HIGHLY STABLE AND DISPERSED Bi MODIFIED NiO CATALYST FOR THE OXIDATIVE DEHYDROGENATION OF n-BUTANE TO BUTADIENE

BY

GAZALI TANIMU

A Thesis Presented to the

DEANSHIP OF GRADUATE STUDIES

KING FAHD UNIVERSITY OF PETROLEUM & MINERALS

DHAHRAN, SAUDI ARABIA

In Partial Fulfillment of the
Requirements for the Degree of

MASTER OF SCIENCE

In

CHEMICAL ENGINEERING

MAY-2016

KING FAHD UNIVERSITY OF PETROLEUM & MINERALS

DHAHRAN- 31261, SAUDI ARABIA

DEANSHIP OF GRADUATE STUDIES

This thesis, written by GAZALI TANIMU under the direction of his thesis advisor and approved by his thesis committee, has been presented and accepted by the Dean of Graduate Studies, in partial fulfillment of the requirements for the degree of **MASTER OF SCIENCE IN CHEMICAL ENGINEERING**.

Dr. Sulaiman S. Alkhattaf
(Advisor)

Dr. Muhammad S. Bashammakh
Department Chairman
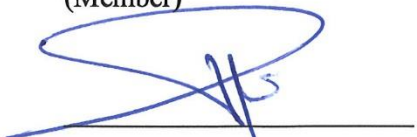
Dr. Basim A Abussaud
(Co-Advisor)

Dr. Salam A. Zummo
Dean of Graduate Studies

Dr. Muhammad S. Bashammakh
(Member)

2/6/16

Date

Dr. Nadhir Al-Baghli
(Member)

Dr. Isam Al-jundi
(Member)

To Almighty Allah and to my beloved parents; Alhaji Tanimu Umar and Malama Huwailat Muhammad, May ALMIGHTY Allah continue to shower his mercy onto them as they trained me when I was young

ACKNOWLEDGMENTS

All thanks be to Almighty Allah, the creator and the sustainer, He whose work is just be and so be it, may His blessings be upon the seal of all prophets, the opener to that which is closed and the seal to that which has passed, our noble Prophet Muhammad (s.a.w), his households, his companions without any exception, and to all those who follow his footsteps till the day of judgment, Amen.

Special thanks to my Parents, Alh. Tanimu Umar and Mal. Huwailatu Muhammad and to the entire members of the family. I must thank them for among others, the moral and spiritual upbringing, untiring financial support and encouragement, without which my attainment of this height wouldn't have been possible. Also to acknowledge are my uncles and aunties for their support and prayers, may Allah continue to guide us onto the right path, ameen.

My sincere appreciation goes to my supervisor Dr. Sulaiman Saleh Alkhattaf for his valuable time and motivations given to me during the entire life span of this research project. I wish to also lodge my vote of thanks to my co-advisor Dr Basim A Abussaud, my committee members Dr Isam Aljundi, Dr Muhammad S Bashammakh and Dr Nadhir Albaghli and to all the lecturers of Chemical Engineering Department who have left no stone unturned to ensure I acquired all requisite knowledge to face the future challenges. I remain humbly appreciative.

Also to acknowledge is Dr Rabindran Balasamy Jermy, I find it difficult to qualify him using one word, he is such a nice and very friendly mentor, I learnt a lot from his wealth of his experience professionally and otherwise. I can never forget the contributions of the following gentlemen towards the success of research, they include Dr Muhammad

TABLE OF CONTENTS

LIST OF TABLES

LIST OF FIGURES

LIST OF ABBREVIATIONS

ODH	:	Oxidative Dehydrogenation
BD	:	Butadiene
OC	:	Oxygenate and Cracking
PO	:	Partial Oxidation
BET	:	Brunaeur Emmett Teller
BJH	:	Barret Joyner Halenda
FID	:	Flame Ionization Detector
GC	:	Gas Chromatography
GHSV	:	Gas Hourly Space Velocity
JCPDS	:	Joint Committee on Powder Diffraction Standards
LSQCURVEFIT	:	Least Square Curve Fit
MATLAB	:	Matrix Laboratory
ODE	:	Ordinary Differential Equation
SS	:	Sum of Square Errors
TCD	:	Thermal Conductivity Detector
TPD	:	Temperature Programmed Desorption
TPR	:	Temperature programmed Reduction

WHSV   :   Weight hourly space velocity

XRD   :   X-ray Diffraction

ABSTRACT

Full Name   : [GAZALI TANIMU]

Thesis Title   : [Highly dispersed and stable Bi modified Ni-O supported catalyst for oxidative dehydrogenation of n-butane to butadiene]

Major Field   : [CHEMICAL ENGINEERING]

Date of Degree : [May, 2016]

The effect of different metal oxide species (Ni, Fe and/or Co) oxide-Bi_2O_3 over alumina support, influence of substituting Bi partially/fully with Mo/W, role of different supports and support modifications with MgO were investigated for n-butane oxidative dehydrogenation (ODH) to butadiene. Co-impregnation technique was used to prepare all the catalysts and the physic-chemical properties were studied using BET, XRD, NH_3/CO_2 TPD and H_2-TPR. The catalytic evaluation shows that, for the case of mono main metal, the order of the butadiene selectivity is Ni > Fe > Co, whereas the order of n-butane conversion is Ni > Co > Fe. Among the binary Ni-Fe, Ni-Co and Fe-Co systems, Fe and Co worked to improve the butadiene selectivity and n-butane conversion, respectively. The ternary Ni-Fe-Co system (10Ni5Fe5Co30Bi-O/Al_2O_3) showed the highest butadiene selectivity of 46.3% at the highest n-butane conversion of 30% with good catalytic stability at the reaction condition. The acid and base sites preferably adjusted by ternary main metal combination in hierarchical nano-particle cohabitation of main metal (Ni, Fe and Co) oxide, Bi_2O_3 and Al_2O_3 cooperate to accelerate butadiene selectivity at both 1st and 2nd step dehydrogenations. This fact was verified by the reduction temperature shift to lower and acid/base property change to moderate with temperature programmed H_2 reduction and CO_2/NH_3 desorption, respectively. Substituting Bi with Mo and W showed decrease in performance indicating mainly that they are not as active as Bi_2O_3 (oxygen mobile oxide)

in enhancing redox cycle of the active species. The different supports investigated showed varying performance due to difference in their ability to interact actively with the metal species in terms of dispersion and reducibility as well as acidic/basic character. The kinetics of n-butane oxidative dehydrogenation was also investigated over the ternary metal (10Ni5Fe5Co30Bi-O/Al$_2$O$_3$) catalyst system. The kinetic models were developed based on the experimental data for the catalytic test as obtained in a fixed bed reactor at reaction temperatures ranging from 350-450$^\text{o}$C. Power law model was used and the kinetic parameters were estimated using MATLAB program.

ملخص الرسالة

الاسم الكامل: تنيمو غزالي

عنوان الرسالة: حفاز أوكسيد النيكل (**Ni-O**) المشتت و المستقر و المعدل بواسطة البزموث المستخدم نزع الهيدروجين المؤكسد من البيوتان لإنتاج البيوتاديين

التخصص: الهندسة الكيميائية

تاريخ الدرجة العلمية: مايو 2016

تأثير أنواع أكاسيد المعادن المختلفة (النيكل، الحديد و/أو الكوبالت) وأكسيد البيزموث المحمول على الألمينا، تأثير إستبدال البيزموث كليا أو جزئيا مع المولوبيدنيوم المحمول على التنجستن، و دور الحاملات و تعديل الحاملات مع أكسيد المغنيسيوم تمت دراستها على نزع الهيدروجين المؤكسد من البيوتان لإنتاج البيوتاديين. في حالة المعادن الأحادية الرئيسية،الترتيب من حيث أنتقائية البوتاديين هو النيكل> الحديد> الكوبالت. في حين أن الترتيب من حيث تحويل البوتان العادي هو النيكل> الكوبالت> الحديد. بين التركيبات الثنائية النيكل-الحديد، والنيكل-الكوبالت والحديد-الكوبالت، عملت على تحسين أنتقائية البيوتاديين من البيوتان العادي، على التوالي. أظهر التركيب الثلاثي النيكل-الحديد-الكوبالت (10Ni5Fe5Co30Bi-O/Al$_2$O$_3$) الأنتقائية الأعلى للبيوتاديين و هي 46.3% عند أعلى نسبة تحويل و هي 30% مع أستقرار حفاز جيد نتج عنه تحسينات مضاعفة عن النيكل في أنتقائية البيوتاديين عن طريق الحديد و في نسبة تحويل البيوتان العادي عن طريق الكوبالت. المواقع الحمضية و القاعدية تم تعديلها التعديل الأفضل عن طريق التركيب الثلاثي للمعادن الرئيسية في أزدواج هرمية الجسيمات الصغيرة لأكاسيد المعادن الأساسية (النيكل، الحديد و الكوبالت)، و يعمل معا كل من أكسيد البيزموث و الألمونيا على تسريع أنتقائية البيوتاديين عن الخطوتيين الأولى و الثانية في نزع الهيدروجين المؤكسد. تم التحقق من هذه الحقيقة عن طريق تغير درجة حرارة الإختزال إلى درجة حرارة أقل و تغيير خاصية الحمضية/ القاعدية اإلى معتدلة مع إختزال الهيدروجين مبرمج درجة حرارة و إمتزاز ثاني أوكسيد الكربون/ النشادر، على التوالي. إستبدال البيزموث مع المولوبيدنيوم و التنجستن أظهر انخفاضا في الأداء مما يدل أساسا أنها ليست نشطة مثل أوكسيد البيزموث في تعزيز دورة الأكسدة و الإختزال من الأنواع النشطة. الحوامل المختلفة التي درست أظهرت أداء مختلف نظرا للاختلاف في قدرتها على التفاعل النشط مع أنواع المعادن من حيث التشتت والقدرة على الإختزال

وكذلك الخاصية الحمضية/ القاعدية. تم التحقق من حركية التفاعلات لنزع الهيدروجين المؤكسد من البيوتان على التركيب الثلاثي

للمعادن للعامل الحفاز (10Ni5Fe5Co30Bi-O/Al$_2$O$_3$). تم تطوير النماذج الحركية أستنادا على البيانات العملية لإختبار

الحفاز في مفاعل مثبت عند دراجات حرارة تتراوح من 450-350 درجة مئوية. و قد أستخدم نموذج قانون القوة لتقدير

المعاملات الحركية بإستخدام برنامج Matlab.

CHAPTER 1

INTRODUCTION

1.1 Background

The increase in the demand of olefins and diolefins in most polymer and petrochemical industries especially in Saudi Arabia motivated the interest towards the search for new production techniques different from the conventional methods, using alkanes as the starting raw materials. Light alkanes (lower alkanes of C_2-C_4) are highly available and are relatively less expensive compared to their corresponding alkenes leading to an economic advantage, they are also environmentally non-aggressive products, hence their usage as raw materials in most chemical industries [1],[2],[3],[4],[5].

The present worldwide usage about 80% of ethylene is in the production of a wide variety of commercially important chemicals such as polyethylene, polystyrene, ethylene dichloride straight chain, higher alkenes and so on. The market for ethylene has been growing at a rate of 2–5% per year. The global capacity of ethylene is around 150 million tons as of 2012, and it reached 160 million tons at the end of 2015 [6]. The demand of 1-butene in the world industries is about 1.3 million metric tons per year and that of butadiene is 10 million in 2006 and is has reached 13 million tons at the end of 2015 with 3-4% annual increment [7]. Butadiene is used mainly as a monomer in the manufacture of polymers such as synthetic rubbers including styrene butadiene rubber (SBR), Polybutadiene rubber (PBR), Nitrile rubber which are tough and/or elastic which is commonly used for the production of tires [8],[9].

1

The commercial (conventional) methods for olefins production includes: steam cracking process which is a gaseous one phase homogeneous reaction occurring at temperatures greater than 800°C, it involves the decomposition of hydrocarbon feed stocks using steam producing different products like alkanes, alkenes and molecular hydrogen [10]. Catalytic cracking process is a process used for upgrading streams from the refinery (heavy and low-value). It uses mainly vacuum gas oil, residue and de-asphalted oil as feed stocks and convert them into light and higher value products like gasoline. Olefins are mainly obtained as co-products in this process in a low amount [10]. Catalytic dehydrogenation process is a reaction that involves the decomposition of alkanes (saturated) into olefins (unsaturated) and H_2 molecule. It is the reverse of hydrogenation reaction. All these processes produces high purity olefins but have major drawbacks as they both are endothermic reactions, leads to coke formation thereby deactivating the catalyst, they are thermodynamically limited reactions hence only produce acceptable yields at high temperatures. Selectivity is difficult to control at such temperatures and finally they are highly energy intensive [6],[11],[12],[13],[14],[15].

Oxidative dehydrogenation of alkanes is an alternative irreversible reaction used for the production of olefins and diolefins. It is an exothermic reaction that occurs at lower temperature and the catalyst used can obtain oxygen directly from the feed stream without requiring additional re-oxidation. The presence of oxygen in this method reduces coking and extends catalyst life time [16],[17],[18].

The major challenge in oxidative dehydrogenation is selectivity control mainly due to parallel and consecutive reactions resulting from the combustion of reactant (partial

2

oxidation) to CO and CO_2, the correct co-feeding of oxygen can reduce this effect together with selectivity improvement by proper catalyst design and formulation [19],[20],[21].

The catalytic performance for ODH is related to the surface acidity/basicity property and reduction-oxidation (redox) property. The lattice oxygen of the catalyst is involved in oxidation process oxidizing hydrogen and olefins intermediates. After which the surface of the catalyst that has been reduced earlier is restored back to normal state by gas phase oxygen adsorption. The evolution of the lattice oxygen is promoted by the interaction between the metal oxides [22].

1.2 Commercial Industrial Technologies

Dehydrogenation reaction is an endothermic process requiring high reaction temperature (600-700°C) for an economical conversion. Butane dehydrogenation requires higher temperature compared to butene for the same conversion. At these high temperatures, many side reactions including cracking and secondary reactions occur, hence the need for a selective catalyst and short residence time [23].

Dehydrogenation reactions unit available in the industries used mainly transition metals like platinum, tin, vanadium and chromium supported on alumina catalysts. Alumina as a support compared to other supports like silica, Titania, zirconia etc has high thermal stability, mechanical strength and strong catalyst regeneration capabilities. The major drawback of alumina is that it speeds up undesired side reactions like cracking and isomerization resulting from its acidic sites, this in turn lead to coke formation and deposition. Some of the established technologies for dehydrogenation process with their

3

catalysts, reactor type, reaction condition and reported conversions and selectivities are
summarized in Table 1.1.

Table 1.1: Commercial dehydrogenation processes

Process name	Catofin	Oleflex	STAR	FBD	Linde/BASF
Licensor	Lummus	UOP	Uhde	Snamprogetti	BASF
Feed	C_3 or C_4	C_3 or C_4	C_3 or C_4	C_3 or C_4	C_3 or C_4
Catalyst	CrO_x/Al_2O_3	$Pt/Sn/Al_2O_3$	$Pt/Sn/Zn/Ca/Al$	CrO_x/Al_2O_3	Pt-Sn/Zr
Reactor	Adiabatic FB	Adiabatic MB	Adiabatic/Oxy	Continuous	Isothermal FB
Temperature/°C	590-650	550-620	550-590	550-600	500-600
Pressure (bar)	0.3-0.5	2-5	1.1-1.5	5-6	>1
Conversion/%	C_3:48-65 C_4: 60-65	C_3:25 C_4:35	C_3:40	C_3:40 C_4:50	C_3:30
Selectivity/%	C_3:82-87 C_4:93	C_3:89-91 C_4:91-93	C_3:89	C_3:89 C_4:91	C_3:90

1.3 Objectives

The main objectives of this research are:

➢ To develop a highly dispersed and stable Bi-modified NiO catalyst for oxidative dehydrogenation of butane to butadiene.

➢ To test the influence of various supports, metal species (Iron and Cobalt), modifiers (Molybdenum and Tungsten) and Acidity/basicity controller (MgO modifications) on the catalyst.

➢ To kinetically study the reaction using the best catalyst.

This are discussed in detail as below:

1.3.1 Synthesis and Characterization of Bismuth and Nickel based catalysts

• Preparation of modified bismuth and nickel oxide based catalysts using co-impregnation, incipient wetness and successive impregnation methods

• Physico-chemical properties determination of the catalysts using characterization techniques

• Testing of the catalysts in the fixed bed reactor (BELCAT) system for their activity and selectivity

• To study the stabilities of the catalysts with best performance in order to confirm their suitability or otherwise for long term usage.

1.3.2 Kinetic modelling of the best catalyst in the fixed bed reactor

• To predict the steps in the rate mechanism using kinetic model

• To estimate the kinetic parameters in the rate equation

• To fit the experimental data into a proposed model to validate the model

1.4 Scope and Outline of the work

The scope of this research will be limited to the synthesis, characterization and testing of the highly dispersed and stable Bi-modified NiO supported catalyst for n-butane ODH to butadiene. This has been broken down to the following chapters

Chapter two discuss a detailed literature review on catalytic oxidative dehydrogenation. Previous work done and the challenges faced and possible solutions taken to address the challenges.

Chapter three will discuss the laboratory section of the work from the equipment used for the experiments together with the procedures followed for the synthesis, characterization and catalyst testing

Chapter four deals with the results obtained from the experimental runs, all the results from characterization of the synthesized catalysts and their detail discussions together with the effects of various conditions varied during the experimental runs. Presented also is the results of the kinetic modelling from model derivation up to the parameters estimation using non-linear regression analysis

Chapter five presents the conclusions that will be drawn from the research together with recommendations for future work.

CHAPTER 2

LITERATURE REVIEW

2.1 BUTADIENE

Butadiene is an unsaturated aromatic hydrocarbon produced as a secondary product from the dehydrogenation (hydrogen abstraction process) of a saturated hydrocarbon mainly butane. Normal butane is first dehydrogenated to form butylene (primary product) and finally butadiene is formed from the dehydrogenation of butylene [1]. Butadiene is a colorless, non-corrosive gas or liquid with a mild aromatic or gasoline-like odor at room temperature, it is highly reactive, toxic and flammable hence classified as a hazardous chemical [24]. Butadiene is mainly polymerized for the production of synthetic rubber. A homo polymer from butadiene (Polybutadiene) is a liquid material and very soft, while Acrylonitrile butadiene styrene (ABS), Styrene butadiene (SBR) and Acrylonitrile butadiene (NBR) produced as copolymers from butadiene and styrene are elastic and tough. Automobile tires producing companies mainly used SBR [8].

2.1.1 Uses of Butadiene

The major use of butadiene is in the production of polymers which have variety of usage domestically and industrially, they improve the performance and functionality of domestic products, safety and also reduces costs of the products. Butadiene-based polymers are used in construction materials, automobiles, Computer and telecommunication equipment, packaging and household articles [24],[25],[26].

2.2 CONVENTIONAL METHODS FOR BUTADIENE PRODUCTION

1,3-Butadiene is produced mainly by the following three methods in the industries:

- Steam cracking of saturated hydrocarbons

- Catalytic dehydrogenation of n-butane and 1-butene (Houdry process)

- Oxidative dehydrogenation of 1-butene (O-X-D process)

2.2.1 Steam Cracking

This process accounts for over 95% of global butadiene production, butadiene is produced as a co-product in the steam cracking of paraffinic hydrocarbons and is purified in a butadiene recovery process. It is a gas phase homogeneous reaction where the feed stocks are fed to a pyrolysis furnace and mixed with steam to be cracked at temperatures in excess of $800^{o}C$. The reaction is highly endothermic and energy intensive and it produces a variety of products (pyrolysate) including olefins, hydrogen and paraffins. Fig. 2.1 shows a typical steam cracking reactor.
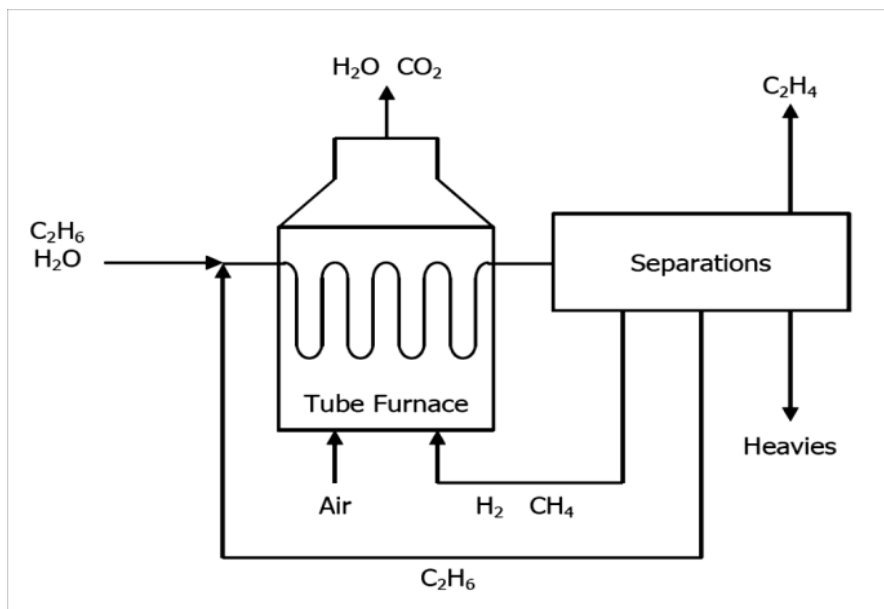
Fig. 2.1: Steam cracking furnace [10].

Depending on the feedstock that is fed to the steam cracker, we have light crackers for gaseous feed like ethane and propane and it produces very low quantity of C4 compounds and heavier co-products while heavy crackers used for liquid feed like gas oils, naphtha and condensates produces much higher quantity of butadiene. Table 2.1 reports a typical yield of steam cracking products from different feedstocks. Depending on the feedstock and the plant operation, butadiene content in C4 compounds can be as high as 75% [24], [10].

Table 2.1: Steam cracking products for different feedstocks [10].

Yield of products (wt%)	Gas feeds			Liquid feeds	
	Ethane	Propane	Butane	Naphtha	VGO
H_2 and methane	13.0	28.0	24.0	26.0	23.0
Ethene	80.0	45.0	37.0	30.0	25.0
Propene	1.1	14.0	16.4	14.1	14.4
1,3-butadiene	1.4	2.0	2.0	4.5	5.0
Mixed butenes	1.6	1.0	6.4	8.0	6.0
C_5^+	1.6	9.0	12.6	18.5	32.0

2.2.2 Catalytic Dehydrogenation

This is a reaction with positive enthalpy change (endothermic) hence requires huge amount of heat and is generally carried out using catalysts. In dehydrogenation of alkanes, the paraffins decompose into an alkene and H_2 molecule and is generally favored by the addition of steam that lowers the partial pressure of the alkanes and also reduces isomerization, polymerization and coke deposition [27],[28].

A common dehydrogenation process is the Houdry process (developed in 1993), it is a single step process of hydrogen abstraction from butane. It uses chromia-alumina catalyst which is usually regenerated after few minutes of usage using air to burn off the coke layer. It is an adiabatic process and butadiene yield is up to 63%. Another dehydrogenation

process is the Dow process which utilizes butenes in the presence of steam to produce butadiene. The catalyst used in this process is Ca-Ni phosphate stabilized with Cr_2O_3, the heat of dehydrogenation is provided by the superheated steam, the conversion achieved is up to 50% and a selectivity of 90%. The catalyst is also regenerated and the product is isolated from reaction mixture using extractive distillation. Shell and Phillips petroleum also developed paraffin dehydrogenation processes using Fe-Cr oxide catalysts with K_2O additive and Fe oxide bauxite catalyst respectively. Typical dehydrogenation reaction is as shown.

$$\left(\Delta H = +\begin{matrix} 30 \text{ kcal} \\ 126 \text{ kJ} \end{matrix} / \text{mol} \right)$$

.... (2.1)

$$\left(\Delta H = +\begin{matrix} 26 \text{ kcal} \\ 109 \text{ kJ} \end{matrix} / \text{mol} \right)$$
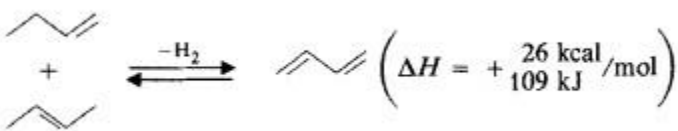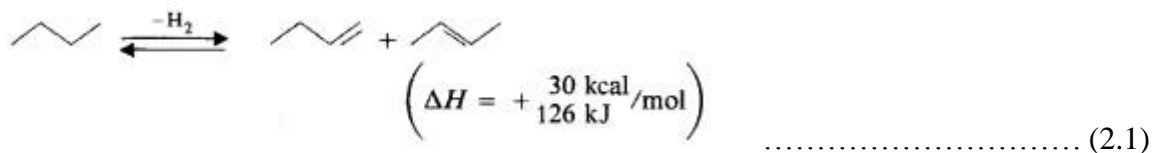
2.2.3 Oxidative Dehydrogenation of Butenes (O-X-D Process)

This process uses oxygen (from air) as a co-feedstock in the production of butadiene. The oxygen acts to displace the equilibrium between butenes and butadiene towards greater production of the diolefins. It removes H_2 by combustion producing water as a byproduct, initiates dehydrogenation by hydrogen abstraction and also oxidatively regenerate the catalyst. It is an exothermic process hence requires low temperature and improved catalyst lifetime compared to the dehydrogenation process. A common O-X-D process is the Phillips process that produces butadiene from n-butenes with steam and air using a fixed bed catalyst at 480-600°C. The resulting conversion is 75-80% and a selectivity of 88-92%.

PetroTex also developed process of butadiene production using O-X-D with a heterogeneous catalyst and reaction performed at 500-600ºC, a selectivity of up to 93% and conversion of 65% were reported.

2.3 OXIDATIVE DEHYDROGENATION OF ALKANES

Oxidative dehydrogenation of alkanes is an alternative irreversible reaction used for the production of olefins and diolefins. It is an exothermic reaction in which the byproduct produced is water instead of hydrogen and occurs at lower temperature. The catalyst used can obtain oxygen directly from the feed stream without requiring additional re-oxidation. The presence of oxidant (like oxygen) in the method also reduces catalyst deactivation by coking due to the efficient removal of coke and its precursors thereby extending catalyst life time [16],[29].

The major challenge in oxidative dehydrogenation is selectivity control mainly due to parallel and consecutive reactions resulting from the combustion of reactant (partial oxidation) to CO and CO_2, the correct co-feeding of oxygen can reduce this effect together with selectivity improvement by proper catalyst design and formulation [19].

The activity and selectivity of a catalyst for ODH depends on its acidic/basic properties and reduction-oxidation (redox) characteristics. The catalyst is reduced by losing its lattice oxygen which is used in the reduction reaction with water as byproduct, it then adsorbs molecular oxygen from the feed to regain its earlier oxidation state. The interaction between the metal components of the catalysts (active species and support) plays a great role in the availability or otherwise of the lattice oxygen for the reaction [30].

Several researchers reported vanadium oxide and chromium oxide as active species with different oxides as carriers (Alumina, Silica, Titania, Zirconia, Ceria etc) showing good results for the ODH of lower paraffins [31],[32],[33]. The catalytic performance relies on the type of carrier, catalyst loading and synthesis method [34]. Hakuli et al [35] investigated different chromia supported catalysts and concluded that alumina and silica-supported chromium oxides were the most effective for the production of lower olefins. Vanadia supported on basic supports not acidic or neutral oxides have been found to be the most selective catalysts for propane oxidative dehydrogenation as reported by Corma et al [36]. Volpe et al [37] concluded from his investigation on n-butane dehydrogenation using VOx supported on USY, NaY, γ-Al_2O_3 and α-Al_2O_3 that VOx/USY has the highest activity and selectivity due to VOx monolayer and its mild acidity. Investigation on the reactivity of vanadia on various supports was conducted by Arena et al [38] and the conclusion drawn was that vanadia was more reactive on amphoteric oxides with TiO_2 having the highest reactivity and that the dispersion and reducibility of the active phase is greatly influenced by the acidic/basic property for the support.

Chromia-Alumina is a dual functional catalyst due to its acidic function obtained from the support and dehydrogenation function due to chromium oxide. Vuurman et al [39] reported that the catalytic dehydrogenation properties of the Chromia-Alumina catalyst are due to surface chromium oxide species and not the bulk chromium oxide phases like CrO_3 or Cr_2O_3. De Rossi et al [40] investigated propane dehydrogenation on Chromia/Silica and Chromia/Alumina catalysts and concluded that, the active sites for the dehydrogenation are Cr^{III} and not Cr^{II} species and that Chromia supported on zirconia has the highest activity compared to silica and alumina supports. This is because the proper coordination of

chromium on the surface sites of zirconia is preserved and the oxygen ion necessary for reduction (H_2 abstraction) is more readily available.

Jibril et al [41] investigated the oxidative dehydrogenation of isobutane on chromium oxide-based catalyst, they tested different supports (Al_2O_3, TiO_2, MgO, and SiO_2), different chromium precursors and partially substituting the chromium with some metals (V, Ni, Co, Mo and Bi). They concluded that, chromia supported on alumina has the best performance with chromium nitrate as the best precursor and that partial substitution of chromium by the metals has little or no contribution on the catalyst performance with Nickel addition slightly increasing the selectivity with same conversion.

Ajayi et al [22] studied n-Butane dehydrogenation over mono and bimetallic MCM-41(highly dispersed Silica) catalyst under oxygen free atmosphere by varying the weight percent of the metals in the catalyst. They concluded that 1.2Cr2.8V/M-41 has the highest butane conversion and butene selectivity.

2.4 CATALYST DEVELOPMENT FOR LOWER ALKANES ODH

The catalyst systems studied by several researchers as obtained from literature for oxidative dehydrogenation of lower alkanes can be grouped into three.

- ➢ Catalyst based on alkali and alkali earth metals
- ➢ Catalyst based on noble metals
- ➢ Catalyst based on oxides of transition metal

2.4.1 Catalyst based on Alkali and Alkali Earth Metals

Catalysts based on Group 1 and 2 metals show good olefin selectivity for ethane and propane, of this catalyst systems the most prominent one is Li/MgO. Although Li/MgO

combination shows reasonable activity [42], [43], the catalyst is usually promoted with halogens mainly chlorine. Hence, halides have high significance towards achievements of good yields resulting from their acidic properties that positively affects dehydrogenation reaction. These catalysts activate ethane at temperature above 600 ^{o}C to form ethyl radicals that react in the gas phase [44]. Addition of Tin oxide (SnO_2), Lanthanium oxide (La_2O_3), Neodymium oxide (Nd_2O_3), or Dysprosium oxide (Dy_2O_3) further improves the performance of Li/MgO [45]. Ethene yield is up to 77% when Dy_2O_3 is used as a promoter and a remarkable selectivity is achieved when the reaction temperature gets closer to melting point of LiCl [45]. Propene is the best alkene produced through oxidative dehydrogenation of propane. Ethene can as well be synthesized in large quantity via catalytic dehydrogenation, chemical industries still maintain steam cracking for ethene production [10].

2.4.2 Catalysts based on Nobel Metals

Catalysts in this group have active species that contains noble metals such as Platinum, Rhodium, Palladium, which are very efficient catalysts for combustion. Paraffins can be converted to alkenes using nobel metal catalysts under specific reaction conditions like reduced contact times and little oxygen supply [10]. At lower temperatures these noble metal catalysts are usually non-selective, however they can be used for selective oxidation at temperature around 1000°C, and non-oxidative same phase reactions greatly influence the formation of products. The selectivity is enhanced by high alkane-oxygen ratio as well as a higher temperature. This leads to nearly complete conversion of oxygen in a way that non-oxidative conversion of paraffins results like steam reforming together with cracking. The catalyst mainly deactivates due to coking and sintering [46]. Enclosing the active nobel

15

metals in a passive support helps mitigate the deactivation. The over layer of support suppresses the oxidative dehydrogenation process and prevents sintering of metals with decrease in coke formation for high temperature reactions.

2.4.3 Transition Metal Oxides based Catalyst

This category of catalyst allows low temperature activation of alkanes relative to group I and II as well as nobel metals. Hence the performance of catalysts for this group is usually better. The oxidative dehydrogenation reaction of lower paraffins using oxides of metals in the transition series on a support occurs via the mechanism of Mars Van Krevelen, in which lattice oxygen in the catalysts is used for oxidizing the paraffin as well as the reoxidation by the gas phase molecular oxygen [22],[47]. Some factors dictates the performance of the catalyst like the redox properties, chemical nature of the active oxygen species and the acid-base character, which in turn depend on the loading and dispersion of the transition metal and the kind of support used [34].
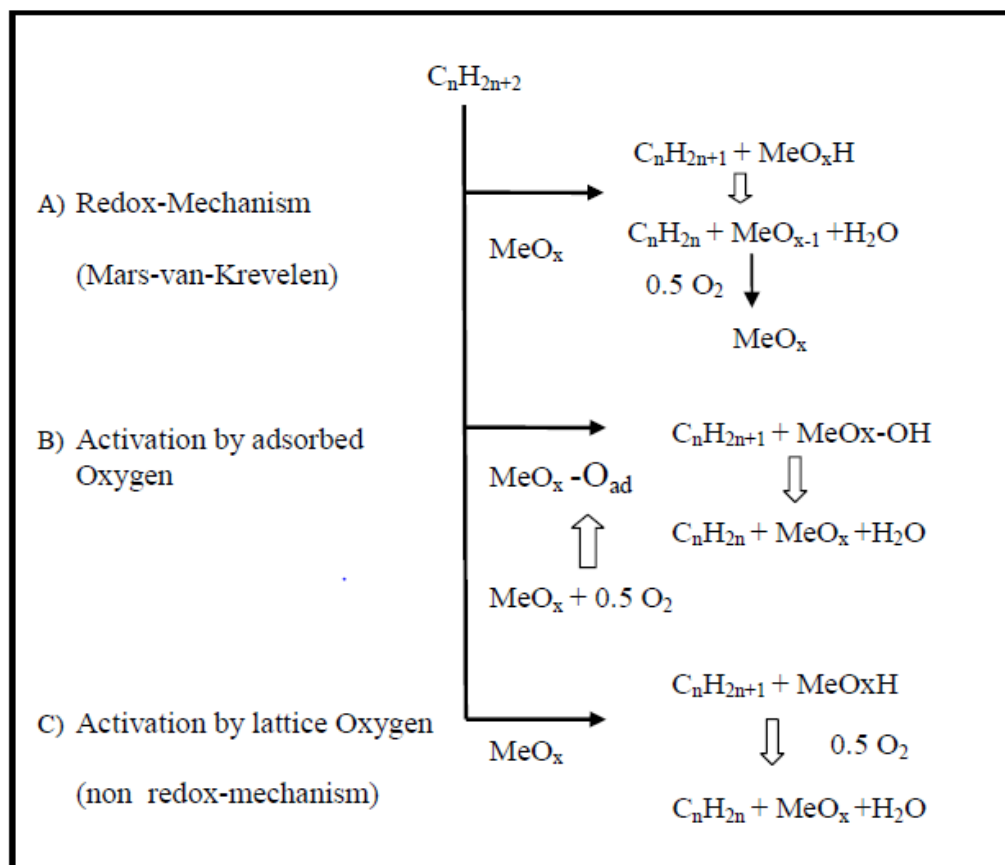
Fig. 2.2: Oxidative dehydrogenation of lower alkanes on transition metal oxides reaction steps [10].

Transition metal oxides have reducible oxygen (surface lattice oxygen) that partake in oxidative dehydrogenation in the absence of gaseous oxygen. Even though, the active oxygen specie partake also in other non-selective routes of ODH resulting to COx. The two most important systems are the molybdenum-based catalytic system and the vanadia–based catalytic system although from literature the molybdenum systems are less active. Figures 2a and 2b show a plot of ethylene and propylene selectivities against conversion for various catalytic systems respectively.
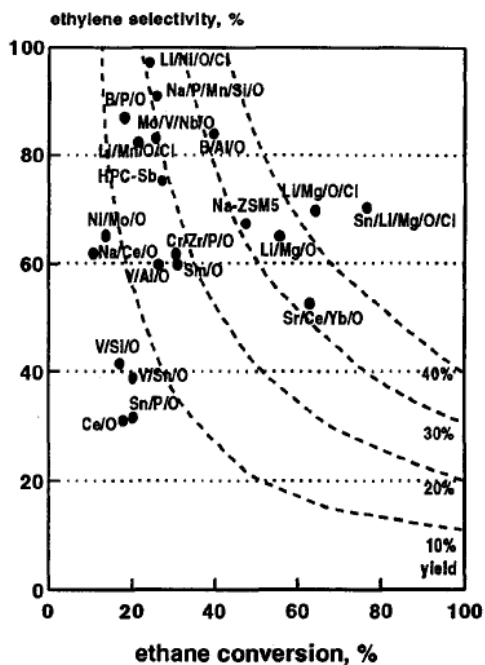
Fig. 2.3a: Ethylene selectivity for various catalytic systems [44].
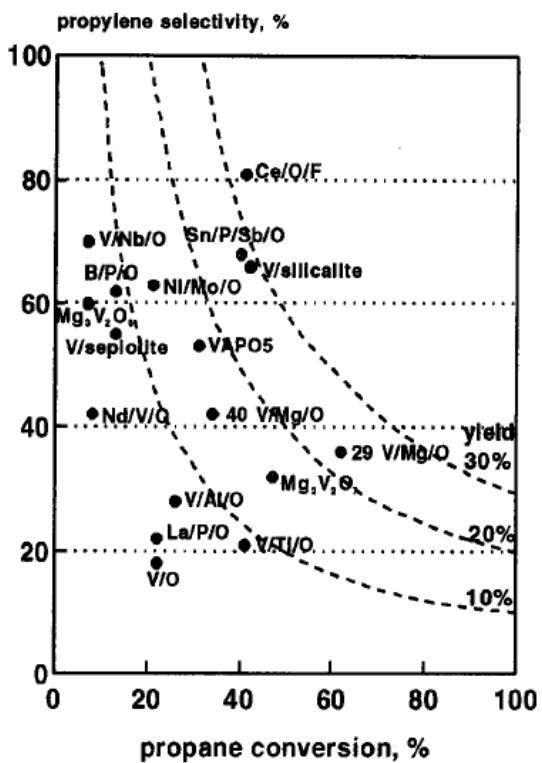
Fig. 2.3b: Propylene selectivity for various catalytic systems [44].

For ethane, the ethylene yield values shown are close to, and sometimes even better than the corresponding values obtained from steam cracking although for propane ODH the values are not too interesting from an industrial point of view. Conditions leading to best propylene yields also leads to production of remarkable amount of ethylene, hence finding a catalyst of industrially acceptable conversion to this olefin is still a major goal [48].

2.5 PROPERTIES OF CATALYST USED FOR ODH

The catalysts used for oxidative dehydrogenation reaction have some basic characteristics that influenced the activity and the selectivity of the catalyst. They are discussed as follows;

2.5.1 Active Lattice Oxygen Species

Metal oxides used as active species for ODH of paraffins have lattice oxygen which participate in the reduction reaction process. The difference in the affinity of the active oxygen species to bind with paraffins is among the main factors that determines the performance (activity and selectivity) of most metal oxides supported catalysts [49]. A study by Weckhuysen and Keller [50] on vanadium oxide supported catalyst reported that 3 categories of lattice oxygen bonds are associated with the catalysts which are end V=O, intermediate V-O-V and V-O-Carrier bond each with different binding strength. They concluded that the lattice oxygen from the V-O-Support bond is the one that is involved in the catalytic reduction reaction.

2.5.2 Surface Coverage

The dispersion of active metal oxides on the support plays a great role on the performance of the supported catalyst. The dispersion depends on the active metal loading and preparation method [51]. Bell et al [52] and Klose et al [53] investigated the effect of

amount of vanadia loading as the main factor leading to distinguished VO_X species on the surface of the carrier (support). They also investigated different type of supports (TiO_2, SiO_2, Al_2O_3 and ZrO_2) with emphasis on alumina-supported vanadia. The conclusions drawn was with little loading of vanadia, isolated VO_4 species which is highly dispersed is formed, isolated monovanadates changes to polymeric polyvanadates with increase in VO_X density which increases continuously until monolayer coverage is attained. Crystalline V_2O_5 nanoparticles forms at high loading of vanadium.

2.5.3 Support Effect

The physic-chemical properties (surface area and acid-base) of the carrier (support) used in metal supported catalysts significantly determines the selectivities of the olefins produced. This is related to the different interactions (dispersion and reducibility) of the active species on different types of support.

Acidic or basic property of the support controls the catalyst selectivity and reactivity due to their influence on reactants adsorption and product desorption. Catalyst with acidic support favor basic reactant adsorption and acidic product desorption, hence with controlled acidic character of support, a catalyst can be designed with higher selectivity in oxidative dehydrogenation reaction [54]. It was concluded in a work by Blasco and Lopez-Nieto [13] and also by Corma et al [36], that catalysts which are very selective are obtained with oxides of vanadium supported on basic oxide (MgO, La_2O_3) compared to oxides of acidic metals, this is as a result of the strong interaction between acidic V_2O_5 and the basic support leading to highly dispersed VOx species responsible for the higher selectivities to olefins and the opposite is true with acidic supports [13], [55].

2.5.4 Redox Properties of Supported Metal Catalysts

The reducibility of active metal oxides play a great role in their activities and selectivities as catalysts for ODH reactions. This property of the metal oxides is greatly influenced by the type of support used which determines the strength of the lattice oxygen used for the redox process.

Lopez-Nieto investigated the reducibility of vanadium oxide catalysts using temperature programmed reduction on different support oxides and concluded that acid-base property of the support strongly influenced the reducibility of the oxides with a negative effect on basic support oxides [1].

2.6 OXIDATIVE DEHYDROGENATION OF NORMAL BUTANE TO BUTADIENE

This is a reaction that involves series removal of molecule of hydrogen from normal butane forming 1,3-Butadiene in the presence of an oxidant (mainly oxygen) with water as a byproduct. Normal butane is a saturated and highly stable hydrocarbon hence requires high temperature for the activation process, it is slightly different from the ODH of ethylene and propylene because of the presence of two secondary atoms of carbon ($-CH_2-$) hence it has high chance of undergoing side reactions to yield other products as shown in Fig. 2.4.
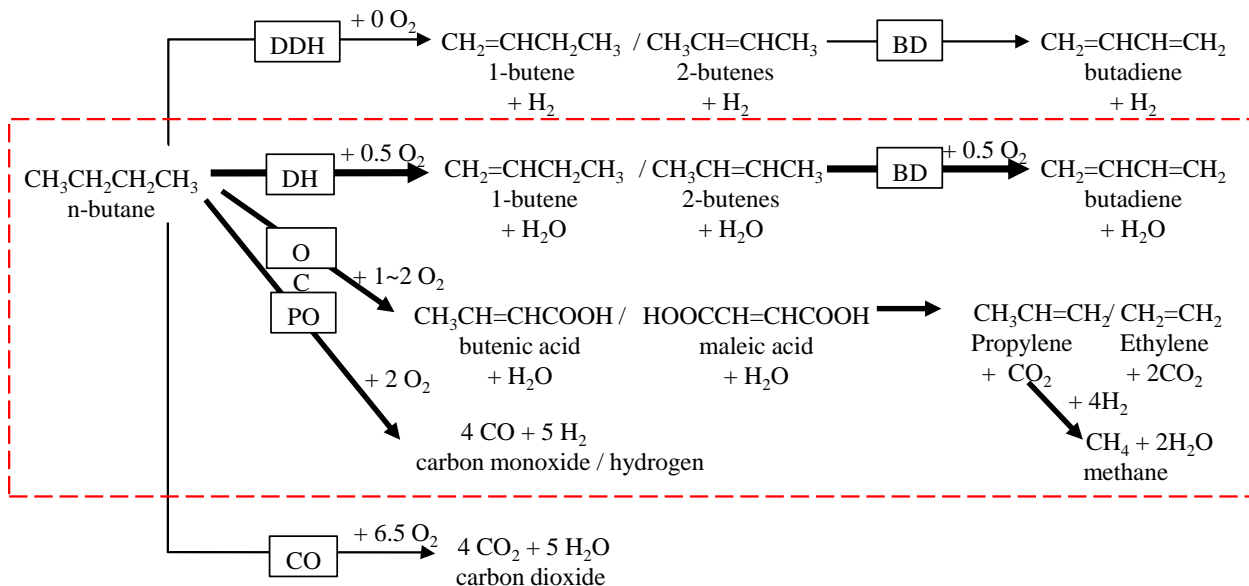
Fig. 2.4: Conversion route of butane to butadiene [56].

(Where DH = dehydrogenation, OC = oxygenates products and cracking and PO= partial oxidation, CO = complete oxidation, DDH = direct dehydrogenation)

2.7 CATALYST DEVELOPMENT FOR BUTANE ODH

Most researchers focus more on the catalyst development for ethane and propane oxidative dehydrogenation with more emphasis on vanadia, molybdena and chromia supported catalysts. Some of the literatures reviewed for the catalyst development for butane ODH are discussed in this section.

Ariola and Nava investigated the ODH of n-butane using Iron-Zinc oxide catalyst. They employed XRD, TPR and Mossbauer spectroscopy to determine the catalytically active phase and concluded that zinc ferrites ($ZnFe_2O_4$) having spinel structure is the selective catalyst for ODH of n-butane to butenes which further produces butadiene in the presence

of ZnO as a modifier. The ZnO interacts with the iron from the zinc ferrite modifying the electron density of the iron which is responsible for the selectivity to butadiene [57].

Armendariz et al studied ODH of n-butane on zinc-chromium-ferrite catalyst. The catalyst was characterized using XRD and Mossbauer spectroscopy. The chromium was added as a promoter that substitutes Fe^{3+} in the octahedral sites which increases the basicity of the lattice oxygen thereby enhancing the selectivities to butadiene and CO_2 [58]

Vasil'ev and Galich reported that the method of active components deposition on the support strongly determines the performance of cobalt-molybdenum and magnesium-molybdenum catalyst used in the ODH of normal butane. Catalyst activity increases proportionally to the number of active components which are cobalt, magnesium and molybdenum especially with a support of low surface area [8].

Xu et al investigated the dehydrogenation of n-butane over vanadia supported on silica gel catalyst using impregnation method of preparation and characterized using XRD, UV-Vis, FTIR, Raman and BET measurements. The influence of VO_x loading and reaction temperature were studied and they concluded that at low VO_x loading and temperature of 590~600°C, n-butane conversion and olefin yield of highest value was obtained [59].

McGregor et al studied the effect of vanadia species in VO_x/Al_2O_3 for n-butane dehydrogenation by varying the vanadium loadings. The catalysts were characterized using FTIR and solid state NMR and concluded from their findings that a strong relationship exist between the surface species of VO_x and the performance of the catalyst with high activity and low selectivity for isolated VO_x species and polymeric VO_x species having greater selectivity to the targeted olefins [15].

Malaika et al investigated the ODH of n-butane to butadiene using chemically modified activated carbon as catalyst. The conclusion was that at low temperature only oxidation takes place leading to the formation of CO_2 but with increase in temperature up to 300^oC and above, 1,3-butadiene and 1-butenes are formed as the major products [16].

Lee et al investigated oxygen mobility influence together with oxygen capacity of $Mg_3(VO_4)_2$ supported with different oxides (Al_2O_3, ZrO_2, MgO, CeO_2) for ODH of n-butane. Their experimental findings shows that at the initial stage of the reaction $Mg_3(VO_4)_2$/MgO is the most active catalyst and $Mg_3(VO_4)_2$/ Al_2O_3 the least active. The activity decreases with time for the MgO catalyst while $Mg_3(VO_4)_2$/ZrO_2 showed stable catalytic activity, hence the conclusion that oxygen mobility and oxygen capacity directly affects the stability of the catalyst activity and the initial catalytic activity respectively [60].

Kwon Lee et al in a similar study investigated the ODH of normal butane to normal butene and 1,3-butadiene over $Mg_3(VO_4)_2$/MgO-ZrO_2 catalyst with varying Mg:Zr in the support. The support was prepared using gel-oxalate co-precipitation method and the catalyst by wet impregnation method and was characterized using XRD, XPS and ICP-AES techniques. They concluded that the catalyst with Mg:Zr of 4:1 has the highest activity and selectivity due to its highest oxygen capacity and acidity as confirmed by TPRO and TPD respectively [61].

Xu et al investigated the catalytic ODH of n-butane over V_2O_5/MO-Al_2O_3 (M= Alkaline earth metals: Mg, Ca, Ba, Sr) with varying V_2O_5 loading. The catalyst were characterized by BET, XRD, FTIR, H_2-TPR and Raman spectra and the results showed that only MgO modified Alumina produce a catalyst with high activity and selectivity while that of Ca, Ba

and Sr showed low activity due to the formation of orthovanadate phase which seldom undergoes reduction. The high activity of the MgO modified Alumina is due to the good dispersion of VOx species due to increased surface area of the support and the existence of crystalline phase of MgO [62].

Jermy et al investigated the catalytic ODH of normal butane to butadiene using Bi-Ni-O/γ-Alumina and reported from their experimental findings that the support itself is selective for the ODH of n-butane to butenes and partial oxidation to CO, the dispersion of NiO on the support reduces the partial oxidation selectivity and enhanced butadiene selectivity. Addition of bismuth to the catalyst was confirmed to give more selectivity to butadiene due to improved NiO dispersion and the redox property of the resulting catalyst [30].

2.8 CATALYTIC PROPERTIES OF NiO SUPPORTED CATALYST FOR BUTANE ODH

The important properties of active metals that influence their performance as active and selective catalyst for oxidative dehydrogenation reaction are redox property and acid/base character. These properties can be enhanced by doping promoters and modifiers to the active metal components and the support as investigated by many researchers, some of which were discussed in the previous section.

Nickel oxide is a relatively less expensive oxide that has been reported to activate short chain alkanes (C_2-C_4) in the presence of molecular oxygen with resulting high activity and at low reaction temperatures. The products obtained however are mainly oxidation products (CO and CO_2) with little dehydrogenation products. NiO has been reported to have improved performance in its activity and selectivity when supported or promoted on

metal oxides. This promotion reduces the selectivity of oxidation products and enhanced that of dehydrogenation [63].

The nature of Ni species and the acidity/basicity of the catalyst are the two factors that influence its performance as a catalyst. The nature of the Ni species are influenced by the valence of the promoters with high valency reducing the concentration of the non-selective non-stoichiometric oxygen in Ni^{3+} species leading to higher selectivity [64]. Lopez-Nieto et al [63] studied the effect of promoted NiO catalysts for the ODH of ethane and concluded from XPS findings that non-stoichiometric Nickel sites Ni^{3+} are involved in the non-selective catalytic processes resulting from the stabilization of electrophilic oxygen species and the removal of these species improves ethylene selectivity. Jermy et al [56] reported that NiO when promoted with Bismuth oxide results in an improved performance, this is due to the participation of Bi_2O_3 as oxygen mobile oxides which is critical in the formation of electrically active grain boundaries in the NiO. Fig. 2.6 shows a pictorial representation of the role of NiO loading on its performance as catalyst for ODH of n-butane as reported by Jermy et al [30]. The mechanism of hydrogen abstraction performed by redox cycle of Ni supported by bismuth oxide species is as shown in Fig. 2.5 as reported by Jermy et al [56]. The redox system by the Ni species is better stabilized with bismuth oxide (which act as controlled O_2- supplier) as hierarchical nanoparticle cohabitation hence making the system highly efficient.
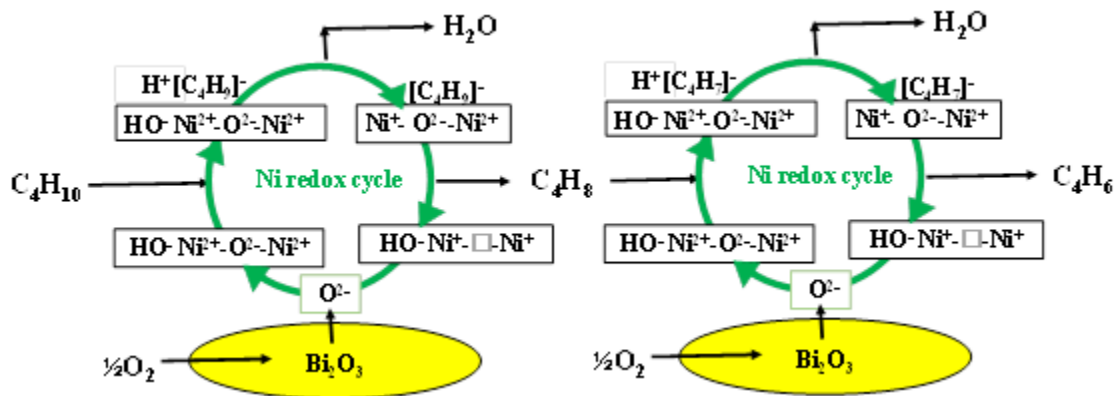
Fig. 2.5: Mechanism of the dehydrogenation performed by redox cycle of Ni (Ni-Bi bimetallic) species [56].

Iron oxide has been shown to be an active site for ODH of butene to butadiene. This is due to its ability to switch easily from Fe^{+2} to Fe^{+3} and vice versa in oxidation/reduction cycle. Park et al [65] reported that if oxygen is added to the catalyst surface, reduced Fe^{+2} reacts with molecular oxygen to form $Fe^{+3}O^-$. The formed O^- dissociates the C-H bonds thereby forming an adsorbed C_4H_7 species and a hydroxyl ion. A second OH^- ion formed will result in adsorbed C_4H_6 with a negative charge which oxidizes Fe^{+3} back to Fe^{+2} through electron release with desorption of butadiene in the gas phase. The two hydroxyl ions formed combined to form water with active site regeneration for further O_2 adsorption. This has been confirmed by electrical conductivity measurements [30].

Cobalt oxide is a good catalyst for various reactions like dehydrogenation, VOC combustion, alcohol oxidation and CO oxidation. Especially in the nanoparticle form, Co_3O_4 shows high surface area and an increased active sites accessibility. Thomas et al [66] reported the use of nanocrystalline cobalt oxide as catalyst for propane oxidative dehydrogenation with almost 100% selectivity to propene.
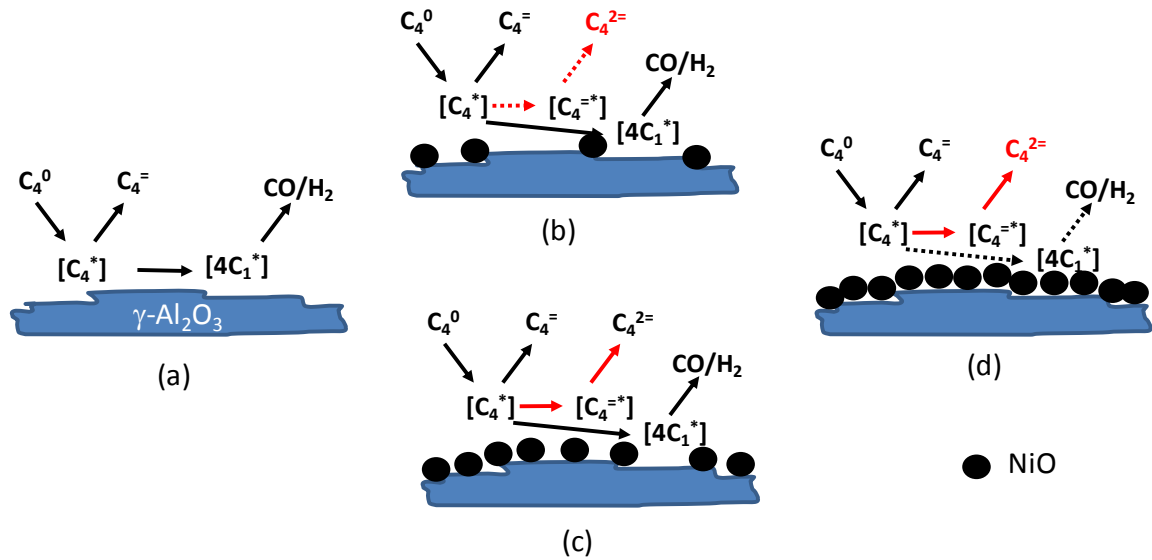
Fig. 2.6: Effect of Nickel oxide loading [30]

2.9 ODH OF PARAFFINS REACTION MECHANISM

The mechanism of oxidative dehydrogenation rely mostly on the paraffin and the catalyst

used, but the basic steps involved in a typical reaction are:

- Alkane interaction with the surface of the catalyst (physisorption)

- Breakage of C-H bond forming alkyl species

- Alkyl species react with nearby surface oxygen (β-elimination) to form olefins

- Reoxidation of the catalyst by molecular oxygen.

2.9.1 Kinetic Models for ODH of Light Alkanes

Light alkanes are gases and their ODH involves solid catalyst, hence forming

heterogeneous system. The catalytic reaction proceeds via the following steps:

- Reactants (Alkanes) diffusion to the catalyst surface

- Reactants adsorption on the catalyst surface

28

- Surface reaction

- Products desorption from the surface of the catalyst

- Products of reaction diffuse from the surface of the catalyst

Based on this reaction steps, the models used for ODH reactions are Eley Rideal model, Langmuir Hinshelwood model, Rake model, Mars Van Krevelen model (Redox model) and power law model.

For ODH reactions using transition metal oxide catalyst, most literatures reported the kinetics following Mars Van Krevelen model (Mechanism of reduction-oxidation) where the active species oxygen participates in the ODH reaction by removing molecule of hydrogen from the paraffin thereby forming water as a byproduct which is removed by surface dehydration. The reduced catalyst is re-oxidized by the gas phase molecular oxygen [10], [67].

For the ODH of n-butane, based on the acidic/basic property of the catalyst, two reaction networks are proposed by several researchers, for a catalyst with basic character alkenes are formed directly from normal butane while 1,3-butadiene as a consecutive reaction product while for catalyst with acidic character, olefins and diolefins are produced firstly from normal butane with CO_x as products of series reaction. Hydrogen removal from normal butane determines the reaction rate while second hydrogen removal/desorption of olefinic intermediate determines the selectivity. Olefinic intermediate desorption rate from catalysts with basic character is higher than that of catalyst with acidic character [68].

CHAPTER 3

EXPERIMENTAL METHODOLOGY

3.1 CATALYST PREPARATION.

The catalysts for used in this research fall into different categories as shown in Table 3.1 and all were synthesized using either co-impregnation technique, successive impregnation or incipient wetness technique for support modification.

3.1.1 Co-impregnation technique

A solution of $Ni(NO_3)_2.6H_2O$ (99% Fisher Scientific) was formed by dissolving 0.99 g of the salt in 160ml distilled water. 0.43 g of Ferric nitrate hydrate and 0.49 g of cobalt nitrate were successfully added to the solution with continuous stirring at $55^{o}C$. To the mixture, 1.39 g of $Bi(NO_3)_3.5H_2O$ (98% Fluka-Garantie) was added with stirring until it dissolved. 2.00 g of Al_2O_3 support was then added and the resulting mixture was stirred continuously for 10 minutes. Air was removed using vacuum from the pore capillaries and the mixture was kept closed overnight at room temperature. It was then dried on a hot plate at $100^{o}C$ until there was no free water and the resulting solid mixture was dried in an oven for 3hrs at $120^{o}C$. All the catalysts were prepared using the above mentioned procedure for consistency. For catalyst testing and characterization, two step calcination method was adopted where the catalyst is heated at a rate of $10^{o}C/min$ up to $350^{o}C$ and maintained for 1hr after which it is raised to $590^{o}C$ at a rate of $15^{o}C/min$ and maintained for 2hr to fully convert the catalyst precursors into their active oxides form.

3.1.2 Successive Impregnation

0.24 g of Ammonium meta tungstate ($(NH_4)_6H_2W_{12}O_{40}$) was dissolved in 60 ml of distilled water to form a solution. 0.92 g of $Bi(NO_3)_3.5H_2O$ (98% Fluka-Garantie) was also dissolved in 120ml of distilled water in a separate beaker. The two solutions were mixed together and added to 2.00 g of Al_2O_3 support in a 250 ml beaker. The mixture was stirred continuously for 10 mins after which air was removed from the pore capillaries using vacuum. The mixture was kept closed at room temperature overnight for ageing. The resulting mixture was dried at 100^oC on a hot plate with stirring for several hours until no free water and finally dried in an oven at 120^oC for 3hrs.

$Ni(NO_3)_2.6H_2O$ (99% Fisher Scientific) solution was formed by dissolving 1.98 g of the precursor in 80 ml of distilled water and poured onto the dried Bi-W impregnated Al_2O_3 support. The resulting mixture was subjected to the same first stage impregnation procedures until dried as-prepared catalyst was obtained.

3.1.3 Incipient wetness followed by Impregnation

0.89 g of Magnesium acetate was dissolved in 2.00 ml of distilled water. This was added dropwise to 2.00 g of Al_2O_3 support. It was then dried under atmospheric condition overnight and calcined at 550 ^oC for 2 hrs at the rate of 5 ^oC/min after which co-impregnation procedure was followed to impregnate the metal species precursors on the modified support.

Table 3.1. Controlling factors of catalysts for Oxidative dehydrogenation of n-butane to butadiene

Main Item	Sub Item		Species/Content (wt %)
Metal Species		SJC01	20Ni 30Bi/Al_2O_3
		SJC28	20Fe 30Bi/Al_2O_3
		SJC30	20Co 30Bi/Al_2O_3
		SJC20	15Ni 5Fe 30 Bi/Al_2O_3
		SJC22	10Ni 10Fe 30Bi/Al_2O_3
		SJC27	5Ni 15Fe 30Bi/Al_2O_3
		SJC21	15 Ni 5Co 30 Bi/Al_2O_3
		SJC23	10Ni 10Co 30Bi/Al_2O_3
		SJC29	5Ni 15Co 30Bi/Al_2O_3
		SJC33	10Fe 10Co 30Bi/Al_2O_3
		SJC31	15Ni 2.5Fe 2.5Co 30Bi/Al_2O_3
		SJC24	10Ni 5Fe 5Co 30Bi/Al_2O_3
		SJC32	5Ni 7.5Fe 7.5Co 30Bi/Al_2O_3
Modifier to Bi	Mo	SJC41	20Ni 20Bi (10)Mo/Al_2O_3
		SJC42	20Ni 10Bi (20)Mo/Al_2O_3
		SJC43	20Ni (30)Mo/Al_2O_3
	W	SJC38	20Ni 20Bi 10W/Al_2O_3
		SJC39	20Ni 10Bi 20W/Al_2O_3
		SJC40	20Ni 30W/Al_2O_3
Support	SiO_2	SJC25	20Ni 30Bi/Silicalite
		SJC02	20Ni 30Bi/formed SiO_2 MSU
		SJC03	20Ni 30Bi/SiO_2 gel (broad) D6
		SJC04	20Ni 30Bi/SiO_2 (new Q10)
	Mesoporous C	SJC36	20Ni 30Bi/mesoporous C
		SJC44	20Ni 10Bi/mesoporous C
		SJC45	10Ni 20Bi/mesoporous C

		SJC46	10Ni 5Fe 5Co 30Bi /mesoporous C
		SJC34	20Ni 30Bi/5MgO-Al$_2$O$_3$
		SJC35	20Ni 30Bi/5MgO-SiO$_2$ (old Q10)
	Modifier to support	SJC05	20Ni 30Bi/5MgO-SiO$_2$ (new Q10)
		SJC06	20Ni 30Bi/5MgO-SiO$_2$ sol (fumed SiO$_2$)
		SJC07	20Ni 30Bi/10MgO-SiO$_2$ (new Q10)

3.2 CATALYST TESTING

All the catalysts testing were done in a fixed bed type of reactor fully integrated with a continuous flow system (BELCAT). It contains a quartz tubular reactor fixed into a stainless steel furnace which passes through reactor furnace thermo well wall. 0.3g of the as-synthesized sample of the catalyst was packed into the reactor. For activation and stabilization, the catalyst was pretreated at higher temperature under flowing air. The system was cooled down to reaction test temperature using nitrogen before commencing the reaction. The contact time for the feed (n-butane) was maintained at 0.093 g-cat.h/mmol. Total reactants flow rates together with inert N$_2$ was maintained at the fixed proportion (31.2 ml/min). The testing of the catalyst was done by changing reaction conditions of temperature (400, 450 and 500°C) and reactant feed ratio (O$_2$/n-C$_4$H$_{10}$) of 1.0, 2.0 and 4.0 mol/mol for oxygen to butane.

Oxidative dehydrogenation reaction is exothermic in nature, hence to monitor the temperature of the catalyst bed, a thermocouple was inserted using a thermocouple well. Online GC (Agilent, 7890N) was used to analyze the reaction products. The GC is

equipped with flame ionization detector (FID) and GC-Gas pro capillary column with dimensions (length=60m, internal diameter=0.32mm) which was used for analyzing hydrocarbons and oxygenates products and a thermal conductivity detector (TCD) with Shin Carbon 80/100 mesh SS Column (having He as a carrier) and MS5A 60/80 mesh SS Column (having Ar as a carrier) for detecting gases including N_2, O_2, CO, CO_2 and H_2. The effluents were identified by comparing with known standard samples. n-butane conversion and products selectivity were determined using carbon balance.

3.3 CATALYST CHARACTERIZATION

All the as-synthesized catalysts were characterized for their physic-chemical properties using the following procedures and techniques as outlined:

For Elemental composition in the various catalysts, ICP equipment ULTIMA 2 (HORIBA Scientific) was used to ascertain the weight percent of the various elements in the catalysts.

For crystallinity test, powder x-ray diffraction (PXRD) was conducted with a desktop x-ray diffractometer Rigaku Miniflex II for a diffraction angle of 5° to 80° using Cu Kα radiation (wavelength $\lambda = 1.5406$ Å) and 30 mA and 40 kV as operating parameters, a step size of 0.02^o and a speed of 2°/min.

Surface area and pore structure measurements (pore surface area, pore volume and pore diameter) were carried out using a Micrometrics ASAP 2020 equipment (Norcross GA). Prior to the adsorption measurements, 0.05g of the calcined catalyst sample was degassed under nitrogen flow for 3hr at 240^oC. The adsorption isotherms were measured at -196^oC (liquid nitrogen temperature). The pore surface area, pore volume and pore diameter were measured using BJH adsorption calculation method.

For redox property and acidic/basic character of the catalyst, temperature programmed reduction (TPR) and temperature programmed desorption (TPD) were conducted in a chemisorption apparatus (BELCAT-A-200). It is made up of a quartz sample holder having a furnace (suitable for high temperature), a mass spectrometer and a thermal conductivity detector (TCD). Injection of gas pulses with standard volume in helium background flow establishes the linearity of the TCD response. The redox property measurement was done using a gas mixture of Ar/H_2 (95/5 vol%) having a total flow rate of $50 cm^3/min$. 100 mg of the calcined catalyst was preheated for 3 hrs at 300^oC in inert He after which it is cooled to room temperature. It was then heated at the rate of $20^oC/min$ up to 900^oC. H_2 intake was recorded with a TCD and CuO was used as a reference for calibrating the consumption of H_2.

Ammonia and carbondioxide temperature programmed desorption (NH_3 and CO_2 TPD) were carried out using the same equipment (BELCAT system) for acidity and basicity measurements, respectively. 100 mg of the calcined catalyst sample was pretreated for 1hr at 500^oC using inert He (50ml/min). It was then exposed to He/NH_3 mixture (He/CO_2 mixture for CO_2 TPD) in volume ratio of 95/5vol% for 30min at 100^oC. Gaseous NH_3 (CO_2) was removed by purging using He for 1hr and then TPD was performed using the same flow of He at a rate of $10^oC/min$ up to 600^oC and the desorbed gas (NH_3 or CO_2) was monitored using mass spectroscopy or TCD detector.

CHAPTER 4

RESULTS AND DISCUSSION

4.1 CATALYST EVALUATION

4.1.1 Sole Metal (Ni, Fe, Co) Catalyst

The influence of different metal species on the performance of catalyst for oxidative

dehydrogenation of n-butane to butadiene in the optimum reaction condition of 450 $^{\circ}$C and

O_2/n-C_4H_{10} = 2.0 is represented in Table 4.1.

Table 4.1: Comparison of catalytic performance for mono main metal in (Ni, Fe or Co)-Bi-O catalyst, Catalyst: 20 wt% main metal-30 wt% Bi-O/Al2O3, Reaction condition: 450 $^{\circ}$C, O_2/n-C_4H_{10} = 2.0

Catalyst main metal	20Ni	20Fe	20Co	10Ni10Fe	10Ni10Co	10Fe10Co	10Ni5Fe5Co
n-C_4H_{10} conversion [%]	**24.0**	**16.2**	**21.4**	**22.2**	**30.7**	**18.3**	**30.0**
Selectivity*[1] [C%]							
DH	75.1	43.3	54.9	54.0	68.9	46.7	66.4
1-C_4H_8	**15.7**	**3.9**	**11.4**	**3.8**	**13.7**	**4.3**	**8.4**
BD	**36.4**	**29.6**	**21.9**	**43.2**	**33.3**	**33.2**	**46.0**
OC	23.7	54.9	45.1	45.7	31.0	52.4	33.4
PO	1.2	1.8	0.0	0.3	0.1	0.9	0.2
BD/DH %	48.5	68.3	39.8	80.1	48.3	71.1	69.2
(1-C_4H_8 + BD)/DH % *[2]	69.4	77.4	60.6	87.1	68.2	80.2	81.8
BD/(1-C_4H_8 + BD) % *[3]	69.8	88.2	65.7	91.9	70.8	88.6	84.6
BD yield	8.7	4.8	4.7	9.6	10.2	6.1	13.8

Butadiene is produced as a second step reaction product from butadiene. The overall reaction including all the side products (partial oxidation, oxygenate and cracking) is shown in Fig.4.1.
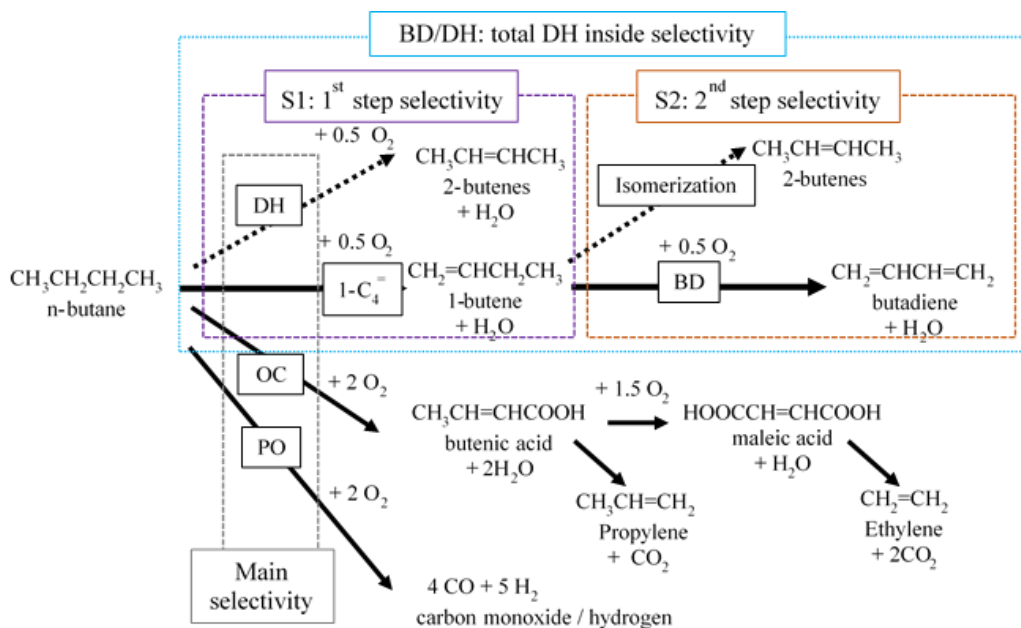
Fig.4.1: Selectivity chart from n-butane to butadiene, DH: oxidative dehydrogenation; BD: butadiene production from butene; OC: oxygenate formation and cracking; PO: partial oxidation to syngas; BD/DH: total DH inside; S1: 1st step of DH inside; S2: 2nd step of DH inside, in Table 1.

From Table 4.1, it can be seen that butadiene selectivity for the sole metals is in the order $Ni > Fe > Co$ while n-butane conversion is $Ni > Co > Fe$, while the overall dehydrogenation selectivity is $Ni > Co > Fe$, conversely oxygenate and cracking selectivity trend is $Fe > Co > Ni$ and all the metal species shows very little partial oxidation selectivity. Ni shows the highest tendency of activating n-butane as well as hydrogen atom abstraction, this fact is possibly due to difference in metal-support interaction and acid-base properties of the metal species which strongly determines the catalyst performance. Table 4.1 also shows the inner

dehydrogenation selectivity to butadiene through the 1-butene intermediate as shown in Fig.4.2.

A) <u>Mixed butene intermediates</u>

B) <u>1-butene intermediate</u>
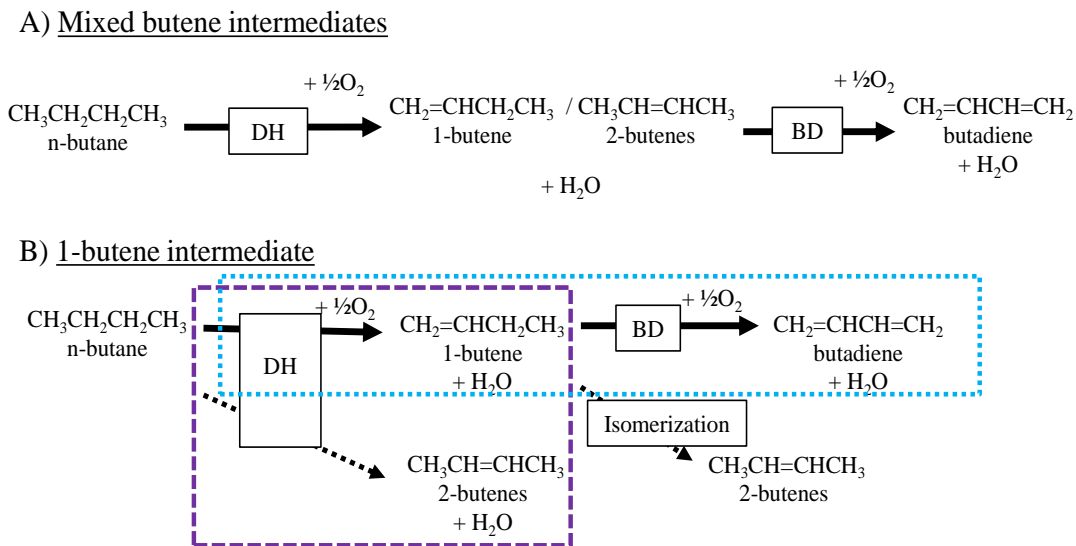
Fig. 4.2. Route inside dehydrogenation for selective conversion from n-butane to butadiene including intermediate and by-product formation. Purple broken and blue dotted line squares mean $*^2$ and $*^3$ in Table 1, respectively.

As can be seen from Table 4.1, for both 1st and 2nd step selectivity, the trend is Fe >Ni > Co, this shows that Fe function as a selective butadiene catalyst due its ability to switch easily from Fe^{+2} to Fe^{+3} and vice versa in oxidation/reduction cycle as reported by Park et al [65] eventhough it shows low activity for the overall reaction. Hence, Ni sole metal catalyst is the best among the three metals owing to its relative high activity and selectivity to butadiene.

4.1.2 Binary Metal (Ni-Fe, Ni-Co, Fe-Co) Catalyst

In order to investigate further the metal species effect on the catalytic performance for oxidative dehydrogenation reaction of n-butane to butadiene, the sole metal species were combined to form binary metals by substituting partially the 20 wt% of Ni from the

standard catalyst (20Ni-30Bi-O/Al₂O₃) as shown in Table 4.1. This shows that partial

substitution of Ni by Fe up to 50 % substitution increases butadiene selectivity due to an

improved dispersion on the support and redox properties enhancement. The activity was

slightly constant for 50 % substitution but decreases with increase in Fe substitution, which

is probably due to decrease in metal-support interaction and increase in catalyst acidity as

manifested in the successive increase in oxygenate and cracking selectivity. Main

selectivity of dehydrogenation as represented in Fig.4.1 also decreases with increase in Fe

substitution. Partial oxidation selectivity remain very low even after substitution. This trend

of conversion and selectivity is depicted clearly as shown in Fig.4.3.
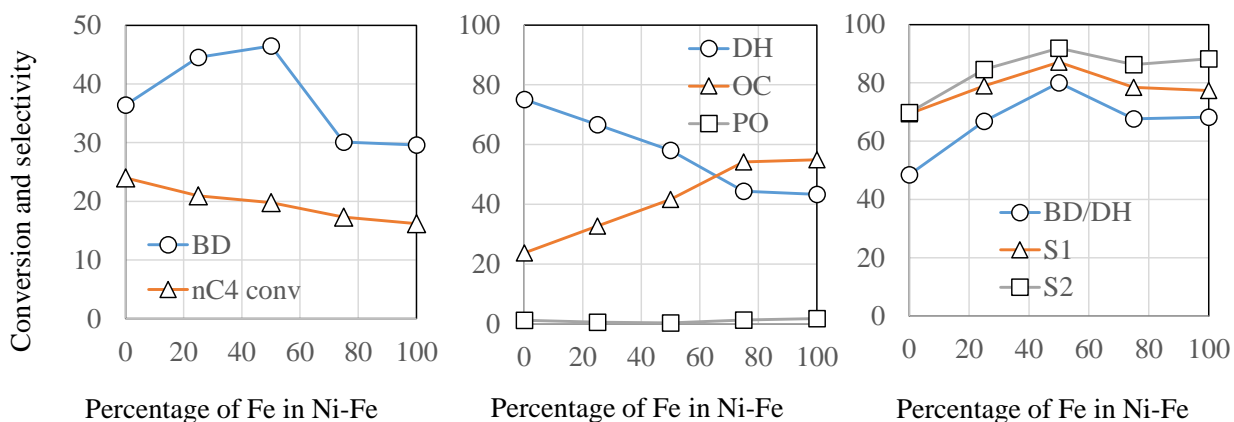
Fig. 4.3: Comparison of catalytic performance for binary main metal in (Ni-Fe)-Bi-O catalyst, Catalyst: 20 wt% main metal-30 wt% Bi-O/Al₂O₃, Reaction condition: 450 ᵒC, $O_2/n\text{-}C_4H_{10} = 2.0$

Fig.4.3 clearly shows the influence of combining Ni-Fe in a binary metal combination on

n-butane conversion and butadiene selectivity. Also, it greatly improves (1-C_4H_8 +

BD)/DH: selectivity at 1st step dehydrogenation, BD/(1-C_4H_8 + BD): selectivity at 2nd step

dehydrogenation, and BD/DH: two step total selectivity, = [(1-C_4H_8 + BD)/DH] x [BD/(1-

C$_4$H$_8$ + BD)] especially up to 50 % substitution which is also due an enhanced redox property as well as Ni-Fe-O, Bi$_2$O$_3$ and Al$_2$O$_3$ hierarchical nanoparticle cohabitation.

Ni-Co binary metal oxide combination was also studied to show its own influence on the catalyst performance as represented in Table 4.1. From the table it can be seen that, Ni-Co binary metal oxide combination improves the catalyst activity (increased in conversion) mainly due to high surface area and an increased accessibility to active sites by cobalt oxide nanoparticle as reported by Junjiang et al [69]. It shows only little improvement in butadiene selectivity at 25 % substitution after which decrease in selectivity was observed. Ni-Co combination showed a gradual increase in oxygenate and cracking selectivity due to change in catalyst acidity by Co oxide substitution. A very negligible partial oxidation selectivity was observed indicating no activity completely by the various catalyst in favor of that reaction pathway. Also, this Ni-Co catalyst combination shows little improvement in both 1st step dehydrogenation selectivity, 2nd step dehydrogenation selectivity and the overall two step selectivity. It shows a fluctuating pattern as shown in Fig.4.4. This is due to the inability of Co to improve butadiene selectivity probably due to its weak strength in facilitating H$_2$ abstraction in both 1st and 2nd step dehydrogenation.
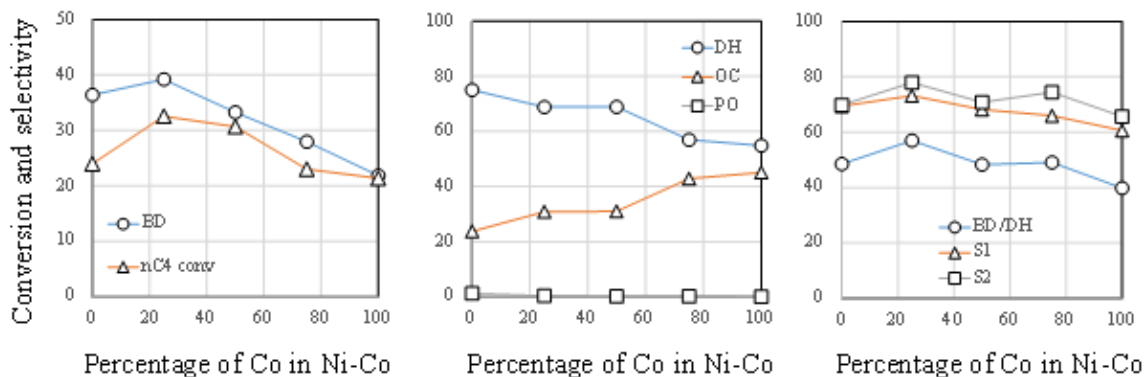
Fig.4.4. Comparison of catalytic performance for binary main metal in (Ni-Co)-Bi-O catalyst, Catalyst: 20 wt% main metal-30 wt% Bi-O/Al_2O_3, Reaction condition: 450 oC, O_2/n-C_4H_{10} = 2.0

Fe-Co binary metal oxide system was also investigated and the results shows that the catalyst performance directly depicts the properties of the two sole metal oxides. Co oxide property improves the n-butane conversion higher than sole metal Fe catalyst and Fe oxide acts to improve butadiene selectivity. Main selectivity of DH, OC and PO also lies between that of the two sole metals as shown in Table 4.1.

4.1.3 Ternary Metal (Ni-Fe-Co) Catalyst

The three sole metal oxide investigated were combined with a view of testing their overall effect on the catalyst performance. Fe and Co substituted 50 % of Ni as shown in Table 4.1. The ternary metal combination resulted in high performance mainly due to double improvements of Ni in the butadiene selectivity by Fe due to its redox ability and in n-butane conversion by Co due to its high surface area and easy accessibility to active sites.

Main dehydrogenation selectivity decreases with ternary metal combination resulting to an increase in oxygenate and cracking selectivity possibly due to slight change in catalyst acidity. Partial oxidation selectivity also decreases with ternary metal combination. The

41

variation of the main selectivity with ternary metal substitution is clearly shown in Fig.4.5. Also the ternary metal combination shows clear improvement in butadiene selectivity at both 1st and 2nd step dehydrogenations which is mainly due to change in acid and base sites due to the hierarchical nanoparticle cohabitation of main metal (Ni, Fe and Co) oxide, Bi_2O_3 and Al_2O_3 support.
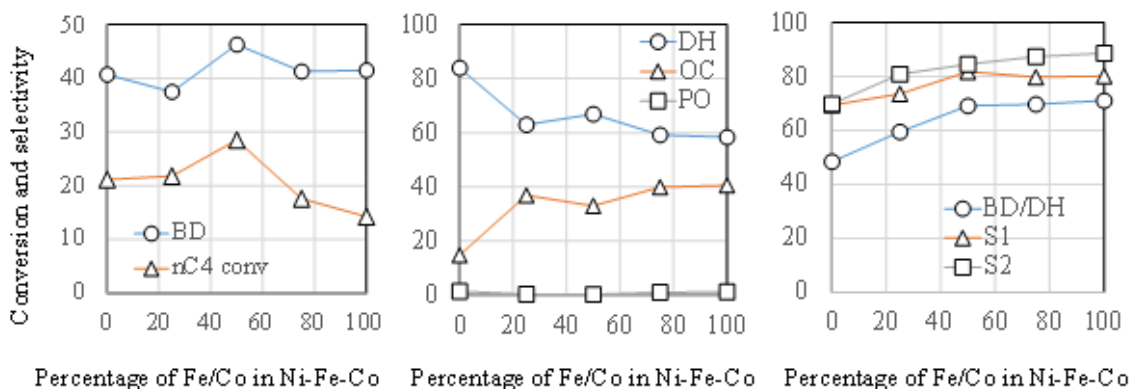
Fig.4.5. Comparison of catalytic performance for ternary main metal in (Ni-Fe-Co)-Bi-O catalyst, Catalyst: 20 wt% main metal-30 wt% Bi-O/Al_2O_3, Reaction condition: 450 °C, O_2/n-C_4H_{10} = 2.0

4.1.4 Catalytic Performance using 1-butene Feedstock

1-butene feed was used in order to confirm the activity and selectivity of the improved ternary metal (Ni-Fe-Co) catalyst for 2nd step dehydrogenation compared to the standard sole metal (Ni) catalyst. The result is presented in Table 4.2 and it clearly shows an improvement in butadiene selectivity but with same activity. Butadiene selectivity at both temperatures and for the two feed stocks is depicted clearly in Fig. 4.6.
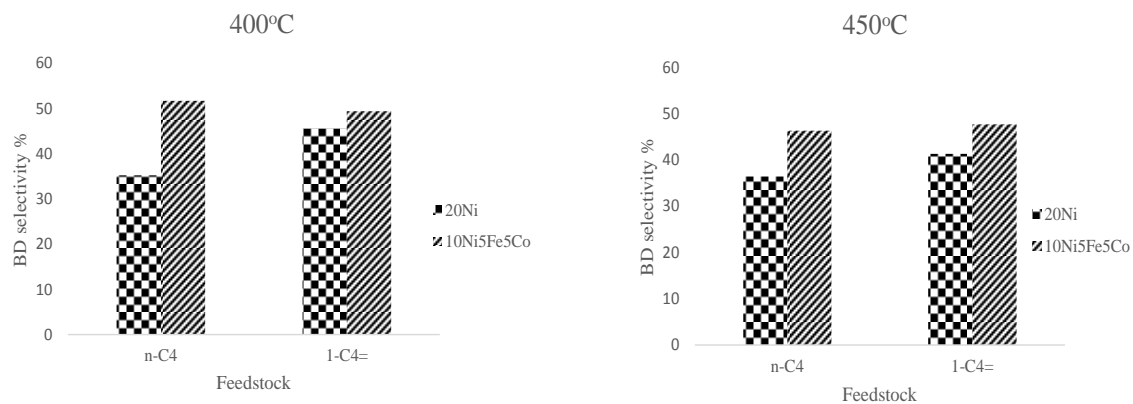
Fig. 4.6: Performance of sole Ni catalyst and ternary metal catalyst with two different feed stocks.

Table 4.2 also shows that no oxygenate and cracking (OC) as well as partial oxidation (PO) products formed at the 2nd step dehydrogenation. It is also clear that dehydrogenation selectivity is the same for both catalysts but different butadiene selectivity which shows difference in isomerization selectivity by the two catalysts. Sole Ni catalyst shows higher isomerization compared to the ternary catalyst due to strong acid sites present in the former but absent in the latter catalyst as was revealed by NH_3 Temperature programmed desorption.

Table 4.2: Comparison between n-butane and 1-butene as feedstock for metal species in (Ni, Ni-Fe-Co)-Bi-O catalyst, Catalyst: 20 wt% (Ni, Ni-Fe-Co)-30 wt% Bi-O/Al_2O_3, Reaction condition: O_2/n-C_4H_{10} = 2.0

Main metal	20Ni				10Ni-5Fe-5Co			
Feed	nC$_4$		1C$_4^=$		nC$_4$		1C$_4^=$	
Reaction temperature: ^oC	400	450	400	450	400	450	400	450
nC$_4$ or 1C4$^=$ conversion	15.0	24.0	72.0	74.3	16.4	28.5	69.6	74.3
BD	35.2	36.4	45.6	41.3	51.7	46.3	49.4	47.7
DH$^+$	94.2	75.1	95.8	93.4	85.1	66.9	95.1	93.3
OC	4.1	23.7	3.3	4.3	14.5	32.9	2.9	4.3
PO	1.7	1.2	0.8	2.3	0.4	0.2	2.0	2.4
BD/DH$^+$	37.4	48.5	47.6	44.2	60.7	69.2	51.9	51.1
BD yield	5.3	8.7	32.8	30.6	8.5	13.2	34.4	35.4

[*1] DH$^+$: dehydrogenation and isomerization, BD: butadiene, OC: oxygenate and the cracked, PO: partial oxidation. [*2] selectivity at 1st step dehydrogenation, [*3] selectivity at 2nd step dehydrogenation

4.1.5 Improved Catalyst Stability

Ternary metal (Ni-Fe-Co) catalyst with the best performance was subjected to stability test under standard conditions: 450 ^oC, O_2/n-C_4H_{10} = 2.0, in order to test its suitability or otherwise for long period of time usage with little decline in performance. The results shows that the catalyst is stable for 10 h as time on stream.
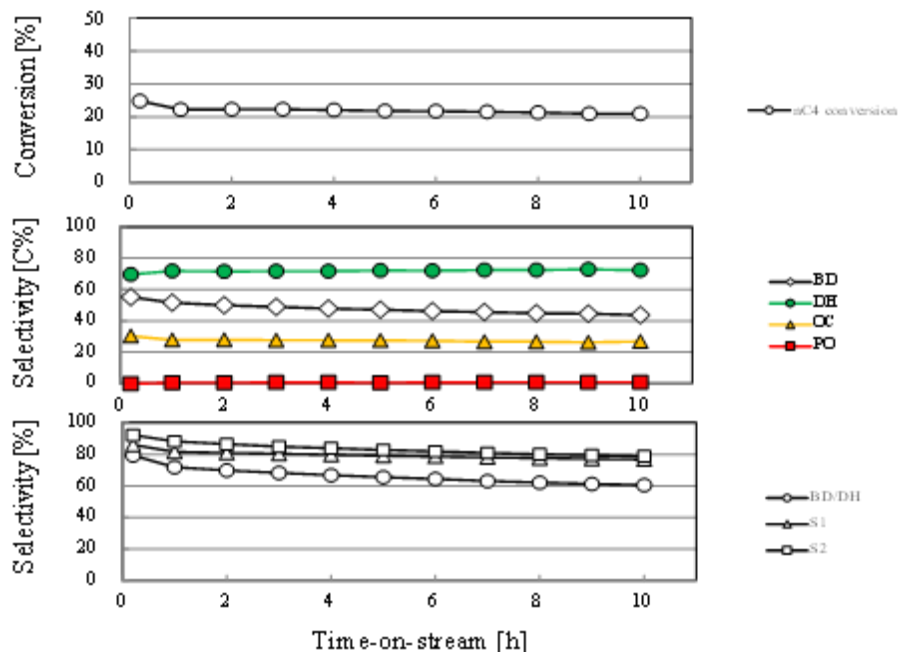
Fig.4.7. Stability of (10Ni-5Fe-5Co)-30Bi-O/Al2O3 catalyst with time-on-stream

It is clear from Fig. 4.7 that the catalyst shows stable activity with little decrease in butadiene selectivity mainly due to decline in 2nd step dehydrogenation selectivity as it shows steep fall with time compared to the 1st step dehydrogenation selectivity and this is possibly caused by active sites poisoning caused by carbon deposits thereby reducing the redox cycle efficiency. Also, main selectivity of dehydrogenation, oxygenate formation and partial oxidation shows an approximate constant trend with slight increase in the overall dehydrogenation selectivity.

4.2 CATALYST CHARACTERIZATION

This section further discussed the various characteristics of the catalyst including their surface area, active sites interaction with support, redox property, crystallinity as well as acid-base properties that determined their suitable performance or otherwise for the oxidative dehydrogenation reactions.

4.2.1 Surface area and pore structure

The BET surface area and the pore structure for all the catalysts (sole metal, binary metal and ternary metal combination) are shown in Table 4.3. All the catalysts exhibited a lower surface area based on weight of catalyst relative to the Al_2O_3 support. The same trend is also observed in the pore surface area and pore volume. The catalysts surface area together with pore structure were also computed based on part weight of support due to metal oxides impregnation. It also shows that surface areas and pore volumes are still lower than that of the support due to pore volume shrinkage caused by metal oxide dispersion on the pore surface.

Table 4.3. Physical properties of 20wt% metal (Ni, Fe and Co)-30wt%Bi-O/Al_2O_3 catalysts.

Catalyst (20wt%metal-30wt%Bi-O/Al_2O_3) Metal species	BET surface area		Pore surface area		Pore volume		Average pore diameter
	$[m^2/g$-catalyst$]^a$	$[m^2/g$-support$]^b$	$[m^2/g$-catalyst$]^c$	$[m^2/g$-support$]^d$	$[cm^3/g$-catalyst$]^e$	$[cm^3/g$-support$]^f$	$[nm]^g$
20Ni	136	218	157	251	0.38	0.61	9.6
20Fe	169	269	191	304	0.45	0.71	9.4
20Co	124	199	150	241	0.36	0.59	9.7
10Fe10Ni	169	270	193	307	0.42	0.67	8.8
10Co10Ni	143	229	161	257	0.38	0.61	9.5
10Fe10Co	153	245	178	284	0.43	0.68	9.6
5Fe5Co10Ni	165	263	184	294	0.41	0.65	8.8

[a]BET surface area, [c,e,g]Surface area, pore volume and average pore diameter measured using BJH isotherm, [b,d,f] Surface area and pore volume calculated by volume based Al_2O_3 using the equation: SA or $PV \times [\Sigma(MO_x/M)+100]/100$, where M=metal wt%; MO_x=metal oxide wt%; SA = Surface Area; PV = Pore Volume.

Pore size distribution was plotted as shown in Fig. 4.8 to further see the influence of metal impregnation and dispersion on the pore structure (pore size distribution) of the catalyst relative to that of the support. Metal oxide dispersion lead mainly to constant/less pore diameter of the catalysts compared to that of the support. It can also be seen that sole metals (Ni, Fe, Co) have closer pore size distribution to the alumina support due to their low dispersion on the support compared to binary metal and ternary metal combinations that resulted in higher metal oxides dispersion.
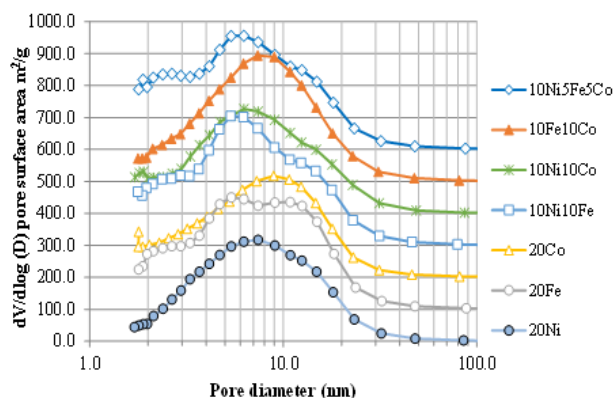
Fig. 4.8: Pore surface area distribution for the main metal composition (mono, binary and ternary of Ni, Fe and Co) in main metal-Bi-O/Al_2O_3 catalyst.

It is clear from Fig.4.8 that metal species combination as is the case with binary metals (Ni-Fe, Ni-Co and Fe-Co) and ternary metal (Ni-Fe-Co) reduces the average pore diameter to lower value compared to the sole metals (Ni, Fe, Co) case which is due to the effect metal mixing has on porosity. Ni and Fe sole metals are more highly dispersed in the support pores than Co due to its larger particles. Main metal species only lead to the change in pore size distribution because Bi_2O_3 contribution is the same in all the catalysts considered. It is also clear from Table 4.3 and Fig. 4.8 that ternary metal combination shows the least pore diameter and lowest pore size distribution which is mainly due to the coexistence of

different particle sizes of Ni, Fe and Co as well as an increased metal dispersion on the support. This findings clearly support the catalyst performance results as discussed earlier.

4.2.2 X-ray Diffraction

The x-ray diffraction (XRD) patterns of the catalysts for sole metal, binary metal and ternary metal combination are presented in Fig.4.9. XRD gives information mainly about phases present in a catalyst, crystal sizes and crystal amount (crystallinity). Intensity of diffraction peaks (peak height) signifies sample crystallinity while peak width signifies crystal sizes.
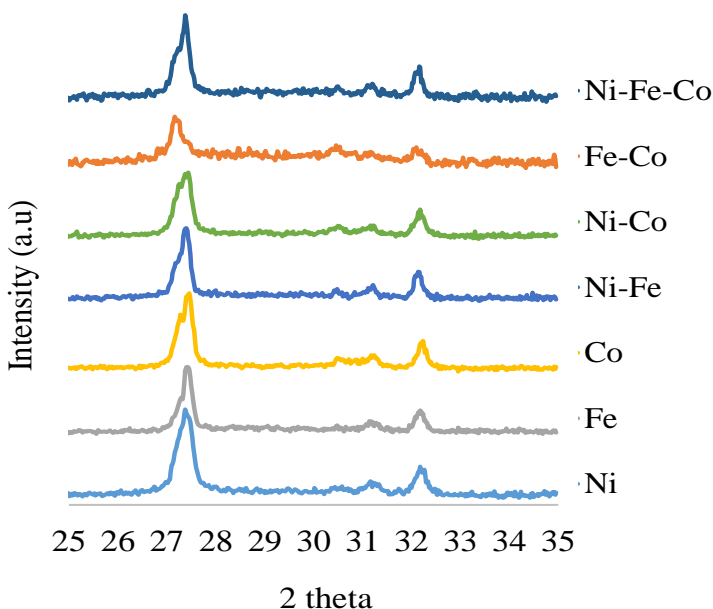
Fig.4.9: X-ray diffraction pattern for the main metal composition (mono, binary and ternary of Ni, Fe and Co) in main metal-Bi-O/Al_2O_3 catalyst

Jermy et al [30] studied NiO peaks in 20Ni-30Bi-O/Al_2O_3 and 20Ni-O/Al_2O_3 and found that no peaks of NiO was observed in 20Ni-30Bi-O/Al_2O_3 indicating that NiO is highly dispersed with a crystal size of 3 nm which cannot be detected by XRD, it only works to

promote Bi_2O_3 transition from tetragonal β-phase to monoclinic α-phase as compared to 30Bi-O/Al_2O_3 that showed only β-phase which is highly crystalline and active for butadiene formation. Hence, diffraction angle of 25° to 35° was chosen to clearly show the characteristics peaks of Bi_2O_3 phase transition due to the proximity of phases angles of 27.15° and 27.38° for α and β phase respectively. Standard catalyst (20Ni-30Bi-O/Al_2O_3) calcined at 590 °C shows α-Bi_2O_3 of 40 % and β-Bi_2O_3 of 60 % as reported by Jermy et al [56], this was used as a basis for comparing the metal species (Fe/Co) substituted catalysts. For the sole metals (Ni, Fe, Co), both Fe and Co catalysts shows lower diffraction peak indicating less crystallinity and α-Bi_2O_3 of higher percentage with broader peak width resulting from their smaller crystal sizes compared to Ni catalyst, where Fe and Co metal species make Bi_2O_3 less active as an oxygen supplier.

For the binary metal and ternary metals, it is clear that with the percentage increase of Ni substitution by Fe and Co, the peak height decreases and peak width broadens mainly due to increased metal oxide dispersion caused by the substitution. This property coupled with the substitution influence on the redox property and acid/base character as will be discussed, strongly determines the overall catalyst performance.

4.2.3 Temperature Programmed Desorption (NH_3/CO_2-TPD)

This techniques were used to determine the acidity/basicity of the catalysts in which NH_3-TPD is for acidic character and CO_2-TPD for basic character. The values (acid and base amount) obtained for the metal species substitution (sole metal, binary metal and ternary metal) are as shown in Table 4. The amount of acid/base related to NH_3/CO_2 desorbed was deconvolved to three strengths of weak, moderate and strong acid/base.

NH$_3$-TPD has spectra showing first desorption peak between 100-250 ºC which is a region of weak acid fraction followed by a region of moderate acid fraction at temperature between 250-400 ºC and then a peak at > 400 ºC indicating strong acid fraction. Catalysts of higher acid sites shows low dehydrogenation selectivity but favors oxygenate and cracking selectivity. Butadiene selectivity is not only determined by the acid sites in a catalyst but by the optimum acidic/basic sites ratio with higher basicity favoring desired butadiene production as reported by Raju et al [70] . Fig. 4.10 shows the plot for NH$_3$/CO$_2$-TPD for the metal species investigated.
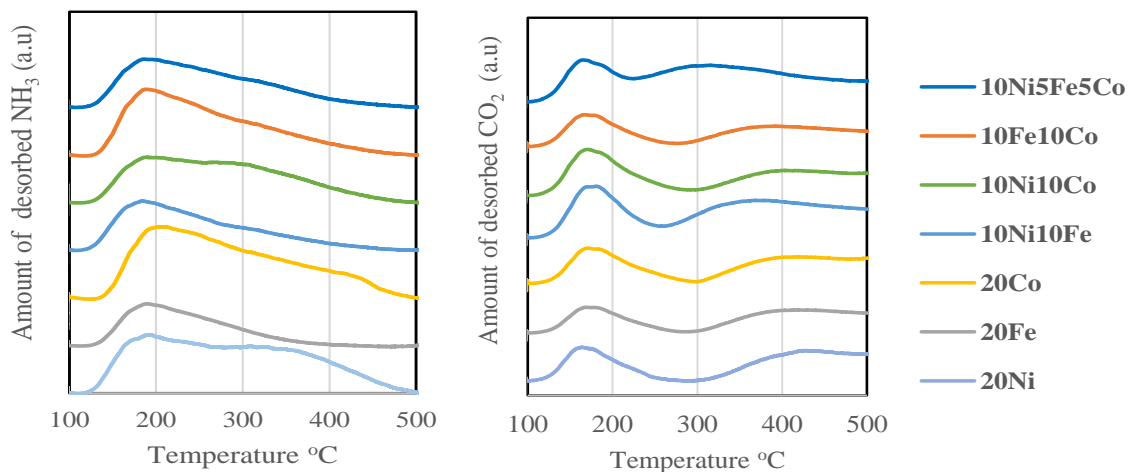
Fig. 4.10: NH$_3$ and CO$_2$-temperature programmed desorption for the main metal composition (mono, binary and ternary of Ni, Fe and Co) in main metal-Bi-O/Al$_2$O$_3$ catalyst

It is clear from Fig. 4.10 that the sole metals showed regions on weak acid fraction and medium acid fraction which makes them have high acidity and their resulting relative low butadiene selectivity. Binary metals showed an improved butadiene selectivity due to their

high weak acid fraction with little or no medium acid fraction. Ternary metal combination shows only weak acid fraction hence its highest butadiene selectivity.

For CO_2-TPD, two distinct peaks are mainly observed at (150-170 $^{\circ}$C) and (300-400 $^{\circ}$C) indicating weak and strong basic sites respectively and this results mainly due to the interaction of CO_2 with the surface hydroxyl groups. It is also clear from Fig. 4.10 that sole metals show mainly regions of weak base fraction with low moderate/strong base fractions. Ternary metal combination showed a reduced weak base fraction with a broad and enlarged moderate base fraction.

Table 4.4: Metal species substitution temperature programmed analysis (NH_3 and CO_2-TPD)

Catalyst	CO_2-TPD Base amount [mmol/g]*1				NH_3-TPD Acid amount [mmol/g]*2			
	I	II	III	Total	I	II	III	Total
20Ni	0.073	-	0.173	0.246	0.115	0.169	0.097	0.381
20Fe	0.061	-	0.123	0.184	0.072	0.049	-	0.121
20Co	0.067	-	0.134	0.201	0.176	0.202	0.095	0.473
10Fe10Ni	0.107	-	0.254	0.361	0.077	0.056	-	0.133
10Co10Ni	0.087	-	0.124	0.211	0.159	0.093	0.059	0.311
10Fe10Co	0.086	-	0.140	0.226	0.155	0.094	0.071	0.320
5Fe5Co10Ni	0.114	0.234	-	0.348	0.131	0.077	0.052	0.260

*1: I (170 $^{\circ}$C peak): weak base, II (300 $^{\circ}$C peak): moderate base, III (400 $^{\circ}$C peak): strong base *2: I (100-250 $^{\circ}$C): weak acid, II (250-400 $^{\circ}$C): moderate acid, III (>400 $^{\circ}$C): strong acid

From Table 4.4, it can be seen that the total acidity/basicity directly determines the performance of the catalysts mainly in butadiene and oxygenate/cracking products selectivity as well as 1st and 2nd step dehydrogenation selectivities. High basicity and low acidity favors dehydrogenation selectivity while the reverse favors oxygenate and cracking products formation. Jermy et al [56] reported the proposed reaction route and catalyst active sites for oxidative dehydrogenation of n-butane to butadiene over a Ni-Bi-O/Al_2O_3, and based on our findings, it became a fact that substituting Ni with Fe or/and Co in binary and ternary metal combination leads to basicity moderation and reduction in acidic strength resulting to improved 1st and 2nd step dehydrogenation selectivity, followed by butadiene selectivity. The presence of Fe in the ternary catalyst added to its basic character that improves H_2 abstraction from both n-butane and butene intermediate hence improving the selectivity to butadiene. Co presence improves the activity due to its acidic character that helps improves butene intermediate desorption with an overall increase in the catalyst activity.

4.2.4 Temperature Programmed Reduction

This is used to determine the extent of catalytic active sites reducibility which strongly determines the catalyst activity. It is obtained using the reduction peak maxima as well as the amount of H_2 uptake (mmol/g). Peak position depends on calcination temperature as reported by Jermy et al [56] and the study shows that four peaks are involved corresponding to I (low), II (low-middle), III (high-middle) and IV (high) H_2 consumption temperature. The changes in reduction temperature are related to the state of NiO, Bi_2O_3 and support nanoparticles interaction. The 1st two peaks are related to NiO species, 3rd reduction peak is associated to Ni and Bi oxide species reduction and the final peak corresponds to isolated

bismuth oxide species. It has also been proven that NiO species are reduced mainly by n-butane and butene intermediate and are re-oxidized by lattice oxygen species without oxygenate formation. The presence of oxygen enhances Ni redox cycle and reduces coke deposition caused by excessive reduced Ni species. Fig. 4.11 shows the TPR profiles of the catalysts studied.
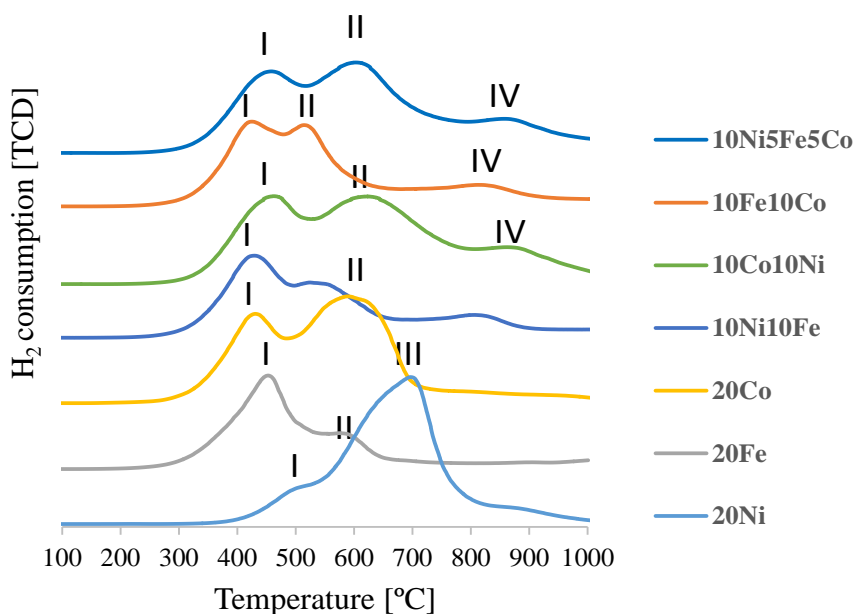
Fig.4.11: H_2-temperature programmed reduction for the main metal composition (mono, binary and ternary of Ni, Fe and Co) in main metal-Bi-O/Al$_2$O$_3$ catalyst.

From Fig.4.11 it can be seen that all the metal substituted catalysts showed lower reduction temperature peaks indicating the presence of more reducible species which agrees with the report by Ajayi et al [47] and is due to increased metal species interaction. Mechanism of dehydrogenation performed by redox cycle of sole main metal Ni species with Bi$_2$O$_3$ has been explained by Jermy et al [56]. Combined main metal species caused reducibility to

shifts to low and middle temperature region which has high concentration of oxygen species making reduction/oxidation very easy and hence favors oxygenate and cracking products formation. The results presented in Table 4.1 show high OC selectivity by all the mono, binary and ternary metals compared to the sole Ni catalysts.

4.3 Modeling of Reaction on Metal (Ni-Fe-Co) Oxide Species

Catalytic performance in oxidation reactions depends mainly on the acid/base character and the redox properties of the catalyst. Acidic/basic ratio of a catalyst is very important as it influence its hydrogen abstraction capability. Basicity of a catalyst is needed for alpha position methyl carbon hydrogen atom removal from n-butane. For selective butadiene production, the catalyst should have acidic character for adsorption of butene as well as basic sites for selective protons withdrawal. Metal species combination leads to adjusted acid and base sites preferable for highly selective oxidative dehydrogenation mainly due to the hierarchical nano-particle cohabitation of the main metal (Ni, Fe and Co) oxide, Bi_2O_3 and Al_2O_3 as represented in Fig. 4.12.
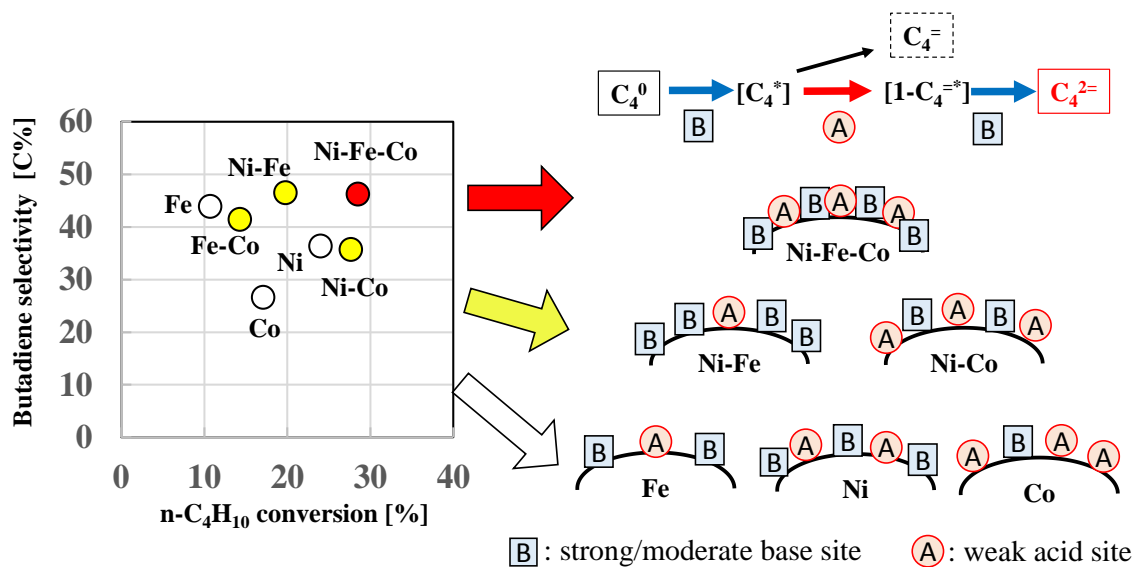
Fig. 4.12. Model of concerted metal effect on acid-base cohabitation over ternary metal (Ni-Fe-Co)-Bi oxide/ Al_2O_3 catalysts for oxidative dehydrogenation of n-butane (C_4^0) to butadiene ($C_4^{2=}$)

4.4 Ni-(Mo-W-Bi)-O Catalyst

Bi_2O_3 has been shown to be the main oxygen supplier (oxygen mobile oxide) for the Ni redox cycle in oxidative dehydrogenation of n-butane to butadiene using Ni-Bi-O/Al_2O_3 catalyst. In order to confirm that role, Mo and W were used to partially/totally substitute Bi from the standard catalyst (20Ni30Bi-O/Al_2O_3). The obtained result is tabulated in Table 4.5.

Table 4.5: Comparison of catalytic performance for various metal in Ni-(Bi, Mo, W)-O catalysts, Catalyst: 20 wt% Ni-30 wt% Bi-O/Al_2O_3, Reaction condition: 450 $^{\circ}$C, O_2/n-C_4H_{10} = 2.0

Catalyst main metal	30Bi	13.77Mo	30W	4.6Mo20Bi	9.18Mo10Bi	10W20Bi	20W10Bi
n-C_4H_{10} conversion [%]	**20.1**	**16.2**	**18.5**	**15.8**	**10.4**	**23.2**	**20.7**
Selectivity*1 [C%]							
DH	89.4	29.0	13.6	74.5	56.4	70.5	40.6
1-C_4H_8	**18.7**	**4.5**	**2.6**	**14.3**	**9.4**	**11.2**	**6.1**
BD	**43.3**	**13.2**	**4.5**	**34.3**	**26.5**	**36.9**	**20.8**
OC	9.2	16.4	18.8	10.8	9.4	12.9	20.0
PO	1.5	54.7	67.6	14.8	34.2	16.6	39.3
BD/DH %	48.5	45.6	32.9	46.1	47.0	52.3	51.3
(1-C_4H_8 + BD)/DH % *2	69.4	61.3	51.9	65.3	63.7	68.2	66.3
BD/(1-C_4H_8 + BD) % *3	69.8	74.4	63.3	70.6	73.9	76.8	77.3
BD yield	8.7	2.1	0.8	5.4	2.8	8.5	4.3

*1 DH: dehydrogenation, BD: butadiene, OC: oxygenate and the cracked, PO: partial oxidation.*2 selectivity at 1st step dehydrogenation, *3 selectivity at 2nd step dehydrogenation

Many researchers have reported the use of Bi-Mo promoted multicomponent oxide catalysts for the ODH of butenes to butadiene with good performance [65], [71]–[74]. Jermy et al [56] have shown that Bi/Ni atomic ratio required for an optimum performance of the standard catalyst is 0.42. Hence weight percent of both Mo and W were calculated while maintaining this ratio. From Table 4.5, it can be seen that the activities of Bi, Mo and W oxides is in the order Bi > W > Mo which is mainly due to the interaction of the active metal species (Ni) and the support (Al_2O_3) with the oxides. The oxides acts as oxygen

supplier for the oxidation/reduction cycle of the NiO. Bi_2O_3 compared to the other oxides also show a very high dehydrogenation selectivity of 89.4 [C%] with MoO_3 and WO_3 favoring partial oxidation and oxygenate and cracking products formation. This is due to their inability to cause efficient hydrogen abstraction from both n-butane and butene intermediate and that consequently leads to their very low butadiene selectivity. As evident from the reaction scheme in Fig.2.4, for partial oxidation as well as oxygenate and cracking routes, excess amount of oxygen is needed which is an indication that MoO_3 and WO_3 oxides supplied an uncontrolled oxygen amount that favor those reactions. Consequently, both catalysts of MoO_3 and WO_3 showed low 1st and 2nd step dehydrogenation selectivities.

Binary combination of the oxides (Bi-Mo and Bi-W) showed performance which is intermediate of the two extremes of the two oxides. Even though partial substitution of Bi with W showed an improved activity possibly due to the increased dispersion and enhanced accessibility to active sites but it still shows low dehydrogenation as well as butadiene selectivity. This shows that the redox cycle of the metal reduces with Bi substitution thereby increasing selectivity to undesired partial oxidation and cracking products.

The trend of Mo-Bi performance is as shown in Fig. 4.13. It is clear from the figure that butadiene selectivity decreases with increased loading of Mo. The conversion also decreases with a slight increase when Mo completely substitutes Bi. Conversely, partial oxidation increases with increasing Mo weight percent which clearly indicates that Ni-MoO_3 is more selective towards CO_x products formation. This is because of the interaction of the oxides which facilitates oxidation reaction in preference to dehydrogenation. This is also related to acidity/basicity character of the catalyst as will be revealed by NH_3/CO_2 temperature programmed desorption.

Butadiene overall selectivity and 1st and 2nd selectivities showed an almost constant trend with increase in Mo content.
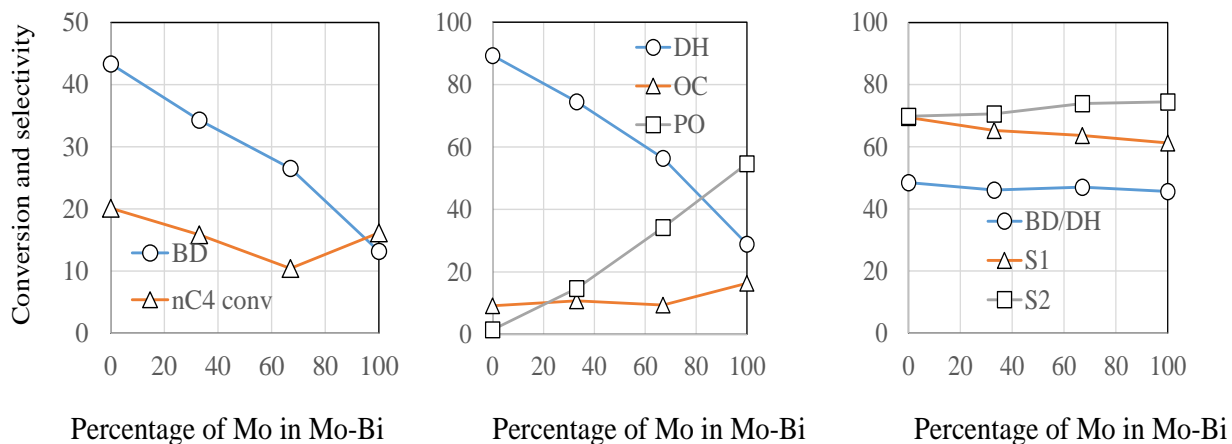
Fig.4.13. Comparison of catalytic performance for metal species in Ni-(Mo-Bi)-O catalyst, Catalyst: 20 wt% Ni-30 wt% Bi-O/Al_2O_3, Reaction condition: 450 °C, O_2/n-C_4H_{10} = 2.0

In order to study further, the influence of substituting Bi with Mo on the catalytic performance, O_2/n-C_4H_{10} molar ratio of 1, 2 and 4 were studied at a reaction temperature of 400°C as shown in Fig.4.14. Conversion increases clearly with increase in the molar ratio with a great increment in the case of only Bi and Mo. This increment is because excess oxygen activates n-butane feed especially for other competitive reactions of partial oxidation and oxygenate and cracking.
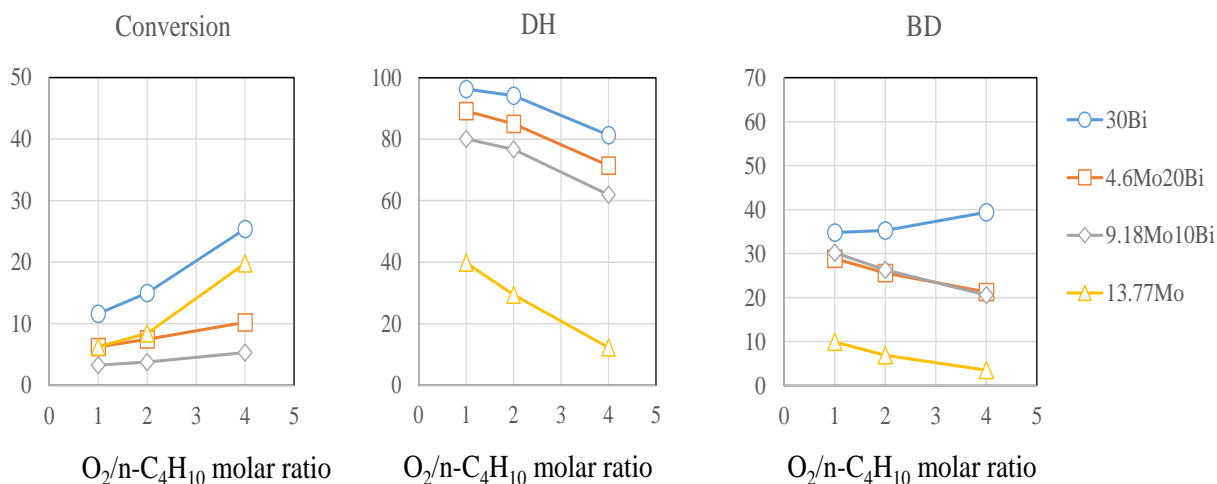
Fig.4.14. Comparison of catalytic performance for metal species in Ni-(Mo-Bi)-O catalyst, Catalyst: 20 wt% Ni-30 wt% Bi-O/Al_2O_3, Reaction condition: 400 ºC

Main dehydrogenation selectivity decreases with increase in O_2/n-C_4H_{10} molar ratio with 20Ni13.77Mo catalyst showing the greatest decrease of less than 20[C%] for O_2/C_4 = 4.0, which is due to decrease in catalyst selectivity towards dehydrogenation reaction and hence butadiene formation, on the contrary, partial oxidation increases. The trend of W-Bi performance shown in Fig. 4.15. It is clear from the figure that butadiene selectivity decreases with increased loading of W. The conversion increases with partial substitution of Bi with W indicating that there is an enhanced dispersion with W and Bi, this decreases for only W showing that Bi is more active than W which agrees with the report of Solsona et al [75] who reported that catalyst activity and reducibility decreases with increase in W content in Ni-W-O mixed metal oxide catalyst when used for the ODH of ethane. Conversely, partial oxidation increases with increasing W weight percent which clearly indicates that Ni-WO_3 is more selective towards CO_x products formation. This is because of the interaction of the oxides which facilitates oxidation (partial/complete) reaction in

preference to dehydrogenation. This is also related to acidity/basicity character of the catalyst as will be revealed by NH_3/CO_2 temperature programmed desorption.
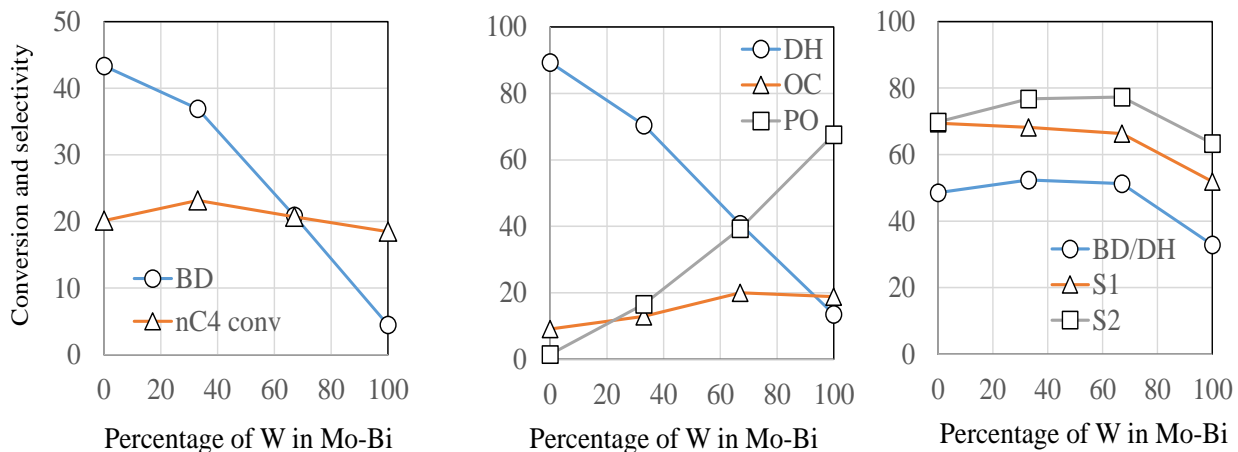
Fig.4.15. Comparison of catalytic performance for metal species in Ni-(W-Bi)-O catalyst, Catalyst: 20 wt% Ni-30 wt% Bi-O/Al_2O_3, Reaction condition: 450 ºC, O_2/n-C_4H_{10} = 2.0

Butadiene overall selectivity as well as 1st and 2nd selectivities showed an almost constant trend for partial W substitution but decreased further for only W. To study further the influence of substituting Bi with W on the catalytic performance, O_2/n-C_4H_{10} molar ratio of 1, 2 and 4 were studied at a reaction temperature of 400ºC as shown in Fig.4.16. Conversion increases clearly with increase in the molar ratio for all the substitution both partial and full even though Bi still maintained higher conversion at the higher O_2/C_4 ratio. This increment is because excess oxygen activates n-butane feed especially for other competitive reactions of partial oxidation and oxygenate and cracking.
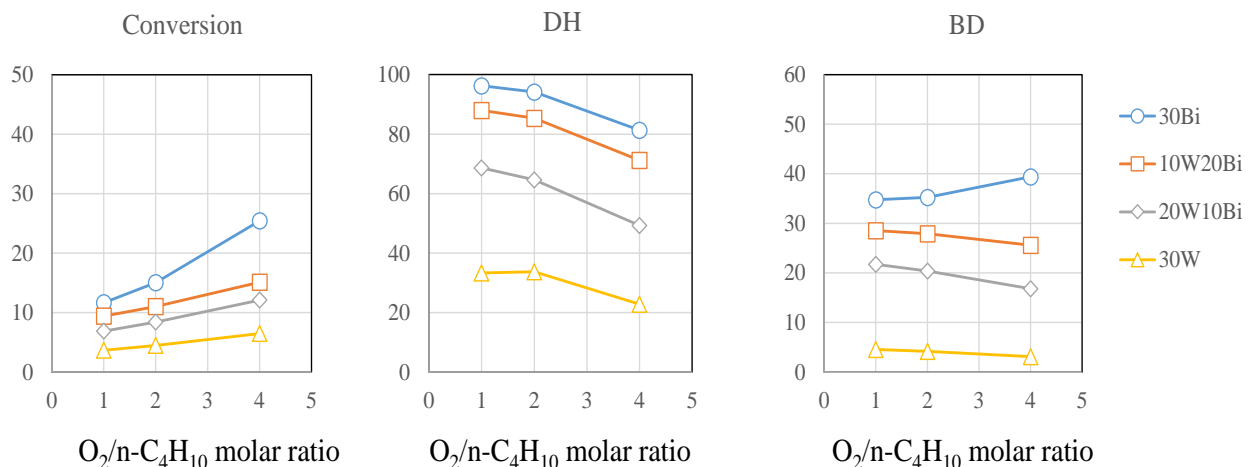
Fig.4.16. Comparison of catalytic performance for metal species in Ni-(W-Bi)-O catalyst, Catalyst: 20 wt% Ni-30 wt% Bi-O/Al$_2$O$_3$, Reaction condition: 400 ºC

It is clear from the figure that main dehydrogenation selectivity decreases with increase in molar ratio showing that as the amount of oxygen increases all the catalysts tends to show reduced dehydrogenation selectivity. The case of Ni-W shows a very low dehydrogenation selectivity which further decreases as the molar ratio increases but on the contrast favors partial oxidation as shown in Table 4.5. Butadiene selectivity also decreases for the W substitution with increase in the molar ratio which is clearly the opposite of Bi catalyst that showed an increase in BD selectivity with increase in molar ratio. For 30wt% W, BD selectivity remained at less than 10 [C%] for all the molar ratios studied, this shows that W-rich catalysts are not selective for dehydrogenation reactions but rather oxidation products. This agrees with the reports by Solsona et al [75], [76] which shows the reaction networks for W-rich catalysts clearly favoring CO$_x$ products.

4.4.1 Catalyst Characterization

4.4.1.1 Surface area and pore structure

The physical properties of all the catalysts (BET surface area and pore structure) are shown in Table 4.6. All the catalysts exhibited a lower specific surface area based on weight of catalyst but maintained almost a constant value when compared per gram of the Al_2O_3 support especially at total Bi substitution by Mo and W. The same trend is also observed in the pore surface area and pore volume. This agrees with the report by Abello et al [77], [78] and Heracleous et al [79]. The decrease in the specific surface area has been attributed to the partial coverage of the pores of the support by molybdenum species and also the presence of W heteroatom that prevents NiO crystallization as reported by Solsona et al [75]. It can also be concluded that the lower surface areas and pore volumes are due to pore volume shrinkage caused by metal oxide dispersion on the pore surface.

Table 4.6. Physical properties of 20wt% Ni-30wt% (Bi, Mo, W)-O/Al$_2$O$_3$ catalysts.

Catalyst (20wt% metal-30wt% Bi-O/Al$_2$O$_3$) Metal species	BET surface area		Pore surface area		Pore volume		Average pore diameter
	[m^2/g-catalyst]^a	[m^2/g-support]^b	[m^2/g-catalyst]^c	[m^2/g-support]^d	[cm^3/g-catalyst]^e	[cm^3/g-support]^f	[nm]^g
Al$_2$O$_3$	283	-	331	-	0.85	-	10.3
30Bi	136	218	157	251	0.38	0.61	9.6
13.77Mo	194	284	206	301	0.48	0.70	9.3
30W	182	297	210	342	0.47	0.76	8.9
4.6Mo20Bi	166	256	186	287	0.45	0.69	9.6
9.18Mo10Bi	187	281	212	319	0.48	0.71	9.0
10W20Bi	159	255	187	300	0.46	0.73	9.8
20W10Bi	174	281	199	322	0.49	0.80	9.9

[a]BET surface area, [c,e,g]Surface area, pore volume and average pore diameter measured using BJH isotherm, [b,d,f] Surface area and pore volume calculated by volume based Al$_2$O$_3$ using the equation: SA or PV×[Σ(MO$_x$/M)+100]/100, where M=metal wt%; MO$_x$=metal oxide wt%; SA = Surface Area; PV = Pore Volume.

4.4.1.2 X-ray Diffraction

The x-ray diffraction (XRD) patterns of the catalysts for Mo and W substituting Bi partially/totally are presented in Fig.4.17. XRD reveals the phases present in a catalyst, crystal sizes and crystal amount (crystallinity). Catalysts crystallinity are detected by the intensity of diffraction peaks (peak height) while peak width signifies crystal sizes.
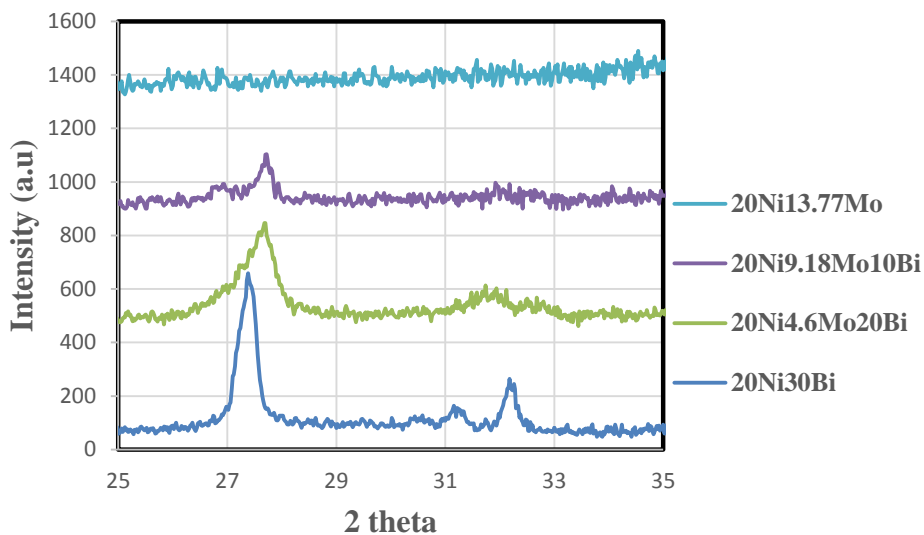
Fig.4.17a: X-ray diffraction pattern for Mo substituting Bi in Ni-Bi-O/Al$_2$O$_3$ catalyst
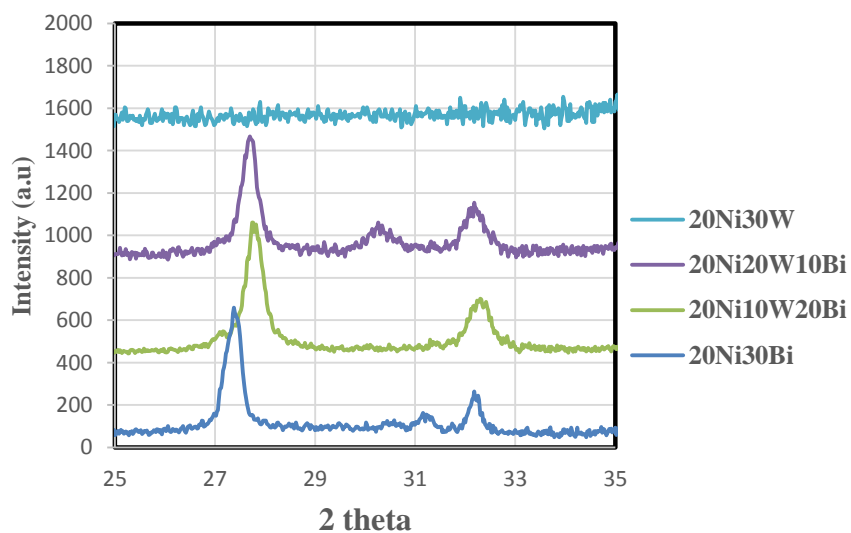
Fig.4.17b: X-ray diffraction pattern for the W substituting Bi in Ni-Bi-O/Al$_2$O$_3$ catalyst

Mo and W compounds mainly showed no diffraction lines due to their amorphous nature and also to some extent dispersion on the support which is in line with the report by Abello

et al that studied Mo/Al_2O_3 catalysts for the ODH of propane and revealed that the XRD of impregnated Mo catalysts only showed characteristic peaks of the support (Al_2O_3) [77]. No peaks of NiO was observed which agrees also with the report by Jermy et al [30]. Heracleous et al also reported that Mo-containing compounds were not detected by XRD due to their amorphous nature [34]. Mo and W catalysts showed almost no peaks for the case of full substitution indicating that no Bi_2O_3 is present and clearly reveals their amorphous nature and dispersion on the support. This also reveals that they showed lower selectivity to butadiene because of their inability to maintain the oxygen supply that stabilizes the redox cycle of the active specie. For the partial substitution, the peak height decreases with increasing Mo content indicating less crystallinity and the peak width broadens which signifies smaller crystal sizes. For W substitution, the peak height remains almost constant but shifted slightly from the β-Bi_2O_3 phase angle indicating the appearance of new crystalline phases which also agrees with the report by Solsona et al [76].

4.4.1.3 Temperature Programmed Desorption (NH_3/CO_2-TPD)

As explained earlier, these techniques are used to determine the acidity/basicity of the catalysts in which NH_3-TPD is for acidic character and CO_2-TPD for basic character. For the case of Mo and W substituting Bi, the amount of NH_3 and CO_2 desorbed are shown in Table 4.7. The amount of acid/base related to NH_3/CO_2 desorbed was deconvolved to three strengths of weak, moderate and strong acid/base.

Cracking and partial oxidation selectivities are favored by catalysts with higher acid sites with low dehydrogenation selectivity. Butadiene selectivity is favored by higher basicity or a relatively low acidic/basic ratio of a catalyst. Table 4.7 clearly shows that the acidity increases with increasing substitution with sole Mo/W having the highest acidity (acidic

sites) and on the contrary the basic character decreases. Fig. 4.18 shows the plot for NH_3/CO_2-TPD for the various substituted catalysts species.
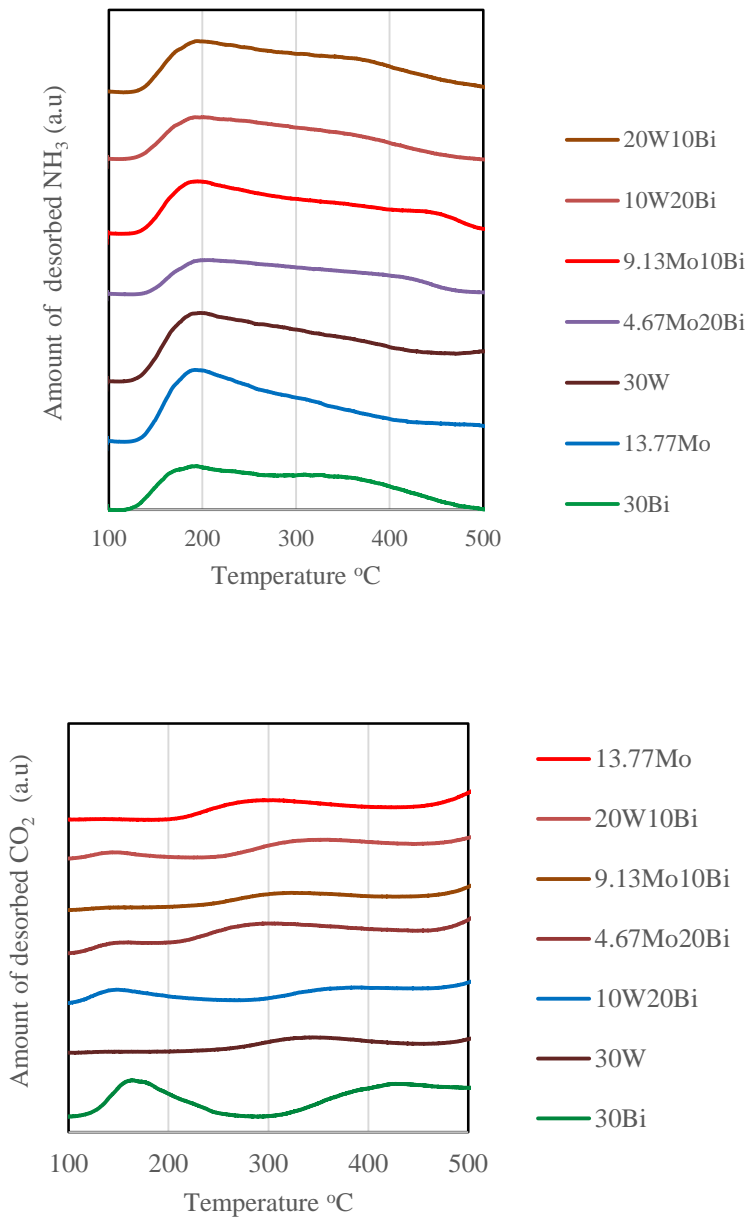
Fig. 4.18: NH_3 and CO_2-temperature programmed desorption for the substitution of Bi by Mo and W in 20Ni-30Bi-O/Al_2O_3 catalyst.

From Fig. 4.18, it is clear that the total substitution of Bi by Mo and W gave catalysts with the three regions of weak, medium and strong acid fractions which makes them have high acidity and their resulting relative low butadiene selectivity. Partial substitution of Mo/Bi and W/Bi catalysts showed an improved butadiene selectivity due to their weak and medium acid fractions only. The reverse is obtained for the case of CO_2-TPD as shown in Fig. 4.18, Mo and W rich catalysts show mainly regions of weak base fraction and moderate base fractions which further decreases as the substitution percentage increases. This further explains why Mo/W substituted showed a consistent decrease in dehydrogenation as well as butadiene selectivities.

Table 4.7: Metal species substitution temperature programmed analysis (NH_3 and CO_2-TPD)

Catalyst	CO$_2$-TPD Base amount [mmol/g][*1]				NH$_3$-TPD Acid amount [mmol/g][*2]			
	I	II	III	Total	I	II	III	Total
30Bi	0.073	-	0.173	0.246	0.115	0.169	0.097	0.381
13.77Mo	0.190	0.251	0.147	0.588	-	0.076	-	0.076
30W	0.380	0.208	0.183	0.771	0.003	0.058	-	0.061
4.6Mo20Bi	0.147	0.130	-	0.277	0.024	0.165	-	0.189
9.18Mo10Bi	0.186	0.097	0.072	0.355	0.004	0.071	-	0.075
10W20Bi	0.138	0.184	-	0.322	0.041	0.047	-	0.088
20W10Bi	0.294	0.191	-	0.485	0.017	0.078	-	0.095

[*1]: I (170 °C peak): weak base, II (300 °C peak): moderate base, III (400 °C peak): strong base [*2]: I (100-250 °C): weak acid, II (250-400 °C): moderate acid, III (>400 °C): strong acid

4.5 Role of Different Supports

The effects of different support on the activity (conversion) and butadiene selectivity in Ni-Bi-O metal species under the typical reaction condition: 450 °C, O_2/n-C_4H_{10} = 2.0 are shown in Table 4.8. The dehydrogenation products includes (DH: 1-butene, t-2-butene, cis-2-butene, 1,3-butadiene: BD), oxygenate formation and cracking products (OC: carboxylic acids and lighter olefins), and partial oxidation (PO: CO and H_2). The other gases CO_2, CH_4, C_2H_6 and C_3H_8 were also detected but in negligible quantities.

Table 4.8: Comparison of catalytic performance for various metal in Ni-Bi-O catalysts, Catalyst: 20 wt% Ni-30 wt% Bi-O/Different supports, Reaction condition: 450 °C, O_2/n-C_4H_{10} = 2.0

Catalyst supports	Al_2O_3	SiO_2	Mesocarbon	Silicalite	MCM41	MSU foam
n-C_4H_{10} conversion [%]	**24.0**	**15.7**	**24.5**	**12.4**	**12.9**	**26.1**
Selectivity*[1] [C%]						
DH	75.1	87.8	35.5	71.0	82.3	86.6
1-C_4H_8	**15.7**	**28.3**	**14.0**	**30.1**	**15.5**	**16.6**
BD	**36.4**	**35.5**	**12.7**	**18.0**	**44.2**	**50.8**
OC	23.7	8.2	64.5	24.0	10.4	11.8
PO	1.2	4.0	0.0	5.0	7.3	1.6
BD/DH %	48.5	40.4	35.7	25.4	53.7	58.7
(1-C_4H_8 + BD)/DH %*[2]	69.4	72.6	75.1	67.8	72.5	77.8
BD/(1-C_4H_8 + BD) %*[3]	69.8	55.6	47.6	37.4	74.1	75.4
BD yield	8.7	5.6	3.1	2.2	5.7	13.2

[1] DH: dehydrogenation, BD: butadiene, OC: oxygenate and the cracked, PO: partial oxidation,[2]selectivity at 1st step dehydrogenation, *[3] selectivity at 2nd step dehydrogenation

The order of the butadiene selectivity as the catalyst support is MSU foam > MCM41 >Al_2O_3 > SiO_2 > Silicalite > Mesocarbon, while n-butane conversion is MSU foam > Mesocarbon > Al_2O_3 > SiO_2 > MCM41=Silicalite. As for main reaction selectivity, DH selectivity Al_2O_3 has the highest followed by SiO_2 while mesocarbon has the least DH selectivity while the opposite trend is observed in OC selectivity, this shows that mesocarbon support serve as a more selective catalyst for cracking owing mainly due to its high acidic character and least contribution to active species redox cycle, it shows good conversion because of the availability of high surface area for good dispersion. Siliceous

materials (SiO$_2$, MSU foam and MCM41) on the other hand showed good butadiene

selectivity but have weak activity, this is due to their inability to activate n-butane and 1-

butene for proper conversion. Silicalite which is a polymorph of silica having a structure

analogous to zeolites also shows low conversion and butadiene selectivity. Additionally,

PO selectivity remains negligibly small in all the supports studied. This fact shows the Ni-

Bi-O metal oxides cannot perform efficiently without the support as catalyst for the ODH

of n-butane to butadiene. Fig. 4.19 depicts clearly the role of supports for the ODH reaction.

Fig.4.19. Comparison of catalytic performance for different supports species in Ni-Bi-O catalyst, Catalyst: 20 wt% Ni-30 wt% Bi-O/support, Reaction condition: 450 ºC, O$_2$/n-C$_4$H$_{10}$ = 2.0

Among the supports, butadiene selectivity over MSU foam in O$_2$/n-C$_4$H$_{10}$ ratio: 2.0 at 450

ºC was the highest (50.8 C%) with the highest n-butane conversion (26.1%) followed by

Al$_2$O$_3$, and MCM41. In particular Al$_2$O$_3$ support showed comparatively less tendency

towards oxygenate and partial oxidation product selectivity. Contrarily mesocarbon

support catalyst has a strong tendency toward OC: oxygenate formation followed by cracking (64.5 C%). Fig. 4.20 shows the main selectivities (DH, OC and PO) for the different supports studied.

Fig.4.20. Comparison of catalytic performance for different supports species in Ni-Bi-O catalyst, Catalyst: 20 wt% Ni-30 wt% Bi-O/support, Reaction condition: 450 °C, O_2/n-C_4H_{10} = 2.0

In Table 4.8, selectivity parameters inside dehydrogenation for selective conversion from n-butane to butadiene through 1-butene intermediate are also shown as (1-C_4H_8 + BD)/DH: selectivity at 1st step dehydrogenation, BD/(1-C_4H_8 + BD): selectivity at 2nd step dehydrogenation, and BD/DH: two step total selectivity, = (1-C_4H_8 + BD)/DH x BD/(1-C_4H_8 + BD), based on the concept for selective conversion from n-butane to butadiene shown in Fig. 3. B) 1-butene intermediate. The values of the parameters in Table 1 shows as for that for the different support system the values of the selectivity at 1st step dehydrogenation: (1-C_4H_8 + BD)/DH are similarly around 70%, while the values of the

71

selectivity at 2nd step dehydrogenation: BD/(1-C$_4$H$_8$ + BD) varies from 75.4% with MSU foam to 37.4% for silicalite which shows that the later has a very low tendency of enhancing H$_2$ abstraction from butene intermediate. From the result, MSU foam shows the highest value of the two step total selectivity: BD/DH (58.7%). Fig.4.21 shows clearly how the 1st and 2nd step dehydrogenation as well total selectivity varies from one support to the other.

Fig.4.21. Comparison of catalytic performance for different supports species in Ni-Bi-O catalyst, Catalyst: 20 wt% Ni-30 wt% Bi-O/support, Reaction condition: 450 ^{o}C, O$_2$/n-C$_4$H$_{10}$ = 2.0

4.6 Support Modification with Magnesia (MgO)

Acidic or basic property of the support controls the catalyst selectivity and reactivity due to their influence on reactants adsorption and product desorption. Catalyst with acidic support favor basic reactant adsorption and acidic product desorption, hence with controlled acidic character of support, a catalyst can be designed with higher selectivity in oxidative dehydrogenation reaction. Appropriate modification of support by MgO led to

an increase in the surface nickel active sites which could easily be reduced and also prevented the formation of $NiAl_2O_4$ spinel species [80].To confirm this, Al_2O_3 and SiO_2 supports that have shown good dehydrogenation tendencies were modified with magnesia (basic oxide) and the effect is as shown in Table 4.9.
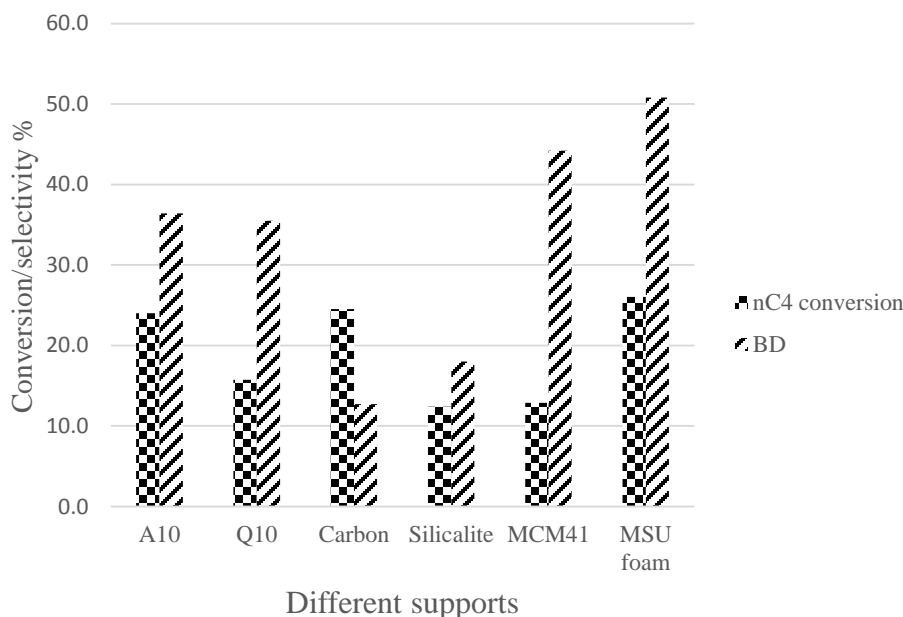
Table 4.9: Comparison of catalytic performance for various supports in Ni-Bi-O catalysts, Catalyst: 20 wt% Ni-30 wt% Bi-O/MgO-supports, Reaction condition: 450 ºC, $O_2/n-C_4H_{10}$ = 2.0

Metal species	20Ni30Bi	20Ni30Bi	10Ni5Fe5Co 30Bi	20Ni30Bi	20Ni30Bi	20Ni30Bi	10Ni5Fe5Co30Bi
Support	Al_2O_3	SiO_2	Al_2O_3	MgO-Al_2O_3	MgO-SiO_2	MgO-fumed SiO_2	MgO-fumed SiO_2
$n-C_4H_{10}$ conversion [%]	24.0	15.7	28.5	20.2	15.0	20.3	14.8
Selectivity*1 [C%]							
DH	75.1	87.8	66.9	65.0	84.3	87.2	89.8
$1-C_4H_8$	15.7	28.3	8.4	16.0	22.7	23.3	16.8
BD	36.4	35.5	46.3	28.6	34.2	40.8	42.8
OC	23.7	8.2	32.9	35.0	10.0	9.2	10.2
PO	1.2	4.0	0.2	0.0	5.7	3.6	0.0
BD/DH %	48.5	40.4	69.2	44.0	40.6	46.8	47.7
$(1-C_4H_8 +$ BD)/DH % *2	69.4	72.6	81.8	68.6	67.5	73.5	66.4
BD/$(1-C_4H_8 +$ BD) % *3	69.8	55.6	84.6	64.2	60.2	63.7	71.9
BD yield	8.7	5.6	13.2	5.8	5.1	8.3	6.3

From Table 4.9, it can be seen that modifying Al_2O_3 with MgO has no effect on the catalyst conversion as it is maintained at 20% but reduces its ability to selectively enhance butadiene production, main dehydrogenation selectivity decreases from 89.4 [C%] to 65.0 [C%] with a resulting increase in oxygenate and cracking products selectivity from 9.2 [C%] to 35.0 [C%], this shows that magnesia modification on Al_2O_3 affects its acidity/basicity ratio which determines its H_2 abstraction ability. MgO modification shows little effect on SiO_2 support in both its activity and butadiene selectivity, this shows that the catalyst acidity/basicity ratio is not affected by the modification. Similarly active metal species (Ni) redox cycle remain unaltered. MgO modification on fumed SiO_2 also shows no effect on the catalyst activity but increases butadiene selectivity, the non-porosity of the fumed silica makes the activity almost constant because there is no effect on metal species dispersion. Fig.22 shows the various catalysts activities and butadiene selectivity.
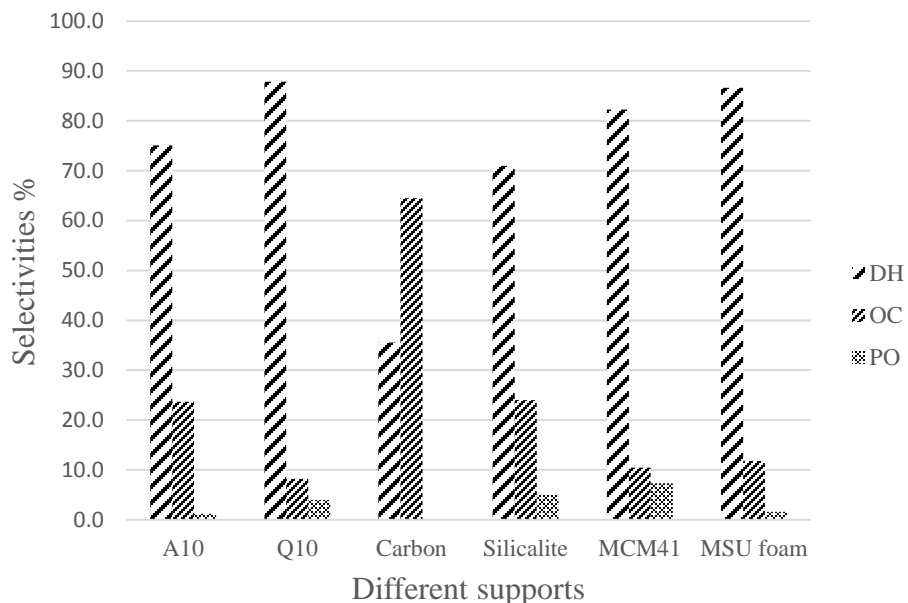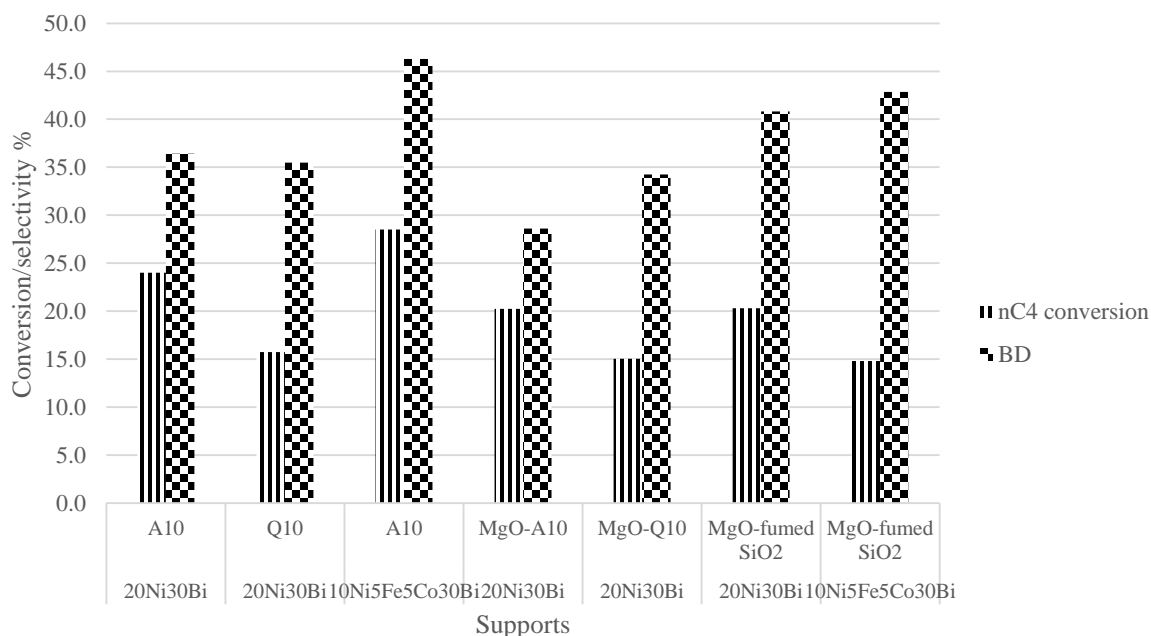
Fig.22. Comparison of catalytic performance for different MgO-supports species in Ni-Bi-O catalyst, Catalyst: 20 wt% Ni-30 wt% Bi-O/MgO-support, Reaction condition: 450 °C, $O_2/n\text{-}C_4H_{10} = 2.0$

Ternary metal composition (10Ni-5Fe-5Co)-30Bi supported on Al_2O_3 and MgO-fumed SiO_2 shows that the active metal species gives a better activity on the Al_2O_3 support due to the high surface area available for metal-support interaction compared to the MgO-fumed SiO_2 support which has less metal-support interaction and hence low activity. Main dehydrogenation selectivity of the ternary catalyst is higher with fumed SiO_2 than with Al_2O_3 which is because mild acidity of the latter act to increase oxygenate and cracking selectivity of the catalyst which is 32.9 [C%] as compared to 10.2 [C%] for the MgO-fumed SiO_2. Fig.4.23 clearly shows how the main reaction selectivities of DH, OC and PO varies from unmodified and modified catalysts.
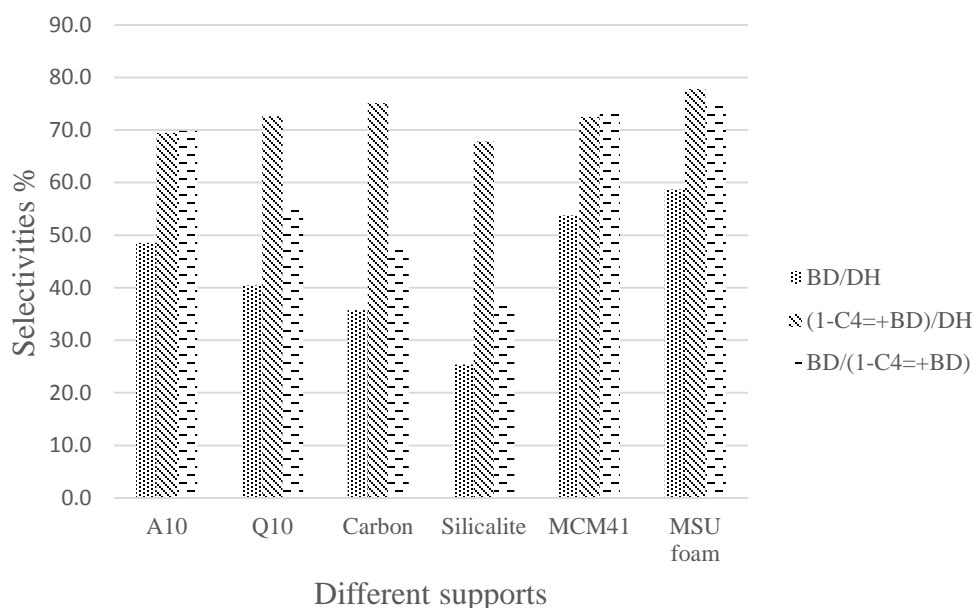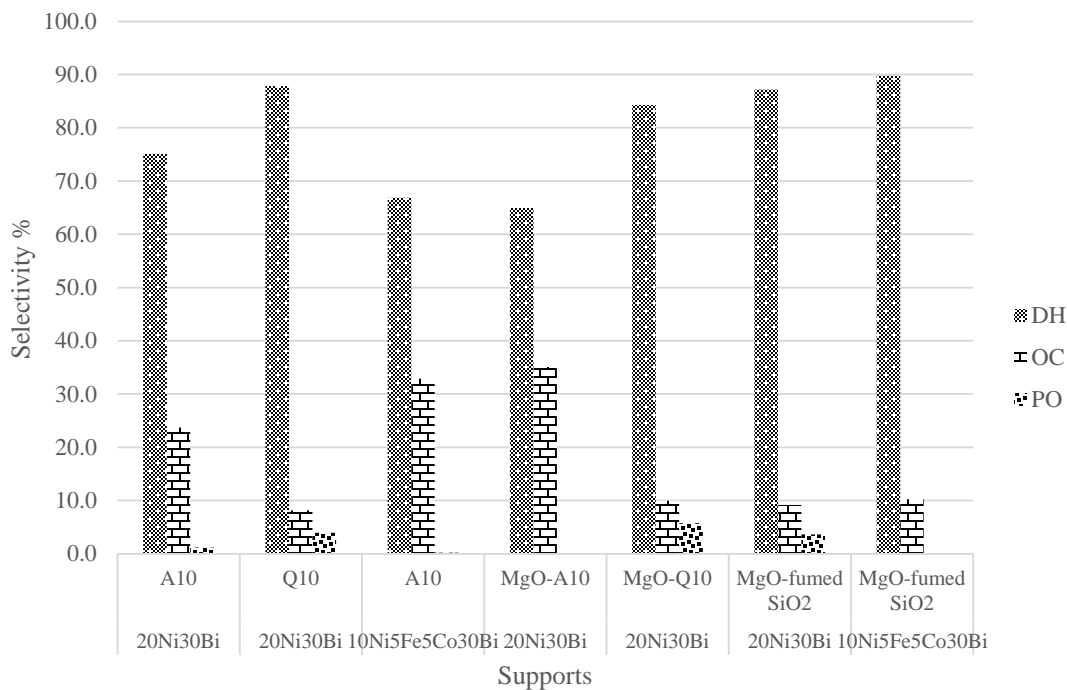
Fig.4.23. Comparison of catalytic performance for different MgO-supports species in Ni-Bi-O catalyst, Catalyst: 20 wt% Ni-30 wt% Bi-O/MgO-support, Reaction condition: 450 °C, $O_2/n-C_4H_{10} = 2.0$

All the catalysts showed low partial oxidation selectivity with SiO_2 and $MgO-SiO_2$ having slightly higher values. For all the catalysts studied, ternary metal combination supported on Al_2O_3 showed the highest overall selectivity as well as 1st and 2nd step dehydrogenation selectivities which is an indication of its ability to abstract H_2 from both n-butane and butene intermediate because of the cooperation of the active metal species (Ni, Fe, Co) in enhancing dispersion and reducibility. Fig.4.24 compares the inside selectivities of both the MgO modified and unmodified catalysts.
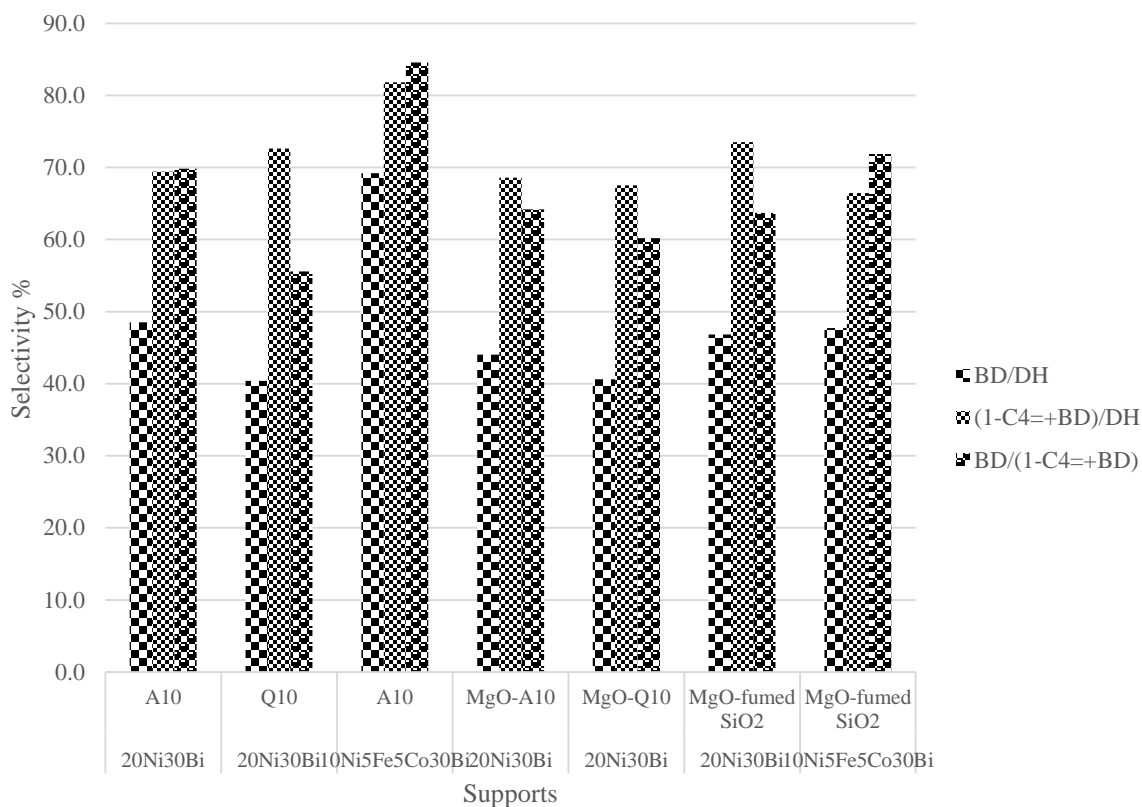
Fig.4.24. Comparison of catalytic performance for different MgO-supports species in Ni-Bi-O catalyst, Catalyst: 20 wt% Ni-30 wt% Bi-O/MgO-support, Reaction condition: 450 °C, O_2/n-C_4H_{10} = 2.0

4.6.1 Catalyst Characterization.

4.6.1.1 Surface area and pore structure

The BET surface area and pore structure of all the catalysts obtained from MgO support modifications are shown in Table 4.10. All the modified catalysts showed a lower specific surface area based on weight of catalyst compared to that of unmodified catalysts which indicates that basic oxide modification has negative effect on the catalysts surface area and the area further decreases with increasing basic oxide content which agrees with the report by Siddhartha et al [80]. The same trend is also observed in the pore surface area and pore

volume especially in the case of modified fumed SiO_2 support due to its non-porous nature. It can also be concluded that the lower surface areas and pore volumes are due to pore volume shrinkage caused by metal oxide dispersion as well as the strong interaction of MgO with the active metal phases which affects the nature of the metal crystallite.

Table 4.10. Physical properties of 20wt%Ni-30wt% Bi-O/MgO-supports catalysts.

Catalyst (20wt%metal-30wt%Bi-O/Al$_2$O$_3$) Metal species	BET surface area		Pore surface area		Pore volume		Average pore diameter
	[m^2/g-catalyst]^a	[m^2/g-support]^b	[m^2/g-catalyst]^c	[m^2/g-support]^d	[cm^3/g-catalyst]^e	[cm^3/g-support]^f	[nm]^g
Al$_2$O$_3$	283	-	331	-	0.85	-	10.3
20Ni30Bi	136	218	157	251	0.38	0.61	9.6
10Ni5Fe5Co	165	263	184	294	0.41	0.65	8.8
Ni/MgO-Al$_2$O$_3$	124	197	146	232	0.37	0.58	10.1
Ni/MgO-SiO$_2$	135	215	141	225	0.45	0.71	12.6
Ni/MgO-fumed SiO$_2$	89	142	87	138	0.56	0.90	26.0
NiFeCo/MgO-fumed SiO$_2$	77	122	75	119	0.60	0.96	32.3

^{a}BET surface area, ^{c,e,g}Surface area, pore volume and average pore diameter measured using BJH isotherm, ^{b,d,f} Surface area and pore volume calculated by volume based Al$_2$O$_3$ using the equation: SA or PV×[Σ(MO$_x$/M)+100]/100, where M=metal wt%; MO$_x$=metal oxide wt%; SA = Surface Area; PV = Pore Volume.

4.6.1.2 X-ray Diffraction

The x-ray diffraction (XRD) patterns of the catalysts having MgO modified supports are shown in Fig.4.25. As discussed in the earlier part, the phases present in a catalyst, crystal

sizes and crystal amount (crystallinity) are revealed by XRD. The crystallinity of the catalysts are detected by the intensity of diffraction peaks (peak height) and crystal sizes are determined by the peak width.
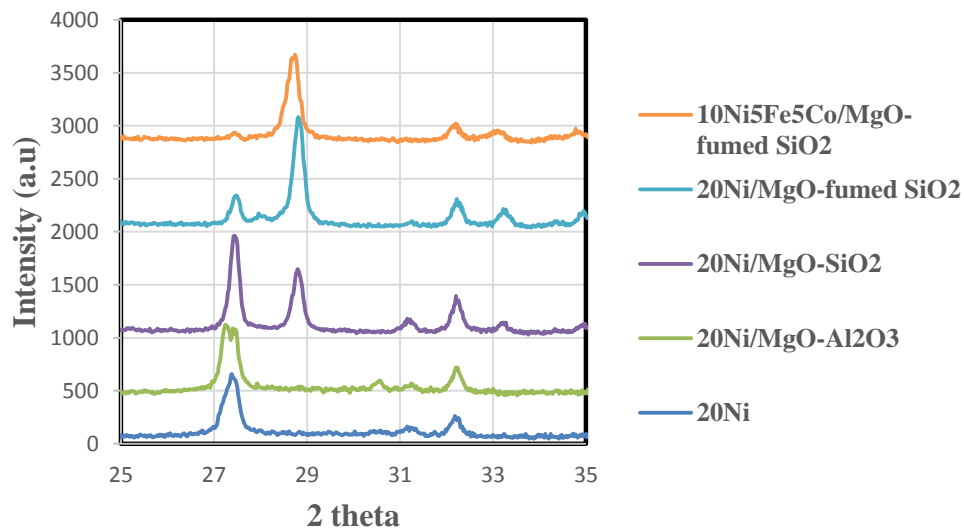
Fig.4.25: X-ray diffraction pattern for the MgO modifying supports Ni-Bi-O/supports catalyst

From Fig. 4.25, it is clear that MgO modification on Al_2O_3 support reduces the β-Bi_2O_3 phase (active phase for butadiene formation) but in contrary increases the α-Bi_2O_3 phase. This explains why BD selectivity decreases for the modified support relative to the unmodified, because the Ni redox cycle is not stabilized due to the inefficient O_2 supply by Bi_2O_3. For the case of MgO-fumed SiO_2 support, Bi_2O_3 peak reduces and almost disappeared for the case of ternary metals, this clearly indicates that the phase becomes highly dispersed in the support phase and only the peaks corresponding to the supports are observed.

4.6.1.3 Temperature Programmed Desorption (NH₃/CO₂-TPD)

The amount of NH_3 and CO_2 desorbed for the case of MgO modified supports catalysts are presented in Table 4.11. The amount of acid/base related to NH_3/CO_2 desorbed was deconvolved to three strengths of weak, moderate and strong acid/base. Fig. 4.26 shows the plot for NH_3/CO_2-TPD for the various substituted catalysts species.
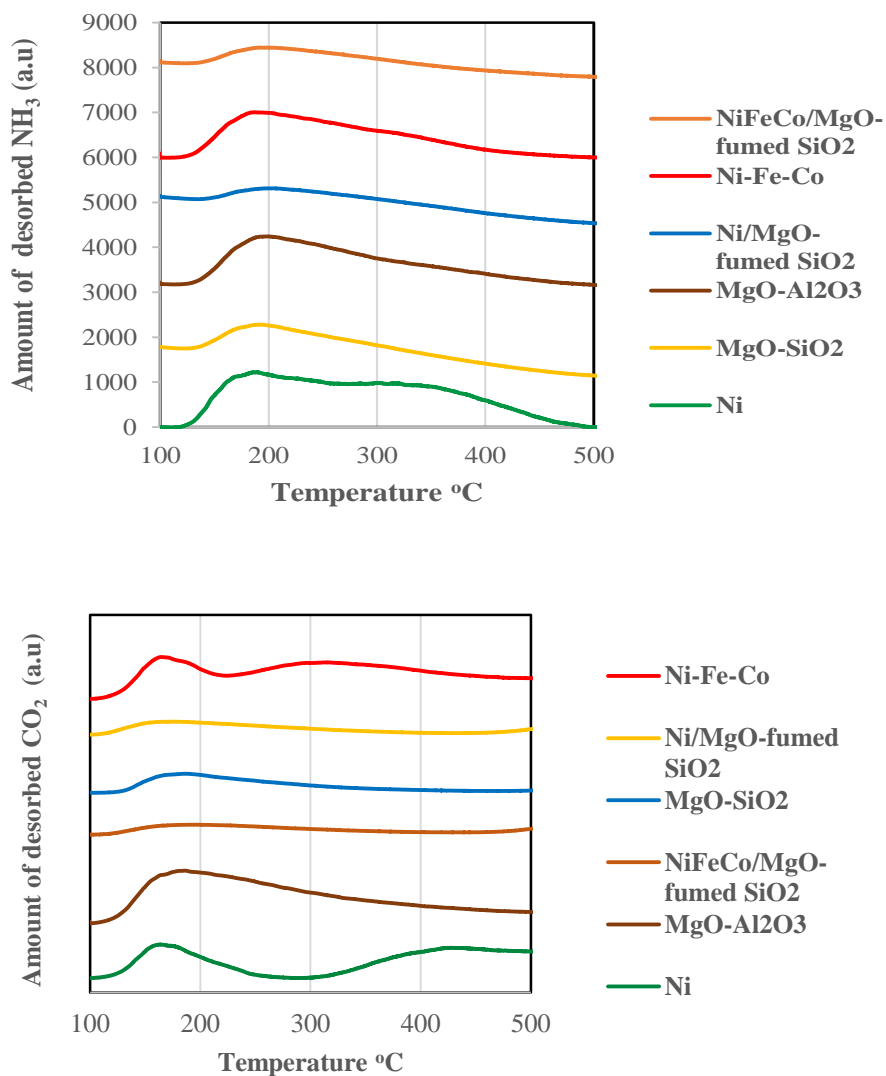
Fig. 4.26: NH_3 and CO_2-temperature programmed desorption for the MgO support modifications in Ni-Bi-O/supports catalysts.

From Fig. 4.26, it can be concluded that MgO modification of the supports lead to a reduction in the catalyst acidity which resulted in an increase in the BD selectivity of the catalysts due to the increased in H_2 abstraction from both n-butane and butenes intermediate by the catalysts. The case of CO_2-TPD for the catalysts did not really show a clear improvement especially for the case of SiO_2 and fumed SiO_2 supports which conclusively indicates that MgO modification on the supports plays little role in the catalyst basic character, but improves on overall the basic/acidic ratio which is required for high BD selectivity.

Table 4.11: MgO support modifications temperature programmed analysis (NH_3 and CO_2-TPD)

Catalyst	CO₂-TPD Base amount [mmol/g]*1				NH₃-TPD Acid amount [mmol/g]*2			
	I	II	III	Total	I	II	III	Total
20Ni	0.073	-	0.173	0.246	0.115	0.169	0.097	0.381
10Ni5Fe5Co	0.114	0.234	-	0.348	0.131	0.077	0.052	0.260
Ni/MgO-Al₂O₃	0.174	-	-	0.174	0.234	0.086	0.034	0.354
Ni/MgO-SiO₂	0.076	-	-	0.076	0.069	0.015	0.004	0.088
Ni/MgO-fumed SiO₂	0.058	-	-	0.058	0.041	0.027	0.006	0.074
NiFeCo/MgO-fumed SiO₂	0.047	0.021	-	0.068	0.055	0.015	0.004	0.074

*1: I (170 °C peak): weak base, II (300 °C peak): moderate base, III (400 °C peak): strong base *2: I (100-250 °C): weak acid, II (250-400 °C): moderate acid, III (>400 °C): strong acid

4.7 Stability Test of Catalysts with Good Performance

Catalysts with the best performance under the various groups studied were subjected to stability test under standard conditions: 450 °C, $O_2/n\text{-}C_4H_{10} = 2.0$, in order to test their suitability for long period of time usage (10 h time on stream). This is in order to confirm whether they have satisfied the three properties that determine catalyst performance (Activity, selectivity and stability). The catalysts are:

4.7.1 20Ni-30Bi-O/Al₂O₃ catalyst

This catalyst is highly stable under both reaction and regeneration conditions which is mainly due to the cohabitating nature of its oxides which greatly enhanced the redox cycle and present great resistance to most forms of deactivation. Also, the support used has high surface area and is very stable under the temperature range for most catalytic reactions. Fig. 4.27 shows the stability diagram of the catalyst showing how the conversion, butadiene selectivity, main selectivities as well as inside selectivities varies with time on stream.
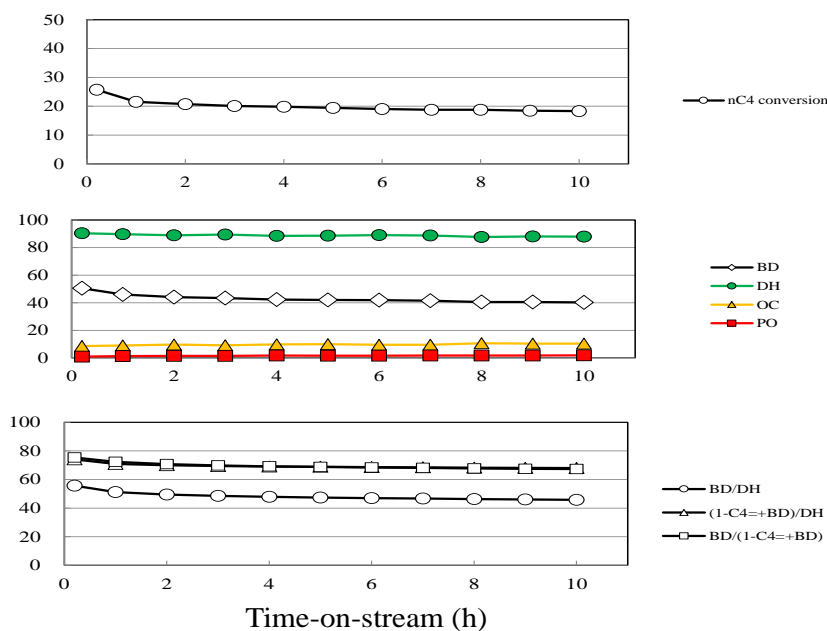
Fig.4.27. Stability of 20Ni-30Bi-O/Al₂O₃ catalyst with time-on-stream

82

From the Fig.4.27, it can be seen that the catalyst activity remain stable around 20% even after the 10h reaction time. Butadiene selectivity, main dehydrogenation selectivity, oxygenate and cracking selectivity and partial oxidation selectivity remained at 40[C%], 90[C%], <10[C%] and negligible respectively. Similarly, 1st and 2nd dehydrogenation selectivity steps also remained at constant values for the whole period. This can be attributed to the efficient redox cycle system by the active species of the catalyst as well as an efficient metal-support interaction as well as good usage of gas phase oxygen to burn off carbon deposits that may otherwise lead to coking thereby deactivating the catalyst by poisoning its active sites.

4.7.2 20Ni-30Bi-O/MSU foam

The stability diagram of the catalyst is shown in Fig.4.28, the catalyst shows a continuous decline in activity from almost 40% to less than 20% after the 10h time on stream. This is a strong indication that the catalyst has no stable performance hence it deactivates fast.
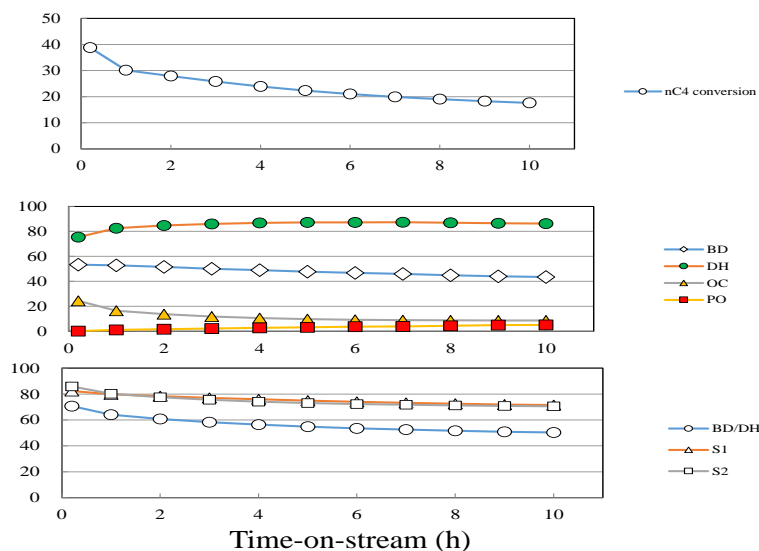
Fig.4.28.   Stability of 20Ni-30Bi-O/MSU foam catalyst with time-on-stream

The catalyst has the same metal species composition as 20Ni-30Bi-O/Al$_2$O$_3$, the only difference is the type of support. This clearly shows that metal-support interaction including dispersion and reducibility of active species on the support as well as the acidic/basic character of the metal/support plays a great role in the overall catalytic performance. MSU foam is a meso structured silica having a very high surface area, hence supposed to show great dispersion of active species but pore blockage by unwanted materials lead to the decline in performance. The catalyst showed an improved main dehydrogenation selectivity but a declining butadiene selectivity.

4.7.3 20Ni-30Bi-O/MgO-fumed SiO$_2$

The performance of the catalyst after 10h time on stream is shown in Fig.4.29, it can be seen that the catalytic activity declines continuously from almost 35% to less than 10%. This indicates clearly that the catalyst is not very stable because it deactivates relatively fast.
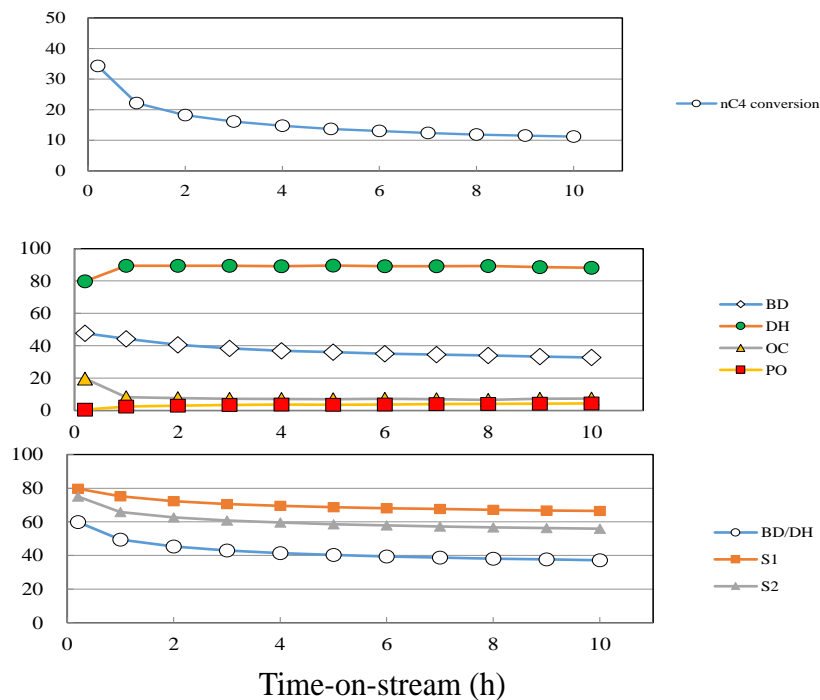
Fig.4.29. Stability of 20Ni-30Bi-O/MgO-fumed SiO$_2$ catalyst with time-on-stream

Fumed-SiO$_2$ support is a finely divided non-porous and highly pure silica powder with particle size in the range of 40 to 50 nm and surface area of about 200 to 400 m^2/g. It is classified as an acidic oxide which is not required for dehydrogenation ability of a catalyst. MgO modification reduces the acidity thereby enhancing the catalyst selectivity and reactivity, due to its strong influence on reactants adsorption and product desorption. This is why the catalyst showed an improved main dehydrogenation selectivity but a decline in butadiene selectivity, due to poor interaction of the active species with the support that affects the redox cycle.

4.7.4 10Ni-5Fe-5Co-30Bi-O/MgO-fumed SiO₂

Fig. 4.30 shows the stability diagram of the catalyst, it shows a continuous reduction in activity from almost 30% to 10% after the 10h time on stream. This is a due to its fast deactivation indicating its low stability. The catalyst has the same support as 20Ni-30Bi-O/MgO-fumed SiO₂ hence followed the same trend in most of the selectivities (main and inside), the only difference is in the active metal species composition, where 20Ni is replaced with 10Ni-5Fe-5Co, this acts only to stabilize the butadiene selectivity relative to the 20Ni catalyst because the combination improves redox cycle due to the ability of Fe to switch easily from Fe^{2+} to Fe^{3+} and vice versa.
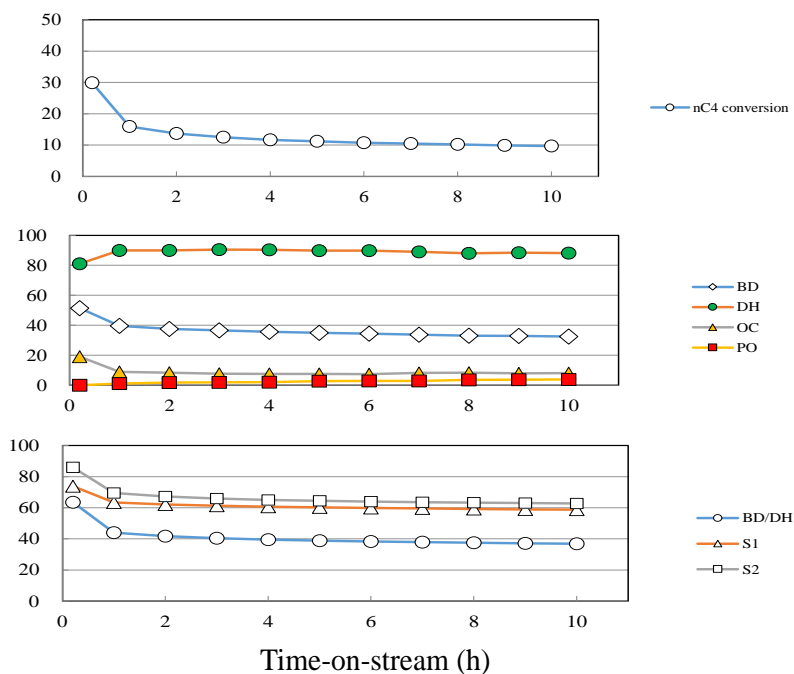
Fig.4.30.   Stability of (10Ni-5Fe-5Co)-30Bi-O/MgO-fumed SiO₂ catalyst with time-on-stream

86

4.8 KINETIC MODELLING OF n-BUTANE ODH OVER 10Ni5Fe5Co30Bi/Al$_2$O$_3$

4.8.1 Model Development

A good kinetic model should contain low reaction steps as well as kinetic parameters but sufficient to describe the basic features of the reaction under study [81],[82]. Oxidative dehydrogenation of n-butane to butadiene has many reactions steps including consecutive and side reactions, this were simplified by lumping all cracked products which are methane, ethane, ethene, propane and propene as one entity. Also, butene isomers (1-butene, cis-2-butene and trans-2-butene) were also considered as one entity (C$_4$ olefin). Partial oxidation scheme that produces CO and H$_2$ were detected in very small quantities, hence neglected.

Scheme one was 1st proposed which involves dehydrogenation and direct cracking of paraffin (n-butane) as shown below;

$$C_4H_{10} + \tfrac{1}{2}\,O_2 \xrightarrow{\;k1\;} C_4H_8 + H_2O + \tfrac{1}{2}\,O_2 \xrightarrow{\;k2\;} C_4H_6 + H_2O$$

$$\searrow k3$$

$$\text{Cracking products}$$
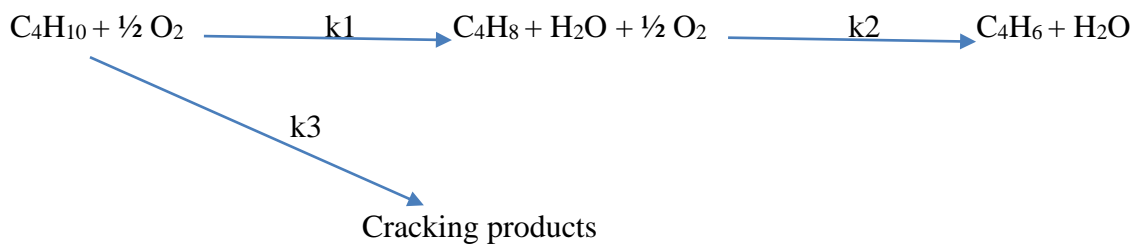
Scheme one: Dehydrogenation and Cracking of n-butane

This was later modified after it failed to give reasonable parameter estimation. Scheme two was later developed which makes more sense due to the fact that it is easier to crack olefins than paraffins especially at the low ODH reaction temperature of 350 to 450°C.

$$C_4H_{10} + \tfrac{1}{2} O_2 \xrightarrow{\quad k1 \quad} C_4H_8 + H_2O + \tfrac{1}{2} O_2 \xrightarrow{\quad k2 \quad} C_4H_6 + H_2O$$

$$\xrightarrow{\quad k3 \quad}$$
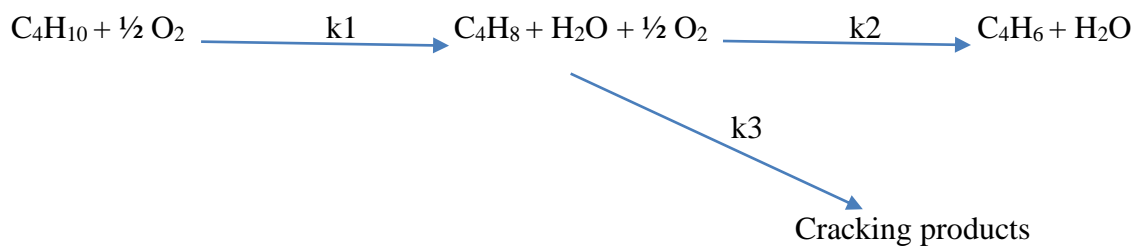
Cracking products

Scheme two: Dehydrogenation of n-butane and cracking of butene intermediate

Table 4.12: Product distribution of n-butane ODH over ternary metal catalyst

Temp (°C)	Contact time (τ)	Weight fraction					Conv [X]
		y_o	y_{nb}	y_{bd}	y_{bu}	y_{cr}	
350	52.71	1.00	0.9658	0.0057	0.0310	0.0006	0.0342
	80.82	1.00	0.9441	0.0110	0.0444	0.0017	0.0560
	105.41	1.00	0.9223	0.0163	0.0578	0.0028	0.0777
	133.52	1.00	0.9207	0.0178	0.0571	0.0037	0.0794
	158.12	1.00	0.9190	0.0193	0.0563	0.0045	0.0810
375	52.71	1.00	0.9513	0.0097	0.0372	0.0018	0.0487
	80.82	1.00	0.9183	0.0223	0.0544	0.0044	0.0817
	105.41	1.00	0.8853	0.0348	0.0715	0.0069	0.1147
	133.52	1.00	0.8808	0.0403	0.0698	0.0077	0.1193
	158.12	1.00	0.8762	0.0457	0.0681	0.0085	0.1238
400	52.71	1.00	0.9152	0.0235	0.0557	0.0046	0.0848
	80.82	1.00	0.8925	0.0352	0.0650	0.0061	0.1076
	105.41	1.00	0.8697	0.0468	0.0743	0.0076	0.1303
	133.52	1.00	0.8544	0.0708	0.0617	0.0112	0.1457
	158.12	1.00	0.8390	0.0947	0.0491	0.0148	0.1610
	52.71	1.00	0.8853	0.0404	0.0644	0.0083	0.1147

	80.82	1.00	0.8614	0.0586	0.0673	0.0109	0.1386
	105.41	1.00	0.8375	0.0767	0.0702	0.0134	0.1625
425	133.52	1.00	0.8331	0.0901	0.0559	0.0188	0.1670
	158.12	1.00	0.8286	0.1035	0.0415	0.0241	0.1714

The experimental results were modelled using power law model and based on the assumption that catalyst deactivation is negligible due to the presence of gas phase oxygen as a co-feed and for the fact that the reactor is a fixed bed, the total reaction rate for each chemical specie i expressed by r_i was evaluated by adding up all the reaction rates at every step j in which the specie i is involved.

$$r_i = \frac{dF_i}{dw} \dots\dots\dots\dots\dots\dots\dots\dots\dots\dots\dots\dots\dots\dots\dots\dots\dots\dots\dots 1$$

$$F_i = \upsilon\, C_i \text{ and } \tau = w/F_{Tm}$$

Also, for a fixed bed reactor, the concentration of species can be calculated using the expression as reported by Tazul et al [83]

$$C_i = \frac{y_i\, F_{Tm}}{MW_{i\; x\, \upsilon}} \dots\dots\dots\dots\dots\dots\dots\dots\dots\dots\dots\dots\dots\dots\dots\dots\dots..2$$

Hence after simplifications, we have the following sets of mole balance (differential equations) obtained from scheme two.

Rate of disappearance of n-butane, r_{nB};

$$-r_{nB} = -\frac{dY_{nB}}{d\tau} = k_1\, C_{nB}^{1/2} * MW_{nB} \dots\dots\dots\dots\dots\dots\dots\dots\dots\dots\dots.3$$

Rate of appearance and disappearance of butene intermediate, r_{Bu};

$$r_{Bu} = \frac{dYBu}{d\tau} = (k_1\,C_{nB}^{1/2} - k_2\,C_{Bu}^{1/2} - k_3\,C_{Bu}^{1/2}\,)*\,MW_{Bu} \ldots\ldots\ldots\ldots\ldots\ldots.4$$

Rate of appearance of butadiene, r_{Bd};

$$r_{Bd} = \frac{dYBd}{d\tau} = k_2\,C_{Bu}^{1/2}*\,MW_{Bd} \ldots\ldots\ldots\ldots\ldots\ldots\ldots\ldots\ldots\ldots\ldots\ldots\ldots\ldots\ldots\ldots.5$$

Rate of appearance of cracked products, r_{Cr};

$$r_{Cr} = \frac{dYCr}{d\tau} = k_3\,C_{Bu}^{1/2}*\,MW_{Cr} \ldots\ldots\ldots\ldots\ldots\ldots\ldots\ldots\ldots\ldots\ldots\ldots\ldots\ldots\ldots.6$$

Where Y_i is the mass fraction of specie i, C_i is the concentration of specie i, MW_i is the molecular weight of specie i.

w is the catalyst weight which was varied from 0.15 to 0.45 g while maintaining constant total mass flow rate (F_{TM}) into the reactor. The activation energy of each reaction step j, E_j is related to the temperature dependent rate constant by the Arrhenius equation.

$$k_j = k_{oj}\,\exp\,[\frac{-Ej}{RT}] \ldots\ldots\ldots\ldots\ldots\ldots\ldots\ldots\ldots\ldots\ldots\ldots\ldots\ldots\ldots.7a$$

k_{oj} is the pre-exponential factor. Re-parameterization of the Arrhenius equation helps in reducing parameter interaction during modelling as reported in many literatures [67], [84], [85]. Hence we have;

$$k_{ij} = k_{0,ij}\,\exp\,[\frac{-Eij}{R}\,(\frac{1}{T} - \frac{1}{T0})] \ldots\ldots\ldots\ldots\ldots\ldots\ldots\ldots\ldots\ldots\ldots.7b$$

Where T_0 is the average temperature of the experimental runs temperature.

4.8.2 Model Assumptions

- Mass transfer limitation is negligible

- Negligible catalyst deactivation

- Excess gas phase oxygen, hence negligible conversion

- Effectiveness factor is unity

- Model assumes only catalytic conversion.

4.8.3 Determination of Model Parameters and Model Discrimination

The kinetic parameters were estimated using non-linear regression analysis. For model evaluation, mole balance equations were combined with temperature dependent specific reaction rate constants with the concentration of various species expressed in terms of weight fraction as obtained from the online GC. The resulting ordinary differential equations were then solved numerically in conjunction with a least square fitting of the experimental n-butane oxidative dehydrogenation data obtained from the fixed bed reactor. MATLAB ODE45 subroutine (Runge-Kutta-Gill method) was used for parameter estimation. For accurate and reliable model and model parameters, the experiments were conducted at four different reaction temperatures (350, 375, 400 and 425ºC) and five different contact times based on catalyst weight of 0.15, 0.23, 0.30, 0.38 and 0.45 g. The criteria for model evaluation is based on the fact that all the rate parameters agrees with physical principles and the optimization criteria is based on minimum sum of squares defined as;

$$SS= \sqrt{\sum_{i=1}^{n}(Ci, \exp - Ci, mod)^2} \quad \dots\dots\dots\dots\dots\dots\dots\dots\dots\dots\dots\dots\dots.8$$

Model discrimination was based on;

- Lower sum of squares

- Correlation coefficient closer to one

- Lower confidence intervals for the estimated parameters.

The values of the model parameters together with their corresponding 95% confidence intervals are presented in Table 4.13. It can be seen from the table that the estimated apparent activation energies of 2nd step dehydrogenation and cracking are 68.8 and 88.5 kJ/mol respectively. This was expected because the ternary metal catalyst ($10Ni5Fe5Co30Bi/Al_2O_3$) is more selective towards dehydrogenation than cracking, hence the lower activation energy.

Table 4.13: Estimated values of kinetic parameters at 95% confidence intervals

Parameters	Values	Model discrimination	Values
k_1^o (mol/gcat.min)	0.857 ± 0.014	Correlation coefficient, R^2	0.9993
k_2^o (mol/gcat.min)	1.93 ± 0.089	Sum of squares, SS	0.0076
k_3^o (mol/gcat.min)	0.198 ± 0.048		
E_1 (kJ/mol)	34.4 ± 2.42		
E_2 (kJ/mol)	68.8 ± 7.57		
E_3 (kJ/mol)	88.5 ± 41.16		

n-C4 conversion was plotted against contact time as shown in Fig.4.31 for both the experimental and model predicted values. It can be seen that the model agrees reasonably to the experimental data especially at low reaction temperatures and low conversion which is due to the fact that at higher temperatures and higher conversions, more complicated model is required to clearly represents the data as this one is a simplified model that lumps many products together.
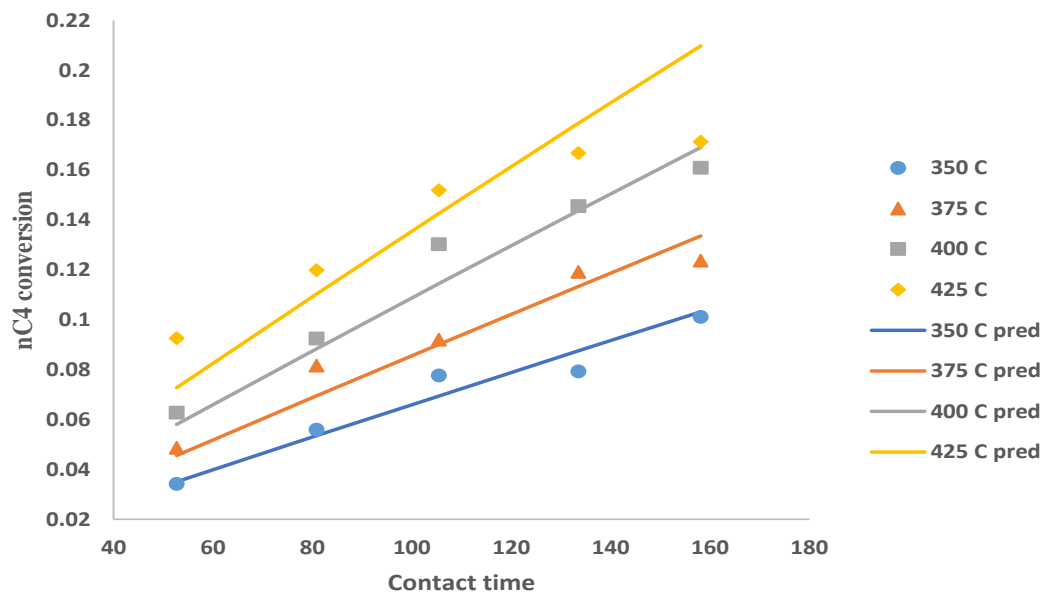
Fig. 4.31: Conversion of n-butane against contact time for both experimental and model predicted.

Also, Butadiene and cracking products mass fractions were also compared for the experimental and model predicted case and it shows a good fitting as shown in Figs. 4.32a and 4.32b respectively, which also validates the developed model.
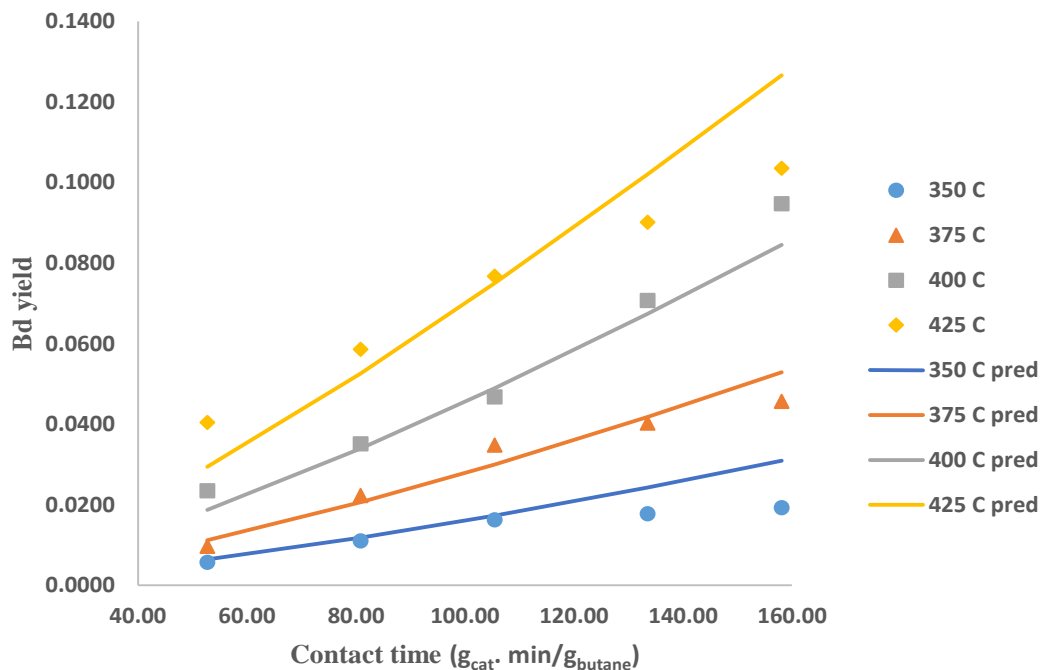
Fig. 4.32a: Experimental vs model predicted values for butadiene yield.
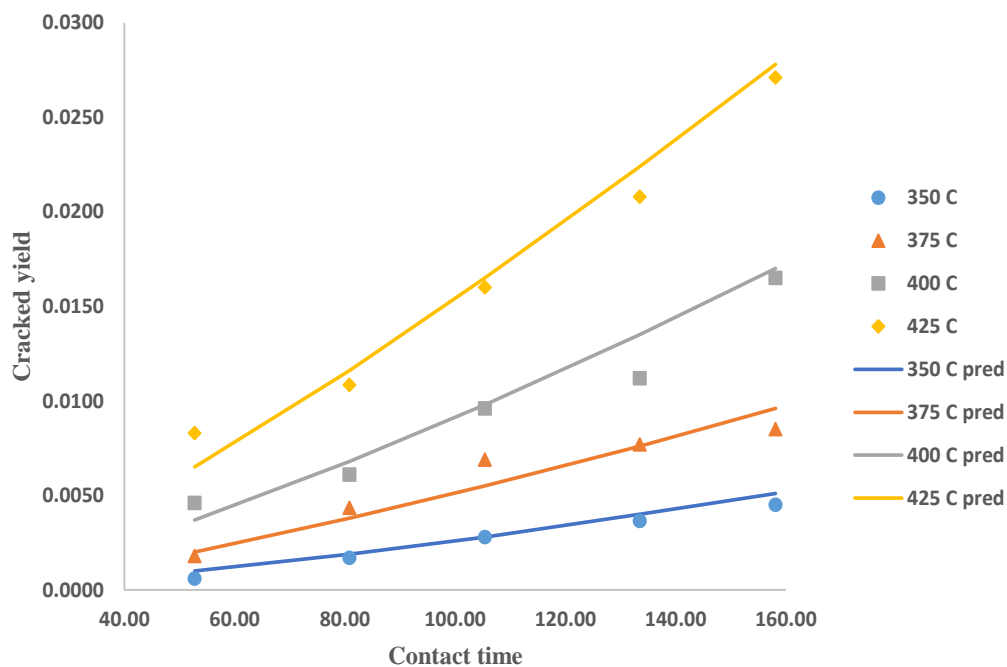
Fig. 4.32b: Experimental vs model predicted values for cracked products yield.

To further show overall agreement between the experimental data and model predicted values, a parity plot as shown in Fig. 4.33 was plotted. It can be concluded from the Figure that the model reasonably predicts the oxidative dehydrogenation reaction over the ternary metal catalyst and also the model discrimination values of 0.9993 and 0.0076 for correlation coefficient (R^2) and sum of squares respectively further give credit to the developed model.
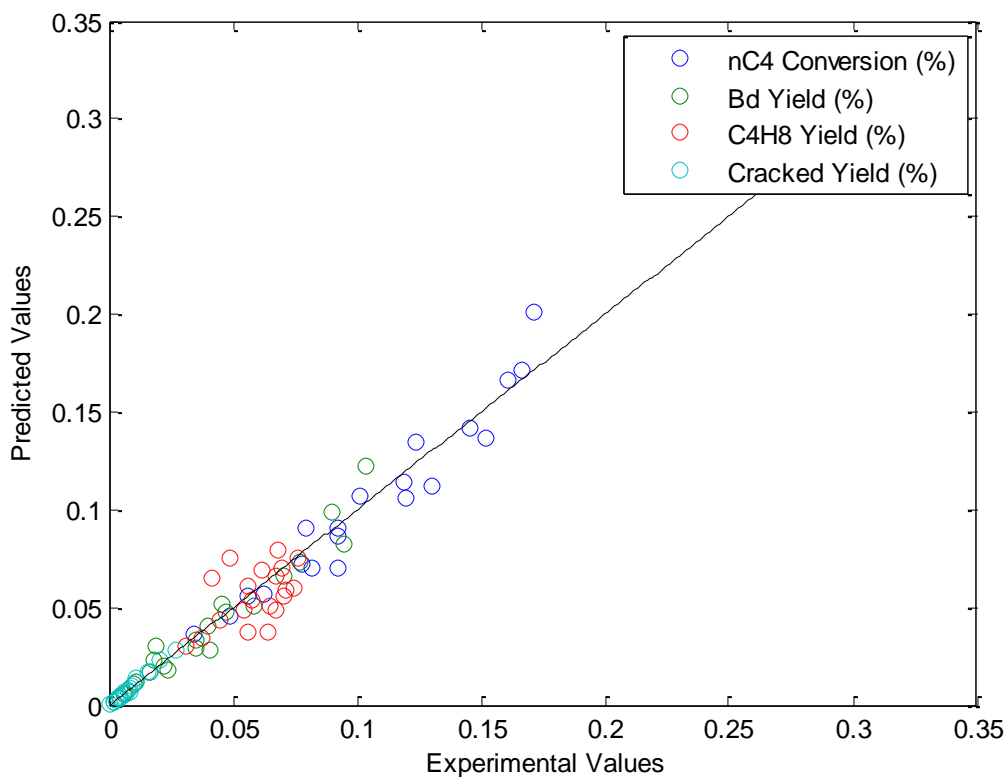
Fig. 4.33: Parity plot between the experimental data and model predicted values.

CHAPTER 5

CONCLUSIONS AND RECOMMENDATIONS

5.1 CONCLUSIONS

The investigation on the effect of main metal species (Ni, Fe and/Co)-Bi-O/Al_2O_3 catalysts on n-butane oxidative dehydrogenation to butadiene showed that binary (Ni-Fe, Ni-Co, Fe-Co) and ternary (Ni-Fe-Co) combination of main metal (Ni, Fe and Co) metals positively influenced the activity and selectivity. The ternary metal combination gave the highest selectivity to butadiene with high activity and stability which is mainly due to double improvements of Ni in butadiene selectivity by Fe due to its improved redox cycle and n-butane conversion by Co due to its high surface and an increased accessibility to active sites by its nanoparticle. The catalyst characterization showed that hierarchical nano-particle cohabitation of main metal (Ni, Fe, Co) oxide, Bi_2O_3 and Al_2O_3 support cooperates to enhanced butadiene selectivity at both 1st and 2nd dehydrogenation steps. This was evident from the low reduction temperature and moderate acidic/basic catalytic character with temperature programmed H_2 reduction and CO_2/NH_3 temperature programmed desorption respectively. Substituting Bi (active as oxygen supplier) with Mo and W gave a declined performance which revealed the fact that Ni as an active specie for dehydrogenation does not interact well with Mo and W and hence its redox ability and dispersion were affected with a resultant inefficiency of H_2 abstraction from both n-butane and 1-butene intermediate. The different supports investigated displayed different performance with MSU foam having the highest activity and selectivity even when compared to Al_2O_3 due to high dispersion ability of the active species by the support, but

deactivates faster which is why it was not used as a basis support for the investigations. Modifying Al_2O_3 and SiO_2 supports with a view of moderating their acidic/basic character which plays great role in desired product (butadiene) selectivity showed little improvement and resulted to a decrease in catalyst stability. The various catalyst stability is in the order 20Ni30Bi-O/Al_2O_3 = 10Ni5Fe5Co30Bi-O/Al_2O_3 > 20Ni30Bi-O/MSU foam > 20Ni30Bi-O/MgO-fumed SiO_2 = 10Ni5Fe5Co30Bi-O/MgO-fumed SiO_2. Kinetic data for n-butane oxidative dehydrogenation over 10Ni5Fe5Co30Bi-O/Al_2O_3 were obtained in the fixed bed reactor. Simple power law model was used to estimate the various kinetic parameters. The model reasonably fits the experimental data with a correlation coefficient of 0.9993 and a sum of squares value of 0.0076. The apparent activation energies of 2nd step dehydrogenation and cracking are 68.8 and 88.5 kJ/mol and shows good 95% confidence intervals which further confirms that the improved catalyst is more selective towards dehydrogenation than cracking.

5.2 RECOMMENDATIONS

The following are recommended for further research work on oxidation of n-butane to butadiene using metal-supported catalyst

- Other preparation methods like precipitation should be investigated in order to compare which method will enhance active metal-support interaction for better catalyst performance.
- Other characterization techniques like Raman spectroscopy, FTIR, UV-vis, HAADF EDX mapping should also be used in order to clearly reveal the active metal species interaction that led to the good performance of the improved catalyst.

- Surface science chemistry of NiO, Bi_2O_3, FeO, Co_3O_4 and Al_2O_3 should further be examined in order to improve the catalyst performance.

- One pot hydrothermal synthesis of the active metal species in the form of hydrotalcites should be investigated

REFERENCES

[1]   J. L. Nieto, "The selective oxidative activation of light alkanes. From supported vanadia to multicomponent bulk V-containing catalysts," *Top. Catal.*, vol. 41, no. 1–4, pp. 3–15, 2006.

[2]   C. Téllez, M. Abon, J. A. Dalmon, C. Mirodatos, and J. Santamaría, "Oxidative Dehydrogenation of Butane over VMgO Catalysts," *J. Catal.*, vol. 195, no. 1, pp. 113–124, 2000.

[3]   E. V Makshina, M. Dusselier, W. Janssens, J. Degrève, P. A. Jacobs, and B. F. Sels, "Review of old chemistry and new catalytic advances in the on-purpose synthesis of butadiene.," *Chem. Soc. Rev.*, vol. 43, pp. 7917–7953, 2014.

[4]   V. V. Chesnokov, A. F. Bedilo, D. S. Heroux, I. V. Mishakov, and K. J. Klabunde, "Oxidative dehydrogenation of butane over nanocrystalline MgO, Al 2O3, and VOx/MgO catalysts in the presence of small amounts of iodine," *J. Catal.*, vol. 218, no. 2, pp. 438–446, 2003.

[5]   M. Setnička, P. Čičmanec, R. Bulánek, A. Zukal, and J. Pastva, "Hexagonal mesoporous titanosilicates as support for vanadium oxide - Promising catalysts for the oxidative dehydrogenation of n-butane," *Catal. Today*, vol. 204, pp. 132–139, 2013.

[6]   A. Qiao, V. N. Kalevaru, J. Radnik, A. Srihari Kumar, N. Lingaiah, P. S. Sai Prasad, and A. Martin, "Oxidative dehydrogenation of ethane to ethylene over V2O5/Nb2O5 catalysts," *Catal. Commun.*, vol. 30, pp. 45–50, 2013.

[7]   W. Yan, Q. Y. Kouk, J. Luo, Y. Liu, and A. Borgna, "Catalytic oxidative dehydrogenation of 1-butene to 1,3-butadiene using CO2," *Catal. Commun.*, vol. 46, pp. 208–212, 2014.

[8]   A. N. Vasil'ev and P. N. Galich, "Catalysts for the oxidative dehydrogenation of butenes and butane to butadiene," *Chem. Technol. Fuels Oils*, vol. 33, no. 3, pp. 185–192, 1997.

[9]   S. Veldurthi, C.-H. Shin, O.-S. Joo, and K.-D. Jung, "Promotional effects of Cu on Pt/Al2O3 and Pd/Al2O3 catalysts during n-butane dehydrogenation," *Catal. Today*, vol. 185, no. 1, pp. 88–93, 2012.

[10]   S. A. Al-Ghamdi, "Thesis: Oxygen-Free Propane Oxidative Dehydrogenation Over Vanadium Oxide Catalysts: Reactivity and Kinetic Modelling," no. December, 2013.

[11]   L. Rodriguez, D. Romero, D. Rodriguez, J. Sanchez, F. Dominguez, and G. Arteaga, "Dehydrogenation of n-butane over Pd-Ga/Al2O3 catalysts," *Appl. Catal. A Gen.*, vol. 373, no. 1–2, pp. 66–70, 2010.

[12]   E. A. Mamedov and V. Cortis Corberan, "Oxidative dehydrogenation of lower alkanes on vanadium oxide-based catalysts. The present state of the art and outlooks," *Appl. Catal. A, Gen.*, vol. 127, no. 1–2, pp. 1–40, 1995.

[13]   T. Blasco and J. M. Lopez-Nieto, "Oxidative dyhydrogenation of short chain alkanes on supported vanadium oxide catalysts," *Appl. Catal. A Gen.*, vol. 157, no. 1–2, pp. 117–142, 1997.

[14]   G. Martra, F. Arena, S. Coluccia, F. Frusteri, and A. Parmaliana, "Factors controlling the selectivity of V2O5 supported catalysts in the oxidative dehydrogenation of propane," *Catal. Today*, vol. 63, no. 2–4, pp. 197–207, 2000.

[15]   J. McGregor, Z. Huang, G. Shiko, L. F. Gladden, R. S. Stein, M. J. Duer, Z. Wu, P. C. Stair, S. Rugmini, and S. D. Jackson, "The role of surface vanadia species in butane dehydrogenation over VOx/Al2O3," *Catal. Today*, vol. 142, no. 3–4, pp. 143–151, 2009.

[16]   A. Malaika, K. Wower, and M. Kozlowski, "Chemically Modified Activated Carbons as Catalysts of Oxidative Dehydrogenation of n-Butane," *Acta Phys. Pol. A*, vol. 118, no. 3, pp. 459–464, 2010.

[17]   N. Ikenaga and S. Onishi, "Oxidative Dehydrogenation of 1-Butene with Lattice Oxygen of V-Mg-Al Complex Oxide."

[18]   I. C. Marcu, I. Sandulescu, Y. Schuurman, and J. M. M. Millet, "Mechanism of n-butane oxidative dehydrogenation over tetravalent pyrophosphates catalysts," *Appl. Catal. A Gen.*, vol. 334, no. 1–2, pp. 207–216, 2008.

[19]   I. Rossetti, G. F. Mancini, P. Ghigna, M. Scavini, M. Piumetti, B. Bonelli, F. Cavani, and A. Comite, "Spectroscopic enlightening of the local structure of VO X active sites in catalysts for the Odh of propane," *J. Phys. Chem. C*, vol. 116, no. 42, pp. 22386–22398, 2012.

[20]   M. Setnička, R. Bulánek, L. Čapek, and P. Čičmanec, "N-Butane oxidative dehydrogenation over VOX-HMS catalyst," *J. Mol. Catal. A Chem.*, vol. 344, no. 1–2, pp. 1–10, 2011.

[21]   M. A. Chaar, D. Patel, M. C. Kung, and H. H. Kung, "Selective oxidative dehydrogenation of butane over VMgO catalysts," *J. Catal.*, vol. 105, no. 2, pp. 483–498, 1987.

[22]   B. P. Ajayi, B. R. Jermy, K. E. Ogunronbi, B. A. Abussaud, and S. Al-Khattaf, "N-Butane dehydrogenation over mono and bimetallic MCM-41 catalysts under oxygen free atmosphere," *Catal. Today*, vol. 204, pp. 189–196, 2013.

[23]   M. Bender, "An Overview of Industrial Processes for the Production of Olefins – C4 Hydrocarbons," *ChemBioEng Rev.*, vol. 1, no. 4, pp. 136–147, 2014.

[24]   W. C. White, "Butadiene production process overview," *Chem. Biol. Interact.*, vol. 166, no. 1–3, pp. 10–14, 2007.

[25] M. L. Pacheco, J. Soler, A. Dejoz, J. M. L. Nieto, J. Herguido, M. Menéndez, and J. Santamar, "MoO 3 / MgO as a catalyst in the oxidative dehydrogenation of n -butane in a two-zone fluidized bed reactor," vol. 61, pp. 101–107, 2000.

[26] J. Herguido, M. Mene, and J. Santamarı, "Oxidative Dehydrogenation of n-Butane in a Two-Zone Fluidized-Bed Reactor," *Ind. Eng. Chem. Res.*, vol. 38, no. DECEMBER, pp. 90–97, 1999.

[27] M. M. Bhasin, J. H. McCain, B. V. Vora, T. Imai, and P. R. Pujadó, "Dehydrogenation and oxydehydrogenation of paraffins to olefins," *Appl. Catal. A Gen.*, vol. 221, no. 1–2, pp. 397–419, 2001.

[28] F. Cavani, M. Koutyrev, F. Trifirò, A. Bartolini, D. Ghisletti, R. Iezzi, A. Santucci, and G. Del Piero, "Chemical and Physical Characterization of Alumina-Supported Chromia-Based Catalysts and Their Activity in Dehydrogenation of Isobutane," *J. Catal.*, vol. 158, no. 1, pp. 236–250, 1996.

[29] F. Urlan, I. C. Marcu, and I. Sandulescu, "Oxidative dehydrogenation of n-butane over titanium pyrophosphate catalysts in the presence of carbon dioxide," *Catal. Commun.*, vol. 9, no. 14, pp. 2403–2406, 2008.

[30] B. R. Jermy, B. P. Ajayi, B. A. Abussaud, S. Asaoka, and S. Al-Khattaf, "Oxidative dehydrogenation of n-butane to butadiene over Bi-Ni-O/γ-alumina catalyst," *J. Mol. Catal. A Chem.*, vol. 400, no. 325329, pp. 121–131, 2015.

[31] M. A. Botavina, G. Martra, Y. A. Agafonov, N. A. Gaidai, N. V. Nekrasov, D. V. Trushin, S. Coluccia, and A. L. Lapidus, "Oxidative dehydrogenation of C3-C4 paraffins in the presence of CO2 over CrOx/SiO2 catalysts," *Appl. Catal. A Gen.*, vol. 347, no. 2, pp. 126–132, 2008.

[32] P. Michorczyk, J. Ogonowski, P. Kutrowski, and L. Chmielarz, "Chromium oxide supported on MCM-41 as a highly active and selective catalyst for dehydrogenation of propane with CO2," *Appl. Catal. A Gen.*, vol. 349, no. 1–2, pp. 62–69, 2008.

[33] T. V. Malleswara Rao, E. Vico-Ruiz, M. A. Bañares, and G. Deo, "Obtaining the best composition of supported V2O5-MoO3/TiO2 catalyst for propane ODH reaction," *J. Catal.*, vol. 258, no. 2, pp. 324–333, 2008.

[34] E. Heracleous, M. Machli, A. A. Lemonidou, and I. A. Vasalos, "Oxidative dehydrogenation of ethane and propane over vanadia and molybdena supported catalysts," *J. Mol. Catal. A Chem.*, vol. 232, no. 1–2, pp. 29–39, 2005.

[35] A. Hakuli, M. E. Harlin, L. B. Backman, and a O. I. Krause, "Dehydrogenation of i-Butane on CrO x / SiO 2 Catalysts," *J. Catal.*, vol. 184, pp. 349–356, 1999.

[36] A. Corma, J. M. L. Nieto, and N. Paredes, "Preparation of V-Mg-O\tcatalysts: Nature of active species precursors," *Appl. Catal. A Gen.*, vol. 104, pp. 161–174, 1993.

[37] N. Ballarini, F. Cavani, A. Cericola, C. Cortelli, M. Ferrari, F. Trifirò, G. Capannelli, A. Comite, R. Catani, and U. Cornaro, "Supported vanadium oxide-based catalysts for the oxidehydrogenation of propane under cyclic conditions," *Catal. Today*, vol. 91–92, pp. 99–104, 2004.

[38] F. Arena, F. Frusteri, A. Parmaliana, G. Martra, and S. Coluccia, *Oxidative dehydrogenation of propane on supported V2O5 catalysts. The role of redox and acid-base properties*, vol. 119. Elsevier Masson SAS, 1998.

[39] M. A. Vuurman, F. D. Hardcastle, and I. E. Wachs, "Characterization of CrO3/Al2O3 catalysts under ambient conditions: Influence of coverage and calcination temperature," *J. Mol. Catal.*, vol. 84, no. 2, pp. 193–205, 1993.

[40] S. Derossi, G. Ferraris, S. Fremiotti, E. Garrone, G. Ghiotti, M. C. Campa, and V. Indovina, "Propane Dehydrogenation on Chromia/Silica and Chromia/Alumina Catalysts," *Journal of Catalysis*, vol. 148, no. 1. pp. 36–46, 1994.

[41] B. Y. Jibril, N. O. Elbashir, S. M. Al-Zahrani, and A. E. Abasaeed, "Oxidative dehydrogenation of isobutane on chromium oxide-based catalyst," *Chem. Eng. Process. Process Intensif.*, vol. 44, no. 8, pp. 835–840, 2005.

[42] B. Tope, Y. Zhu, and J. A. Lercher, "Oxidative dehydrogenation of ethane over Dy2O3/MgO supported LiCl containing eutectic chloride catalysts," *Catal. Today*, vol. 123, no. 1–4, pp. 113–121, 2007.

[43] M. V. Martínez-Huerta, X. Gao, H. Tian, I. E. Wachs, J. L. G. Fierro, and M. A. Bañares, "Oxidative dehydrogenation of ethane to ethylene over alumina-supported vanadium oxide catalysts: Relationship between molecular structures and chemical reactivity," *Catal. Today*, vol. 118, no. 3–4 SPEC. ISS., pp. 279–287, 2006.

[44] F. Cavani and F. Trifiri, "The oxidative dehydrogenation of ethane and propane as an alternative way for the production of light olefins," *Catal. Today*, vol. 24, no. 3, pp. 307–313, 1995.

[45] S. Gaab, M. Machli, J. Find, R. K. Grasselli, and J. A. Lercher, "Oxidative dehydrogenation of ethane over novel Li/Dy/Mg mixed oxides: Structure-activity study," *Top. Catal.*, vol. 23, no. 1–4, pp. 151–158, 2003.

[46] B. Fu, J. Lu, P. C. Stair, G. Xiao, M. C. Kung, and H. H. Kung, "Oxidative dehydrogenation of ethane over alumina-supported Pd catalysts. Effect of alumina overlayer," *J. Catal.*, vol. 297, pp. 289–295, 2013.

[47] B. P. Ajayi, B. Rabindran Jermy, B. A. Abussaud, and S. Al-Khattaf, "Oxidative dehydrogenation of n-butane over bimetallic mesoporous and microporous zeolites with CO2 as mild oxidant," *J. Porous Mater.*, vol. 20, no. 5, pp. 1257–1270, 2013.

[48] F. Cavani, N. Ballarini, and A. Cericola, "Oxidative dehydrogenation of ethane and propane: How far from commercial implementation?," *Catal. Today*, vol. 127, no. 1–4, pp. 113–131, 2007.

[49] V. Murgia, E. Sham, J. C. Gottifredi, and E. M. F. Torres, "Oxidative dehydrogenation of propane and n-butane over alumina supported vanadium catalysts," *Lat. Am. Appl. Res.*, vol. 34, no. 2, pp. 75–82, 2004.

[50] B. M. Weckhuysen and D. E. Keller, "Chemistry, spectroscopy and the role of supported vanadium oxides in heterogeneous catalysis," *Catal. Today*, vol. 78, no. 1–4 SPEC., pp. 25–46, 2003.

[51] S. A. Karakoulia, K. S. Triantafyllidis, G. Tsilomelekis, S. Boghosian, and A. A. Lemonidou, "Propane oxidative dehydrogenation over vanadia catalysts supported on mesoporous silicas with varying pore structure and size," *Catal. Today*, vol. 141, no. 3–4, pp. 245–253, 2009.

[52] K. Chen, S. Xie, A. T. Bell, and E. Iglesia, "Structure and Properties of Oxidative Dehydrogenation Catalysts Based on MoO3/Al2O3," *J. Catal.*, vol. 198, no. 2, pp. 232–242, 2001.

[53] F. Klose, T. Wolff, H. Lorenz, A. Seidel-Morgenstern, Y. Suchorski, M. Pirkowska, and H. Weiss, "Active species on ??-alumina-supported vanadia catalysts: Nature and reducibility," *J. Catal.*, vol. 247, no. 2, pp. 176–193, 2007.

[54] H. H. Kung and M. C. Kung, "Oxidative dehydrogenation of alkanes over vanadium-magnesium-oxides," *Appl. Catal. A Gen.*, vol. 157, no. 1–2, pp. 105–116, 1997.

[55] T. Blasco, "Influence of the Acid-Base Character of Supported Vanadium Catalysts on Their Catalytic Properties for the Oxidative Dehydrogenation of n-Butane," *Journal of Catalysis*, vol. 157, no. 2. pp. 271–282, 1995.

[56] B. Rabindran Jermy, S. Asaoka, and S. Al-Khattaf, "Influence of calcination on performance of Bi–Ni–O/gamma-alumina catalyst for n-butane oxidative dehydrogenation to butadiene," *Catal. Sci. Technol.*, vol. 5, no. 9, pp. 4622–4635, 2015.

[57] H. Armendariz, G. Aguilar-Raos, P. Salas, M. A. Valenzuela, I. Schifter, H. Arriola, and N. Nava, "Oxidative dehydrogenation of n-butane on iron-zinc oxide catalysts," *Appl. Catal. A, Gen.*, vol. 92, no. 1, pp. 29–38, 1992.

[58] H. Armendariz, J. A. Toledo, G. Aguilar-Rios, M. A. Valenzuela, P. Salas, A. Cabral, H. Jimenez, and I. Schifter, "Oxidative dehydrogenation of n-butane on zinc-chromium ferrite catalysts," *J. Mol. Catal.*, vol. 92, no. 3, pp. 325–332, 1994.

[59] Y. Xu, J. Lu, M. Zhong, and J. Wang, "Dehydrogenation of n-butane over vanadia catalysts supported on silica gel," *J. Nat. Gas Chem.*, vol. 18, no. 1, pp. 88–93, 2009.

[60] H. Lee, J. K. Lee, U. G. Hong, Y. Yoo, Y. J. Cho, J. Lee, H. S. Jang, J. C. Jung, and I. K. Song, "Effect of oxygen capacity and oxygen mobility of supported Mg 3(VO 4) 2 catalysts on the performance in the oxidative dehydrogenation of n-butane," *J. Ind. Eng. Chem.*, vol. 18, no. 2, pp. 808–813, 2012.

[61] J. K. Lee, H. Lee, U. G. Hong, J. Lee, Y. J. Cho, Y. Yoo, H. S. Jang, and I. K. Song, "Oxidative dehydrogenation of n-butane to n-butene and 1,3-butadiene over Mg 3(VO 4) 2/MgO-ZrO 2 catalysts: Effect of Mg:Zr ratio of support," *J. Ind. Eng. Chem.*, vol. 18, no. 3, pp. 1096–1101, 2012.

[62] B. Xu, X. Zhu, Z. Cao, L. Yang, and W. Yang, "Catalytic oxidative dehydrogenation of n-butane over V2O5/MO-Al2O3 (M = Mg, Ca, Sr, Ba) catalysts," *Chinese J. Catal.*, vol. 36, no. 7, pp. 1060–1067, 2015.

[63] J. M. L. Nieto, B. Solsona, R. K. Grasselli, and P. Concepcion, "Promoted NiO catalysts for the oxidative dehydrogenation of ethane," *Top. Catal.*, vol. 57, no. 14, pp. 1248–1255, 2014.

[64] E. Heracleous and A. A. Lemonidou, "Reaction pathways of ethane oxidative and non-oxidative dehydrogenation on γ-Al2O3 studied by temperature-programmed reaction (TP-reaction)," *Catal. Today*, vol. 112, no. 1–4, pp. 23–27, 2006.

[65] J.-H. Park and C.-H. Shin, "Oxidative dehydrogenation of butenes to butadiene over Bi–Fe–Me(Me=Ni, Co, Zn, Mn and Cu)–Mo oxide catalysts," *J. Ind. Eng. Chem.*, vol. 21, pp. 683–688, 2015.

[66] T. E. Davies, T. García, B. Solsona, and S. H. Taylor, "Nanocrystalline cobalt oxide: a catalyst for selective alkane oxidation under ambient conditions.," *Chem. Commun. (Camb).*, no. 32, pp. 3417–3419, 2006.

[67] S. A. Al-Ghamdi, M. M. Hossain, and H. I. De Lasa, "Kinetic modeling of ethane oxidative dehydrogenation over VO x/Al2O3 catalyst in a fluidized-bed riser simulator," *Ind. Eng. Chem. Res.*, vol. 52, no. 14, pp. 5235–5244, 2013.

[68] R. Grabowski, "Kinetics of Oxidative Dehydrogenation of C 2 -C 3 Alkanes on Oxide Catalysts," *Catal. Rev.*, vol. 48, no. 2, pp. 199–268, 2006.

[69] J. Zhu, K. Kailasam, A. Fischer, and A. Thomas, "Supported cobalt oxide nanoparticles as catalyst for aerobic oxidation of alcohols in liquid phase," *ACS Catal.*, vol. 1, no. 4, pp. 342–347, 2011.

[70] G. Raju, B. M. Reddy, B. Abhishek, Y.-H. Mo, and S.-E. Park, "Synthesis of C4 olefins from n-butane over a novel VOx/SnO2–ZrO2 catalyst using CO2 as soft oxidant," *Appl. Catal. A Gen.*, vol. 423–424, pp. 168–175, 2012.

[71] J.-H. Park, K. Row, and C.-H. Shin, "Oxidative dehydrogenation of 1-butene to 1,3-butadiene over BiFe0.65NixMo oxide catalysts: Effect of nickel content," *Catal. Commun.*, vol. 31, pp. 76–80, 2013.

[72] J. H. Park, H. Noh, J. W. Park, K. Row, K. D. Jung, and C. H. Shin, "Effects of iron content on bismuth molybdate for the oxidative dehydrogenation of n-butenes to 1,3-butadiene," *Appl. Catal. A Gen.*, vol. 431–432, pp. 137–143, 2012.

[73] J. C. Jung, H. Lee, H. Kim, Y.-M. Chung, T. J. Kim, S. J. Lee, S.-H. Oh, Y. S. Kim, And I. K. Song, "A synergistic effect of α-Bi2Mo3O12 and γ-Bi2MoO6 catalysts in

the oxidative dehydrogenation of C4 raffinate-3 to 1,3-butadiene," *J. Mol. Catal. A. Chem.*, vol. 271, no. 1–2, pp. 261–265.

[74] J. C. Jung, H. Lee, J. G. Seo, S. Park, Y. M. Chung, T. J. Kim, S. J. Lee, S. H. Oh, Y. S. Kim, and I. K. Song, "Oxidative dehydrogenation of n-butene to 1,3-butadiene over multicomponent bismuth molybdate (MII9Fe3Bi1Mo12O51) catalysts: Effect of divalent metal (MII)," *Catal. Today*, vol. 141, no. 3–4, pp. 325–329, 2009.

[75] B. Solsona, J. M. Lopez Nieto, P. Concepcion, A. Dejoz, F. Ivars, and M. I. Vazquez, "Oxidative dehydrogenation of ethane over Ni-W-O mixed metal oxide catalysts," *J. Catal.*, vol. 280, no. 1, pp. 28–39, 2011.

[76] B. Solsona, F. Ivars, A. Dejoz, P. Concepción, M. I. Vázquez, and J. M. López Nieto, "Supported Ni-W-O mixed oxides as selective catalysts for the oxidative dehydrogenation of ethane," *Top. Catal.*, vol. 52, no. 6–7, pp. 751–757, 2009.

[77] M. . Abello, M. . Gomez, and O. Ferretti, "Mo/γ-Al2O3 catalysts for the oxidative dehydrogenation of propane.," *Appl. Catal. A Gen.*, vol. 207, no. 1–2, pp. 421–431, 2001.

[78] M. C. Abello, M. F. Gomez, and L. E. Cadu, "Oxidative Dehydrogenation of Propane over Molybdenum Supported on MgO-γ-Al 2 O 3," *Magnesium*, vol. 5885, no. 95, pp. 2137–2143, 1996.

[79] E. Heracleous, A. F. Lee, I. a Vasalos, and a a Lemonidou, "Surface properties and reactivity of Al 2 O 3 -supported MoO 3 catalysts in ethane oxidative dehydrogenation," vol. 88, no. May, pp. 1–7, 2003.

[80] S. Sengupta and G. Deo, "Modifying alumina with CaO or MgO in supported Ni and Ni-Co catalysts and its effect on dry reforming of CH4," *J. CO2 Util.*, vol. 10, pp. 67–77, 2015.

[81] S. M. Waziri and S. Al-Khattaf, "Kinetics of Ethylbenzene Ethylation with Ethanol over a ZSM-5-Based Catalyst in a Riser Simulator," *Ind. Eng. Chem. Res.*, vol. 48, no. 18, pp. 8341–8348, 2009.

[82] B. P. Ajayi, B. Abussaud, R. Jermy, and S. Al Khattaf, "Kinetic modelling of n-butane dehydrogenation over CrOxVOx/MCM-41 catalyst in a fixed bed reactor," *Prog. React. Kinet. Mech.*, vol. 39, no. 4, pp. 341–353, 2014.

[83] T. I. Bhuiyan, P. Arudra, M. M. Hossain, M. N. Akhtar, A. M. Aitani, R. H. Abudawoud, and S. S. Al-Khattaf, "Kinetics modelling of 2-butene metathesis over tungsten oxide containing mesoporous silica catalyst," *Can. J. Chem. Eng.*, vol. 92, no. 7, pp. 1271–1282, 2014.

[84] T. Odedairo and S. Al-Khattaf, "Kinetic investigation of benzene ethylation with ethanol over USY zeolite in a riser simulator," *Ind. Eng. Chem. Res.*, vol. 49, no. 4, pp. 1642–1651, 2010.

[85] M. Osman, M. M. Hossain, and S. Al-Khattaf, "Kinetics study of ethylbenzene alkylation with ethanol over medium and large pore zeolites," *Ind. Eng. Chem. Res.*, vol. 52, no. 38, pp. 13613–13621, 2013.

VITAE

Name   :TANIMU GAZALI

Nationality   :NIGERIAN

Date of Birth   :9/5/1991

 Email   :gtu4ever@yahoo.com

Address   :Kaduna, Nigeria

Academic Background   :B.Eng. Ahmadu Bello University, Zaria